Detection and estimation of stage-discharge rating shifts for retrospective and real-time streamflow quantification

Matteo Darienzo

▶ To cite this version:

THÈSE

Pour obtenir le grade de

DOCTEUR DE L'UNIVERSITE GRENOBLE ALPES

Spécialité : **Océan, Atmosphère, Hydrologie**

Arrêté ministériel : 25 mai 2016

Présentée par

Matteo DARIENZO

Thèse dirigée par **Michel LANG**,
et co-encadrée par **Jérôme LE COZ** et **Benjamin RENARD**

préparée au sein de l'**unité de recherche RiverLy à INRAE centre de Lyon-Grenoble, France**
dans l'**École Doctorale Terre, Univers, Environnement (TUE)**

Detection and estimation of stage-discharge rating shifts for retrospective and real-time streamflow quantification

Thèse soutenue publiquement le **2 Février 2021,**
devant le jury composé de :

Mme Anne-Catherine FAVRE
Professeure, Université Grenoble Alpes, France, Présidente
M. Gil MAHE
Directeur de recherche, IRD, HydroSciences, Montpellier, France, Rapporteur
M. Dirceu REIS
Professeur, Université de Brasilia, Brésil, Rapporteur
M. Asgeir PETERSEN-ØVERLEIR
Ingénieur spécialiste, Statkraft Energy AS, Oslo, Norvège, Examinateur
M. Michel LANG
Chercheur IDTPE (HDR), INRAE Lyon-Grenoble, France, UR RiverLy, Directeur de thèse
M. Jérôme LE COZ
Chercheur ICPEF (HDR), INRAE Lyon-Grenoble, France, UR RiverLy, Co-encadrant de thèse, Invité
M. Benjamin RENARD
Chargé de recherche, INRAE Lyon-Grenoble, France, UR RiverLy, Co-encadrant de thèse, Invité
M. Arnaud BELLEVILLE
Ingénieur spécialiste, EDF-DTG, Grenoble, France, Invité
Mme Karine DELAMARRE
Ingénieure spécialiste, CNR, Lyon, France, Invitée

CONTENTS

ACKNOWLEDGEMENTS

(among them, my compatriots Marco DM and Andrea B).

My scientific skills are certainly also the results of the patience and professionalism of the supervisors of my previous research experiences: Olivier Boutron, Marion Vittecoq (La Tour du Valat) and Laurent Oxarango (IGE, ex LTHE). Moreover, I got some important skills in hydrometry from my experience at SEGI Ingénierie. Merci beaucoup.

Finally, but not for importance, I deeply thank Olga for her constant support and ability to ease the stress during these years in Lyon ("spasibo bolshoye"). Je remercie tous mes amis à Lyon et tous ceux que j'ai rencontrés en France, ma ovviamente anche tutti i miei amici d'infanzia in Italia con i quali ho cresciuto, e la mia famiglia sempre presente nel momento del bisogno. Grazie infinite.

RÉSUMÉ

Les séries temporelles de débit des rivières sont établies à l'aide de "courbes de tarage", qui sont des modèles avec les hauteurs d'eau en entrée et les débits en sortie. Malheureusement, de nombreuses stations hydrométriques ont une relation hauteur-débit instable, notamment à cause de l'évolution du lit de la rivière lors des crues. Ces "détarages" posent problème à la fois pour l'établissement des séries hydrologiques de long-terme (analyse rétrospective) et pour la fourniture de données en temps réel, par exemple pour la prévision des inondations, avec des incertitudes quantifiées et fiables. Les méthodes existantes pour la mise à jour de la courbe de tarage sont basées sur une analyse statistique des données de calibration (jaugeages) passées ou sur des règles empiriques. Cette thèse a permis de développer des méthodes originales pour la détection automatique des détarages et l'estimation de leur amplitude en rétrospectif et en temps réel : une méthode de segmentation des résidus entre les jaugeages et une courbe de référence, une analyse des récessions du limnigramme et une détection de détarages potentiels à partir d'un indicateur disponible en temps réel (par exemple, transport sédimentaire cumulé). L'approche probabiliste permet d'une part de prendre en compte l'incertitude des informations sur les détarages et d'autre part de quantifier les incertitudes sur les débits calculés. La combinaison des trois méthodes a été appliquée à la station de l'Ardèche à Meyras, en France, qui présente des détarages nets après chaque crue importante. Une bonne détection et estimation des détarages a été observée en rétrospectif et en temps réel. La méthode est générique et, après davantage de validation, applicable en opérationnel à d'autres sites.

ABSTRACT

River discharge time series are established using "rating curves", which are models with stage as input and discharge as output. Unfortunately, many hydrometric stations have an unstable stage-discharge relation, particularly because of the change in the river bed during floods. These "rating shifts" pose a problem both for the establishment of long-term hydrological series (retrospective analysis) and for the delivery of real-time data, for example for flood forecasting, with quantified and reliable uncertainties. The existing methods for updating the rating curve are based on a statistical analysis of past calibration data (the gaugings) or on empirical rules. This thesis aims at developing some original methods for the automatic detection of rating shifts and the estimation of their magnitude in both retrospective and real time: a method of segmentation of the residuals between the gaugings and a base rating curve, an analysis of the stage recessions and a method for detecting potential shifts from an indicator available in real time (e.g. cumulative sediment transport). The probabilistic approach allows on the one hand to take into account the uncertainty of the information on the shift and on the other hand to quantify the uncertainties of the calculated streamflow. The combination of the three methods has been applied to the Ardèche at Meyras, France, which shows net shifts after each major flood. Good detection and estimation of the rating shift has been observed retrospectively and in real time. The method is generic and, after further validation, operationally applicable to other sites.

LIST OF TABLES

1.1 Context and challenges related to discharge quantification

1.1.1 Monitoring streamflow: the rating curve

River discharge, or streamflow, is the volume of water passing through a river cross-section per unit of time (in $m^3.s^{-1}$). Streamflow time series are therefore the baseline data for most hydrological studies. They support decision-making for the management of water resources and aquatic environments and for the prevention of flood risk, erosion and river pollution.

However, for many natural rivers, streamflow time series are not direct observations: indeed, streamflow cannot be measured continuously. Instead, at some specific locations along the river easily accessible and equipped for data logging (called hydrometric stations) the water level (hereafter called "stage") is monitored with a constant frequency (e.g., every 15 minutes) or a frequency increasing with stage variation.

Consequently, streamflow time series are derived from the transformation of continuous measurement of water level via a stage-discharge relation, called the **"rating curve"** [WMO, 2010; Rantz, 1982], hereafter "RC".

1.1.2   Hydraulic principles behind the rating curve

The hydraulic relation between discharge and stage is determined by hydraulic controls. They are classified into two main categories: the **section controls**, characterised by critical flow conditions induced by obstacles or change in the cross-section, e.g., natural riffle, artificial weir, and the **channel controls**, mainly influenced by the bed slope and roughness and characterised by fairly uniform or friction-dominated flow. For both types, elementary controls have been extensively studied in the literature with typical formulas of the power-law form:

$$Q(h) = a(h - b)^c \tag{1.1}$$

linking the discharge Q to stage h, where a is the coefficient related to the physical and geometrical properties of the control (e.g., the channel width, the longitudinal slope, the roughness), b is the offset (with respect to the instrument measuring stage) below which the flow is zero, and c is an exponent related to the type and shape of the hydraulic control [Le Coz et al., 2014]. The term $h - b$ represents the water depth y.

In general several controls add or succeed to each other as flow increases. As an example of very common situations, Figure 1.1 illustrates the hydraulic configuration proposed by Mansanarez et al. [2019] and Sikorska and Renard [2017] for the Ardèche River at Meyras station located in a relatively small catchment of Mediterranean France. At this gravel bed stretch of the river the low flows are controlled by a natural riffle (located almost 50 m downstream of the bridge, where stage is measured) which can be modelled as a rectangular weir section control. The medium-high flows are controlled by the characteristics of the main channel which can be modelled as a wide rectangular channel control. At very high flows, water also flows in the lateral floodplain which can be modelled as a wide rectangular channel control added to the main channel control.

Once the hydraulic configuration has been defined, the RC parameters are calibrated using some occasional stage-discharge measurements (also called "**gaugings**"). Unfortunately, the gaugings are affected by **measurement uncertainty**. While the uncertainty of gauged stage is often neglected for the RC estimation, the uncertainty of gauged discharges cannot be neglected. Standard uncertainty values for the most frequent techniques (e.g., current meters, acoustic
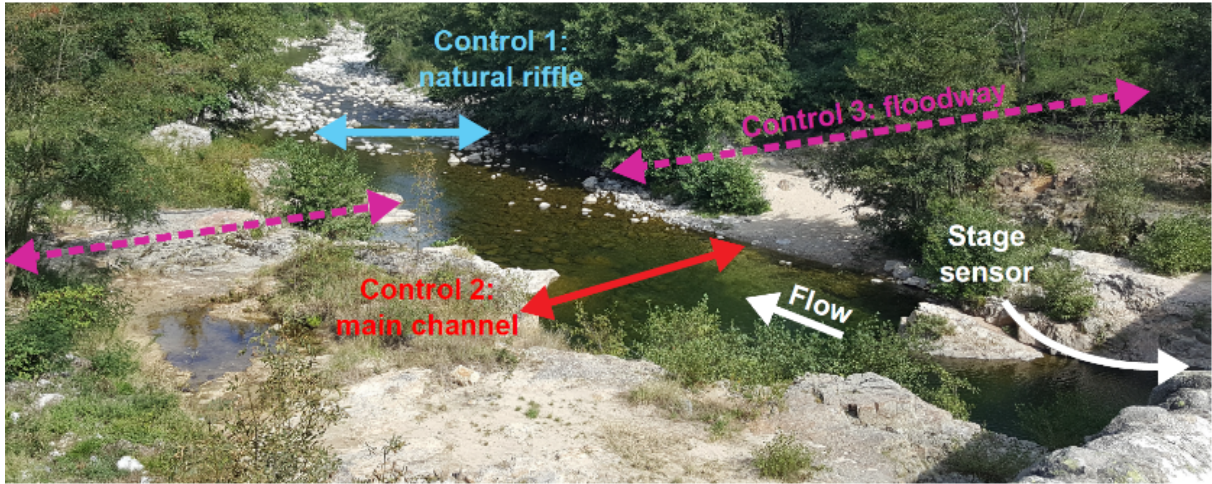
Figure 1.1: The Ardèche River at Meyras station (France), view downstream of Barutel bridge (taken from Mansanarez et al. [2019]): a very common hydraulic configuration.

Doppler current profilers ADCP, surface velocity radar and imagery analysis) have been proposed in the literature [e.g., Le Coz et al., 2014]. As an example, for the Meyras station the gaugings, performed by means of current meters at low, medium and high flows and by means of radar velocimetry at very high flows, are affected by an uncertainty of ± 7 % and ± 10 %, respectively.[1]

1.1.3 Rating curve uncertainty

Estimating the parameters of the RC based on a limited number of uncertain gaugings leads to substantial RC uncertainty. Two sources of uncertainty can be distinguished [Le Coz et al., 2014; Kiang et al., 2018]:

- the **parametric uncertainty** resulting from the imperfect identification of RC parameters;

- the **structural** (also called "remnant" or "epistemic") **uncertainty** related to the imperfection of the considered RC model.

---

[1]Unless specified otherwise, uncertainties expressed as $\pm\ u$ denote the width of a 95 % probability interval. For instance a value x affected by a probability $\pm$ 10 % means that a 95 % probability interval is $[0.9\ x;\ 1.1\ x]$.
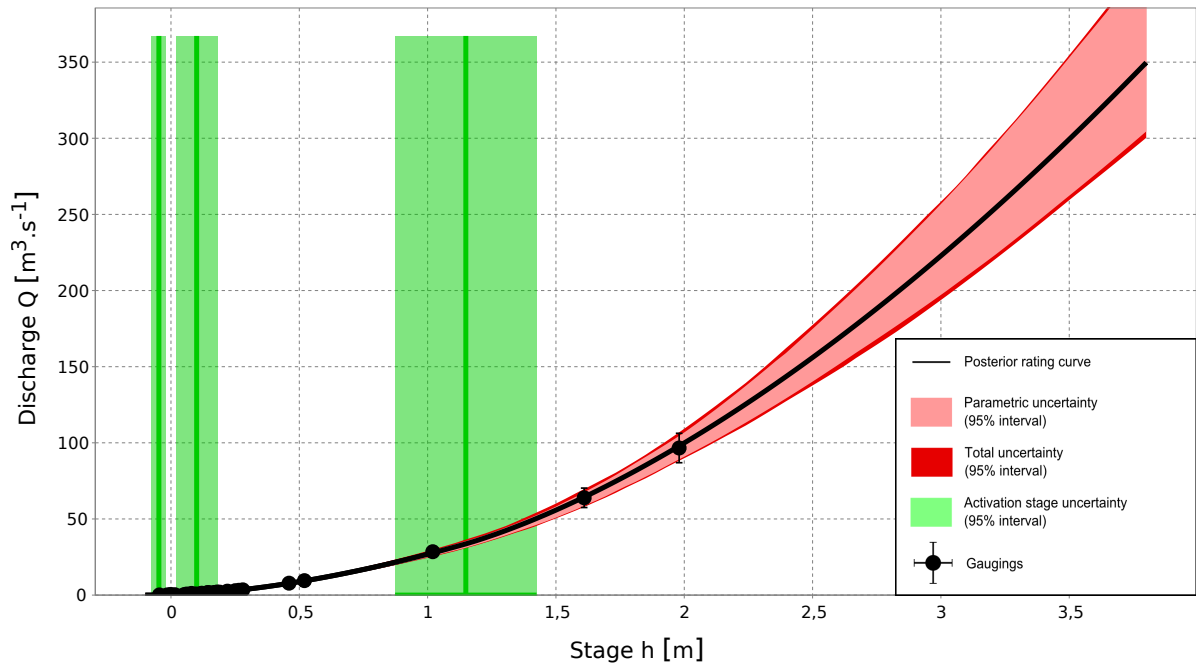
Figure 1.2: RC estimation with quantitative uncertainty for the Ardèche River at Meyras using the BaRatin approach [Le Coz et al., 2014] for the period 07/11/2001 - 08/11/2006.

As an order of magnitude, the total uncertainty is typically of $\pm\ 50 - 100$ % for low flows, $\pm\ 10 - 20\%$ for medium flows, and $\pm 40\%$ for out of bank flows [McMillan et al., 2012].

The various methods for estimating the RC with quantitative uncertainty are in general based on the regression of piecewise power functions accounting for gaugings uncertainty [Kiang et al., 2018]. They basically differ in:

- the assumption they made about the main sources of errors (e.g., structural error not formally accounted for, or accounted for with a standard deviation, constant or linearly increasing with discharge);

- the statistical tools they use (e.g. least square regression, Bayesian inference);

- the amount of hydraulic information used in addition to the gaugings (e.g., the Bayesian approaches allow specifying informative priors on the hydraulic knowledge of the RC parameters);

- the way they estimate the low and high flows outside the gaugings range (e.g., by extrapolation, or by prior specification on the very low flow control and on the flood
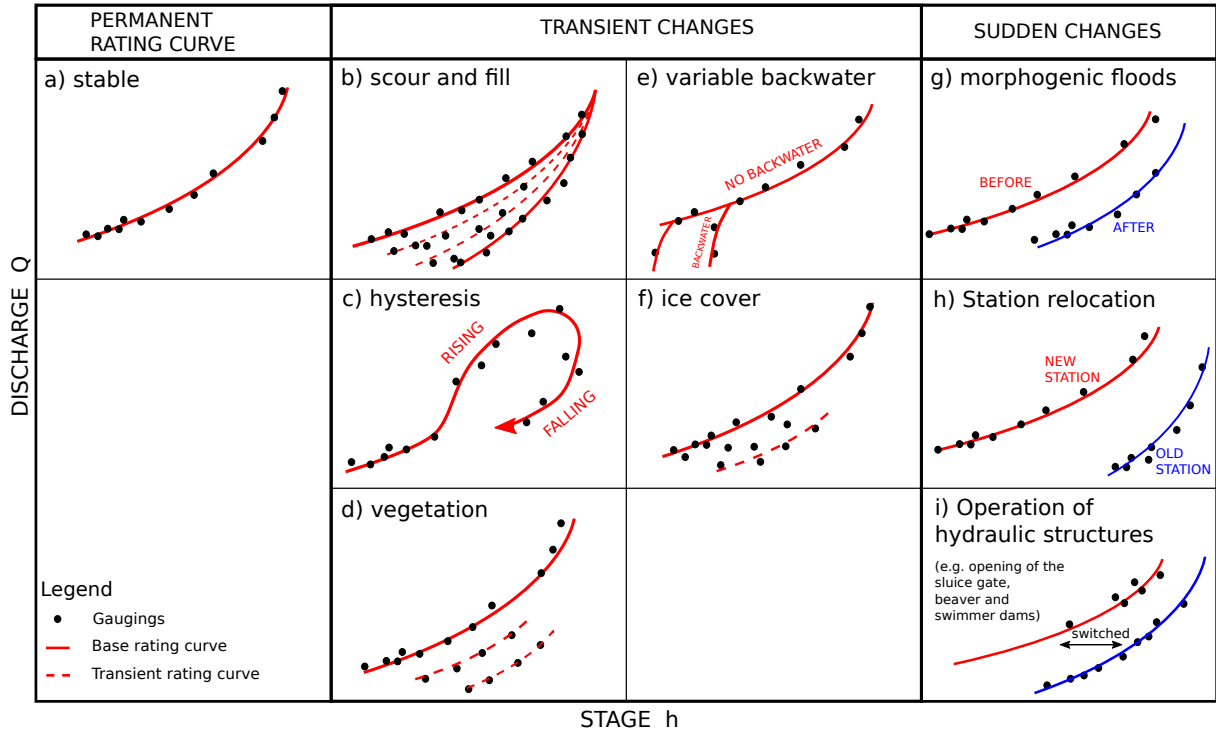
Figure 1.3: *Schematic representation of the different types of rating changes, of both transient and sudden type (modified from Herschy [1998] and Coxon et al. [2015]).*

plain).

As an example, Figure 1.2 illustrates the results of the RC estimation with uncertainty for the Meyras station by using the BaRatin method [Le Coz et al., 2014], which introduces in the Bayesian inference the preliminary hydraulic analysis through the prior specification. The figure does not only illustrate the most probable (maximum a posteriori) RC and the two types of RC uncertainty, but also displays the activation stages, i.e. the stage values corresponding to the transitions between two subsequent controls.

1.1.4   Rating changes

Unfortunately, one of the major issues affecting the RCs is that the stage-discharge relation is not only uncertain but can be unstable and affected by rating changes over time. The rating changes impose episodic or continuous RC updates.

Various causes lead to the RC changing in various ways, including simple translations of the
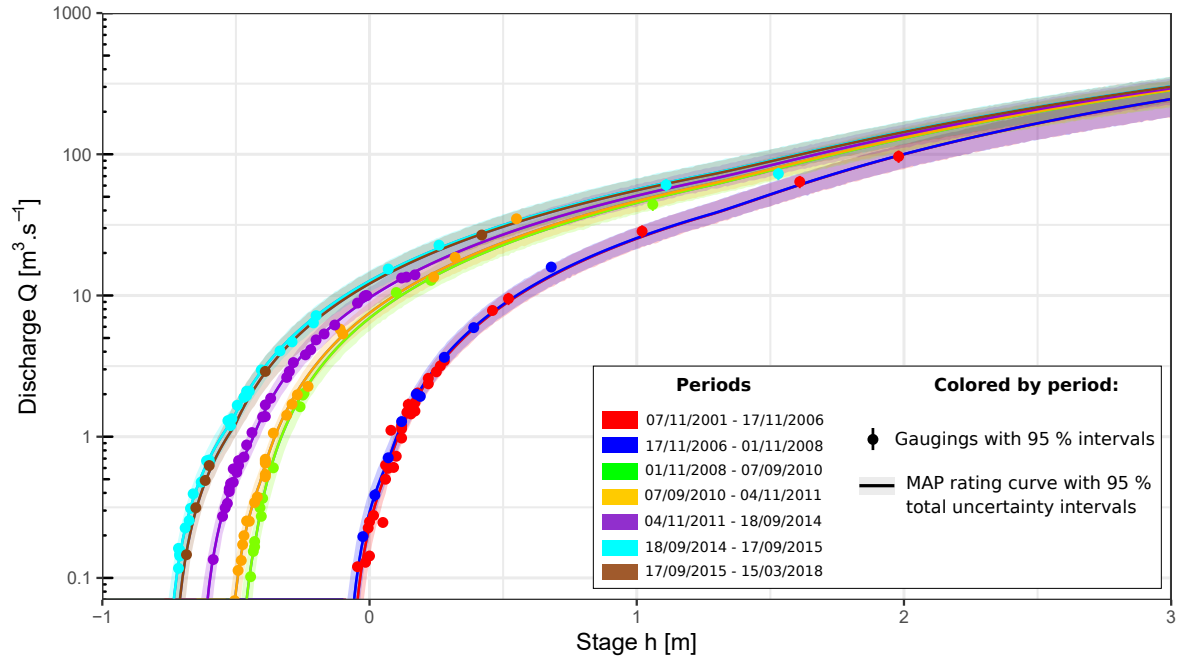
Figure 1.4: Rating shifts affecting the Ardèche River at Meyras station after intense morphogenic floods. Modified from Mansanarez et al. [2019].

whole curve to more complex modifications. The causes of this instability have been extensively studied in the literature (e.g. Herschy [1998]) and some examples are illustrated in Figure 1.3. Rating changes can be classified into two main categories: transient and sudden changes.

Transient changes are caused by progressive phenomena that lead to a wide variety of RC changes, such as sediment dynamics, hysteresis during floods, aquatic vegetation, variable backwater effect and ice sheets covering.

On the other hand, **sudden changes** (hereafter called **rating shifts**) are related to specific and short events inducing net rating changes between before and after the event, such as morphogenic floods, relocation or modification of the gauging station, operation of hydraulic structures such as the change in the opening of sluice gates, dike/levee break, dams built by swimmers or beavers, gravel or sand extraction from the river bed, etc.

In the case of Meyras station (Figure 1.4) the RC changes are most likely caused by sudden vertical shifts of the gravel bed elevation. These shifts are induced by some episodic and intense
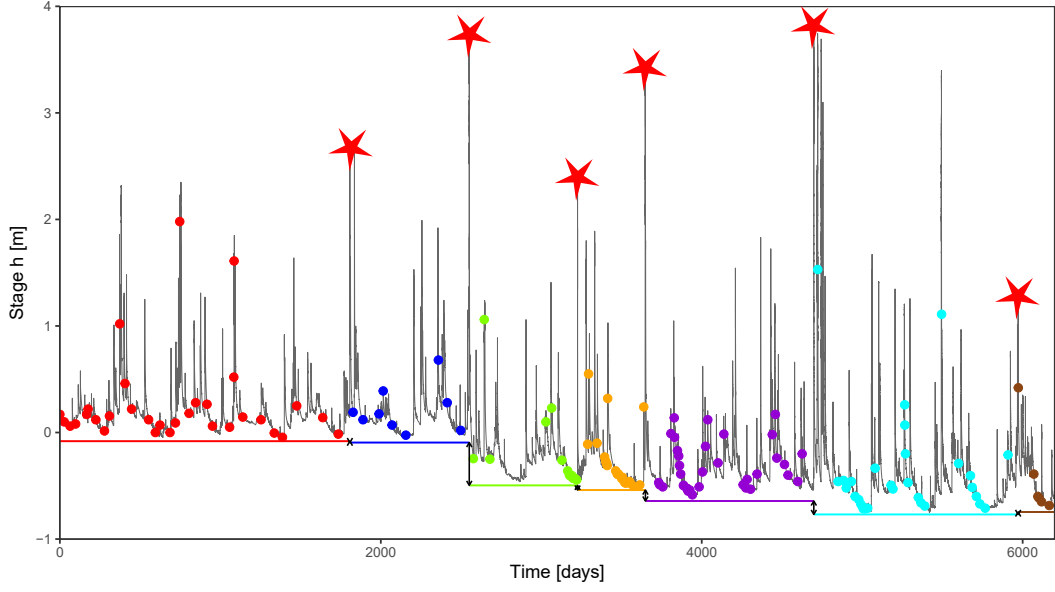
Figure 1.5: Stage record at the Ardèche River at Meyras (France) for the period 07/11/2001 16:19 - 29/10/2018 17:45 (measured by piezometer probe and a bubbler system); 151 gaugings provided by the hydrometric service UHPC Grand Delta for the period 07/11/2001 16:30 - 25/09/2018 10:55 are also plotted (dots). Stars denote morphogenic floods that are suspected to have caused a rating shift.

morphogenic floods (evidenced with stars in Figure 1.5) after which a net vertical degradation of the stage record is observed.

After having characterised the processes affecting the RC stability, the next step is to identify the RC parameters that are more likely to vary over time. For instance processes affecting width, slope and roughness of the channel induce a change in the parameter a of the control equation (Equation 1.1), and processes affecting the channel elevation induce a change in the parameter b. Instead, parameter c, which defines the type and the shape of the hydraulic control, is more rarely affected by rating changes. Moreover, identifying the unstable RC parameters may be very challenging also because some processes may occur simultaneously.

However, determining the nature of the change is not sufficient. The hydrologist also needs to identify among the hydraulic controls of the station which ones are more likely affected. For example in the case of morphological changes induced by floods the low flow section control (e.g. natural riffle) is in general more frequently and severely affected by net shifts than the high flow channel control. This is because the section controls are sensitive to local adjustments

in the bed micro-topography whereas the channel controls are not. Thus, minor events may suffice to induce net shifts at the low-flow controls. To induce net shifts at high flow controls, much greater events are required.

In the Meyras example, assuming that the channel banks have a rigid rocky composition (Figure 1.1), the channel bottom mostly degrades or raises vertically while the channel width remains stable. This induces mainly shifts of the offset parameters of the low flow controls: b_1 (mean elevation of the natural riffle crest) and b_2 (mean elevation of the main channel bed).

1.1.5 Managing rating changes in real time

Tracking and estimating these rating changes in order to update the RC is of primary importance for many operational applications, for instance for flood forecasting, hydroelectricity, compliance with environmental flows and nutrient/pollutant flux limits, administrative decisions related to low flows, restrictions or prohibitions on water diversion (for irrigation, etc.), shutdown of nuclear reactors, etc. [Osorio and Reis, 2016; McMillan et al., 2017].

There is a strong interest in obtaining and communicating values of streamflow in real time, accompanied by quantified uncertainties. This is particularly challenging at unstable hydrometric stations, affected by rating changes.

In the operational practice, the main source of information to detect and estimate RC changes is represented by the gaugings. When a gauging is far away from the last stable rating curve then the practitioner is aware that a potential shift may have occurred. Unfortunately, gauging campaigns are relatively costly and time consuming and can be problematic in particular site and hydraulic conditions. Thus, in general detecting a rating shift may take several months. During this period the official RC is obsolete and the discharge values estimated in real time by using this model might be biased.

This leads to the following questions: how to detect rating shifts as quickly as possible? Which information other then a gauging can be used to this aim? How to manage the uncertainty around the released streamflow data? In real time, when rating shifts cannot be

Figure 1.6: Flood of the Ross River in Townsville, Australia, on February 2019. Source of the photo: http: // media.bom.gov.au/ social/ blog/ 2156/ explainer-what-is-a-flood/ . Credit: Australian Defence Force.

quickly estimated, a solution may be to provide at least an updated uncertainty around the RC, hence around the released streamflow data. The next subsections describe in more details a few practical situations where streamflow and its uncertainty are needed in real time.

1.1.5.1   Flood forecasting and flood risk management

River floods (Figure 1.6) are still nowadays one of the major natural disasters all around the world [UNDRR, 2020]. In real time the decision makers supported by the services in charge of the hydrometric stations use forecasted streamflow to provide reliable and timely flood alert. Thus, a poor streamflow forecasting may have two types of consequences: a) it may fail to issue a warning for a flood event leading to potential loss of life and infrastructure; or b) it may issue a warning for an event that does not occur, which may erode people's trusting in the forecast and lead them to not respond to the next warning.

Two distinct sources of streamflow information are used for real-time flood risk management:

- the real-time observed streamflow (directly measured at some stations or estimated through the RC).

- the forecasted streamflow for the actual and next time steps, usually obtained from hydrological rainfall-runoff models describing the water balance in the river catchement. These models use meteorological data (rainfall, wind, temperature, etc) as input and historic streamflow data for the model calibration.

To reduce flood forecasting uncertainty sources a standard practice is to assimilate the real-time streamflow observations into the forecasting process in order to correct the registered deviations between the uncertain forecasted flows and the uncertain observed flows.

In the case of unstable rating curves the real-time analysis of streamflow data uncertainty is very challenging but is still necessary since it affects the data assimilation process and hence flood forecasting [Ocio et al., 2017]. During floods in June 2016 on the Cher and Seine catchments in France hydrometric services (the DREAL Centre-Val-de-Loire and the DRIEE Ile-de-France) had to extrapolate and re-estimate their rating curves in emergency (the same day), especially due to the difference in floodplain vegetation between summer and winter.

1.1.5.2 Hydroelectric power plants

Hydroelectric power plants can be mainly split in impoundment facilities (where the water is stored in a reservoir controlled by a dam and then released from the reservoir to the penstocks containing the turbines located at a lower elevation) and run-of-river plants (with little or no water storage, composed of a diversion structure, not necessarily a dam, that derives the flow destined to the turbines, example in Figure 1.7a). Both types need to carefully monitor streamflow in order to:

- optimise the energy production, by combining the energy price market, the energy demand cycles and the available streamflow diverted to the turbines (for example Q_2 in Figure 1.7b).

- control the floods through dam operations and to defend structures and workers from dangerous floods. This requires the monitoring of the incoming main streamflow (for example Q_1 in Figure 1.7b).

- guarantee that the instream flow released in the main channel (for example Q_3 in Figure 1.7b) respects the minimum environmental flow (MEF) fixed by the law, to ensure

the ecological continuity along the reach. This requires a correct and fast estimation of this flow in particular during droughts.

A poor real-time streamflow estimation may lead to economical losses for the hydropower company, to material and human losses in case of floods, or to environmental issues during low flows followed by sanctions implemented after Water Authorities investigations.

(a)
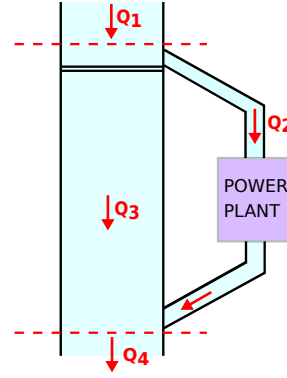
(b)

Figure 1.7: a) Run-of-River hydropower plant along the Rhin River, at Kembs in France, operated by EDF. Source image: https://congress.hydropower.org/2019-paris/programme/study-tours/study-tour-kembs-france/. b) Schematics of a generic Run-of-River hydropower plant with upstream main flow Q_1, derived flow Q_2, instream reserved flow Q_3, downstream flow Q_4.

1.1.5.3 Nuclear Power Plants (NPP)

As for hydropower plants all the phases of the siting, design, construction and real-time operation of an NPP (Figure 1.8a) require accurate streamflow estimation in order to ensure the necessary water supply (in this case water is used for cooling the condenser and the spent-fuel pool), to protect structures and workers against floods, and to ensure a minimum environmental flow. As an example, in 2011, the NPP of Fort Calhoun in Nebraska along the Missouri River was flooded (Figure 1.8b) and shut down (source: https://en.wikipedia.org/wiki/Fort_Calhoun_Nuclear_Generating_Station).

In addition to these issues the NPP needs to avoid or limit accidental pollution, that can be thermal (the hot water released by the NPP to the main stream may

(a)

(b)

Figure 1.8: a) NPP of Tricastin, France (EDF). Source photo: https://en.wikipedia.org/wiki/Tricastin_ Nuclear_Power_Plant. Credit: Marianne Casamance. b) Flood of Missouri River at the Calhoun NPP in Nebraska, 2011. Source photo: https://en.wikipedia.org/wiki/Fort_Calhoun_Nuclear_Generating_ Station. Credit: U.S. Army Corps of Engineer.

induce ecological issues, in particular on the aquatic life) and chemical (related to the concentration and flow of waste waters released by the NPP). The combination of droughts induced by the precipitation deficit and the river water overheating caused by extreme hot weather may force some nuclear power plants to temporarily shut down. In 2018 EDF temporarily shut down three reactors in eastern France, at the Bugey NPP upstream Lyon, at Saint-Alban NPP downstream Vienne on the Rhône River, and at the Fessenheim NPP close to the German border (source: https://www.leparisien.fr/economie/ canicule-arret-d-un-reacteur-de-la-centrale-nucleaire-de-fessenheim-04-08-2018-7843200.php).

In conclusion both water quantity and quality need to be monitored both upstream and downstream of an NPP. The stability of the rating curve at the hydrometric station of the NPP needs to be frequently monitored, in particular if rating changes are suspected to occur often. As an example, the station of the Civaux NPP on the Vienne River is frequently disrupted by aquatic vegetation, thus it is the subject of an intensive gauging joint program by several organizations: EDF-DTG, DREAL.

Figure 1.9: May 2020, a tank containing diesel oil at the Nadezhda plant on the Taymyr peninsula in the Russian Arctic, accidentally released 20 thousand tonnes of oil contaminating more than 20 km of Ambarnaya River. Source photo: https://www.greenpeace.org/international/story/43553/oil-spill-russian-arctic/. Credit: Greenpeace.

1.1.5.4 Accidental pollution

Sudden accidental pollution of a river may occur for several reasons: release of toxic industrial waste water into the river, pipelines failure, rain and snowmelt run-off from contaminated watershed, etc.

In order to describe the transport and the dispersion of the contaminant by water, reliable streamflow data is essential. It is particularly important in real time for the accident forecasting and prevention and/or the estimation of the short and long-term environmental effects. As an example a recent (2020) contamination of the Ambarnaya River in Russia (Figure 1.9) by 20,000 tons of diesel oil was constantly and carefully monitored by state Authorities in order to take actions to limit the environmental consequences.

1.1.5.5 Water-use restrictions

Real-time streamflow data is also of primary importance for those complex systems governed by one or more reservoirs where water resources need to be optimised for multiple uses at the same time: e.g. irrigation (Figure 1.10a), water consumption, hydroelectricity

(a)

(b)

Figure 1.10: a) Water uptake from the river for irrigation purposes. Source photo: https://wmanorthamerica.weebly.com/colorado-river.html. b) Mekong River in Thailand suffering from a terrible drought in the end of 2019. Source photo: https://vietnamtimes.org.vn/mekong-river-facing-severe-drought-amidst-serious-flooding-in-china-21905.html.

production. Administrative decisions related to low flows may lead to restrictions or prohibition of withdrawals.

In France, hydrological situation bulletins have to be released every three weeks or so by water authorities to allow for decisions on water use and allocation during drought seasons.

A severe drought in 2019 has impacted the Mekong River (Figure 1.10b), causing record low water levels in Thailand, Laos, Cambodia and Vietnam. Lack of water had devastating consequences for fish, as well as the tens of millions of people living and working along the river. Poor real-time streamflow estimation in this case may possibly cause political conflicts on the water management since the Mekong River flows through several countries characterised by different water regulation laws.

1.2 State-of-the art for the detection and estimation of rating changes

Several methods (manual or automated) have been proposed in the literature to formally or empirically track and estimate the magnitude of rating changes over time, as reviewed by Mansanarez et al. [2019]. However their applicability to real-time applications is challenging and quite limited.

The transient and sudden changes (mentioned in Section 1.1.4) require different approaches. While transient changes require dynamic modelling or continuous updates of the RC, sudden changes require, firstly, the detection of the shift times with the definition of stationarity periods of the RC, secondly, the RC estimation for each period.

1.2.1 Dynamic modelling of transient changes

In the past, dynamic approaches have existed in the operational practice with gradual modification of the RC (called "correction curve"). These methods are time-intensive and the applied corrections are done without considering the underlying hydraulic controls. Moreover, the calibration of the RCs and the review of the results remain very manual, without quantifying the uncertainties, and unsuitable for real-time management.

Bayesian methods have recently been developed to introduce some physical knowledge about the rating changes. Reitan and Petersen-Øverleir [2011] developed a dynamic model based on time-varying RC parameters within a hierarchical Bayesian framework. Mansanarez [2016] proposed a method for complex ratings, including stage-fall-discharge models for twin gauge stations affected by variable backwater (introducing an additional stage input variable, h_2), and stage-gradient-discharge (SGD) models to address hysteresis due to transient flows and the effect of the flood wave propagation [Mansanarez et al., 2020].

Perret et al. [2021] developed physically-based models to account for the aquatic vegetation dynamics (through the Strickler roughness coefficient, which involves a modification of parameter

a of the RC). The models are calibrated using the gaugings and some qualitative information on vegetation density through a Bayesian approach.

1.2.2   Detecting and estimating sudden changes

Several methods have also been proposed to detect the rating shifts in order to identify the periods characterised by RC stability.

The most common practice to detect a shift is to use gaugings. Some empirical approaches have been proposed, such as the detection of a shift when the gauging departs from the previous RC for more than some predefined threshold. However these approaches do not consider the uncertainty of both the gaugings and the RC. A more formal way to analyse the set of gaugings is to apply a statistical analysis (segmentation) to the residuals between the gaugings and a baseline RC, as proposed by Morlot et al. [2014] (Figure 1.11). A more detailed review on the segmentation issue will be proposed in Chapter 2.

Another way to detect rating shift is to use the stage record, which, contrarily to gaugings, is available in continuous and much cheaper. Łapuszek [2003] demonstrated that analysing the annual minimum stages (called H in Figure 1.12) may be of interest in order to detect anomalies or a trend in river bed evolution. However this method is not suited to the real time application because of its annual time step. A shift may be detected after several years.

Once the periods of validity have been defined, different methods have been proposed in the literature to update the corresponding RC. The "shift correction" techniques (used by USGS and Water Survey of Canada [Rainville et al., 2016]) apply a shift $s(h)$ to the RC offset:

$$Q(h) = a(h - b - s(h))^c \tag{1.2}$$

These corrections allow the hydrologist to account for the hydraulic configuration of the river and to select (based on the expertise) the specific controls assumed to be affected by the shift.

Alternatively, the RC can be estimated by using, in a sequential way, one of the methods mentioned in Section 1.1.3 for RC estimation with uncertainty [Kiang et al., 2018]. However,
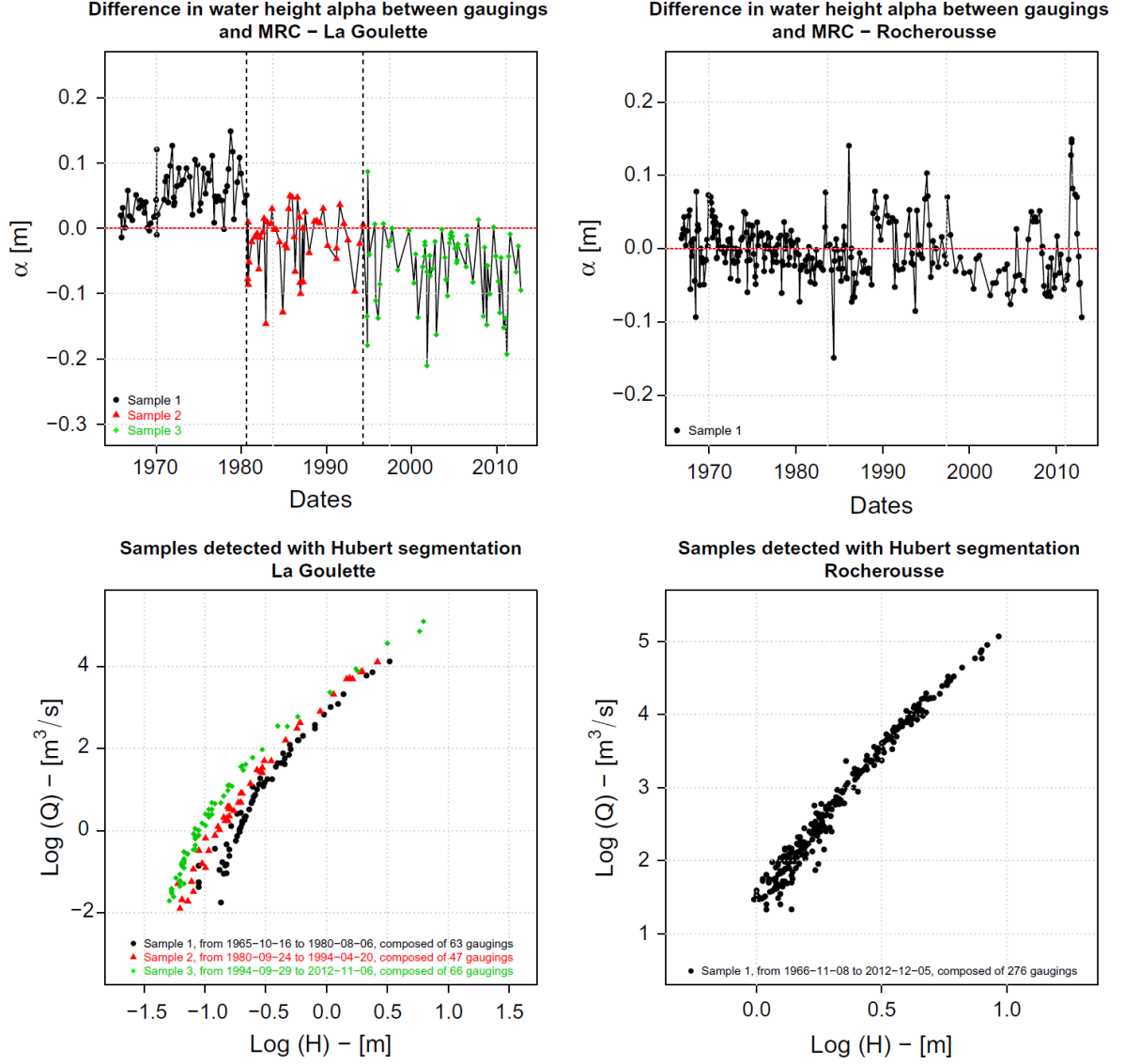
Figure 1.11: Top panels: segmentation procedure applied to the time series of the stage residuals computed between the gaugings and a baseline RC [Morlot et al., 2014]. Bottom panels: associated stage-discharge gaugings.
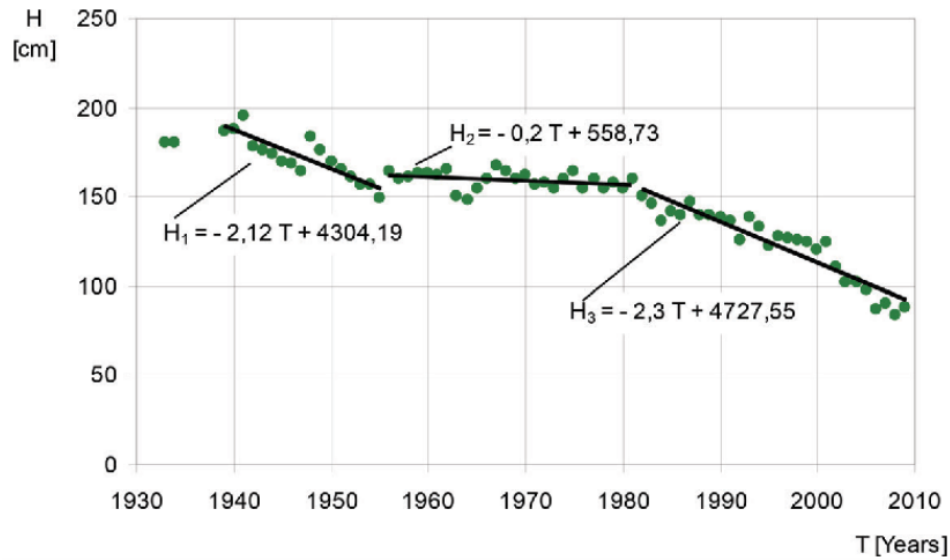
Figure 1.12: Variability of annual minimum stages (H) and estimated linear trends at the Brzegi cross-section on the Nida River [Łapuszek and Lenar-Matyas, 2015].

this becomes challenging for those periods characterised by few (or no) available gaugings, which may cause a large RC uncertainty. Thus a current practice is to re-use some gaugings from other periods to estimate the RC of the current period, therefore assuming that the corresponding controls are stable [Mansanarez et al., 2019]: e.g., this is typically applied to high-flow gaugings [McMillan et al., 2010; Puechberty et al., 2017].

A solution to this issue has been proposed by Mansanarez et al. [2019] who developed stage-period-discharge models for estimating successive RCs and their uncertainty with a transfer of information across periods through a Bayesian approach. In these models, RC parameters that are suspected to shift between periods are specific to each period, while other parameters remain unchanged across all periods. As an example, the application of this method to the Meyras case study is illustrated in Figure 1.4.

1.2.3 Real-time challenges

All the traditional and emerging methods introduced in the previous subsections are usually performed in **retrospective**, thus when the hydrometric data sets are fully available and when a rating shift has already occurred. This is acceptable when the interest of the station managers

is to perform a re-analysis of the historical hydrograph for purposes such as flood frequency analysis or to define the instability level of a station for planning future gauging campaigns.

On the contrary, the use of the traditional methods is quite limited for **real-time** purposes such as the operational applications described in Section 1.1.5, because of their dependence on gaugings (seldom performed and very uncertain if performed during floods) or on the stage record but with a too long time step (year).

Detecting a rating shift (real or suspected) may be required in real time, e.g., during floods or soon after, without waiting for the next gaugings. To this aim, station managers use visual control (more seldom bathymetry surveys) and all kind of information on, e.g., river works, gravel mining operations, vegetation growth or ice jams. These methods are, in the opinion of the operational staff themselves, unsatisfactory, in particular because they are not formalized and hardly reproducible but it is the best that can be done with the tools currently available.

Moreover, each type of process causing rating change is associated with a different time step. During floods, the rating change induced by morphological change or due to hysteresis may occur in a period of a few hours or a few days. During a period of growth of aquatic vegetation the rating change may occur for several months with observable changes at a daily/weekly/monthly time step. A different time step may be used also depending on the operational application. For flood forecasting purposes or in the case of accidental pollution the hydrometric services and water authorities may want to update the RC or at least its uncertainty, for example, every 15 minutes or every hour during/after the event. Instead for water restrictions during droughts a weekly/monthly time step may suffice.

The real-time management of the RC was the initial motivation for the development of the GesDyn method [Morlot et al., 2014] by EDF and LTHE through the PhD thesis of Morlot [2014]. However, the real-time application could not be achieved because a new gauging is required to trigger an RC update, with no specific mechanism to update the curve or its uncertainty *in between* gaugings.

Alternatively, the operational services often analyse the spatial and temporal behavior of several stations to detect potential shifts by examining the hydrographs from correlated stations (upstream-downstream station, station located in a tributary river or in a neighboring catchment, etc.). A change in the regression between the stations (e.g., after a flood) leads to question the rating curves of the two stations [Puechberty et al., 2017]. This method is usually based on a monthly time step, thus its applicability during floods is limited. Moreover, it requires the existence of a hydrologically comparable and stable station, which is never granted.

In addition, rainfall-runoff modelling is widely available and is used for real-time purposes by operational services [Puechberty et al., 2017; Lucas, 2018]. A rating shift may be detected by comparing the output of such models with the streamflow obtained from the RC. The advantage of this approach is the use of other sources of information usually available in real time (i.e., the inputs of the hydrological model such as precipitation, wind, temperature) and the use of a daily time step which may be more suitable for real-time purposes.

1.3 Objectives and outline of the manuscript

An efficient and transparent strategy to allow real-time decision making based on streamflow data is to integrate in real time any potential rating shift and to provide the associated uncertainties on the streamflow estimation. Such a strategy may typically indicate that there is an urgency to carry out control gaugings to confirm/invalidate the suspected shift. It may also lead to a large streamflow uncertainty during the period of time when a shift is suspected but not yet confirmed or invalidated. Forecasters and decision-makers in particular need to have real-time data, even if more uncertain, without gaps or delays, but they must then have information on uncertainty to be able to make informed decisions. With this in mind, this PhD work focuses on the issue of detecting and estimating rating shifts in retrospective as well as in real time. In particular, the main objectives are to develop and validate:

1. tools for the detection of **effective** rating shifts using essentially the gaugings and the stage record.

2. tools based on proxy models for the detection of **potential** rating shifts using the only information always available in real time: the stage record.

3. a general real-time framework for the streamflow quantification based on the sequential re-estimation of the RC accounting for potential shifts.

As regards the first objective two tools for detecting effective rating shifts are presented:

- An original segmentation procedure applied to the time series of the residuals computed between the gaugings and a reference rating curve (**Chapter 2**). The method uses all available gaugings to detect shifts and identify homogeneous periods. It performs a recursive multi-change point detection and accounts for both gaugings and rating curve uncertainties. It expresses the change point as a time rather than a position and provides uncertainty on the change points. The text in Chapter 2 is a slightly modified version of the article "Detection of Stage-Discharge Rating Shifts Using Gaugings: A Recursive Segmentation Procedure Accounting for Observational and Model Uncertainties" published in Water Resources Research journal [Darienzo et al., 2021].

- An original stage-recession analysis to detect changes in the recession shape over time (**Chapter 3**). The method aims at detecting and estimating step changes in the river bed elevation using the stage record as an input. It is based on: the extraction of all available recessions; the estimation of a recession model through a Bayesian approach; the detection of shifts in specific parameters of the recession model over time. The text in Chapter 3 is also written as a journal article that will be submitted shortly.

As regards the second objective, **Chapter 4** describes a tool for detecting potential rating shifts caused by morphological changes during floods. The tool is based on a sediment transport proxy analysis and is of particular interest for real-time applications. Using the stage record, it computes a cumulative bed load estimate for each flood event in order to identify the events more likely to cause a net river bed change.

The third objective of this PhD work will be treated in **Chapter 5** by discussing the results of a first proof-of-concept application of a real-time streamflow estimation framework. In particular, the real-time framework requires:

- One tool for estimating the RC estimation and its uncertainties. In this manuscript the Bayesian approach (and in particular the BaRatin method [Le Coz et al., 2014]) will be preferred because of its ability to include in the statistical inference the physical knowledge of the rating shift through the prior specification of RC parameters).

- At least one tool for detecting and estimating rating shifts in a real-time context, and thus capable of providing a continuous information about the RC stability. This tool needs to be calibrated and validated through a retrospective analysis that consists in detecting and studying all past rating shifts.

The general perspectives for future work including possible improvement, potential operational application of the tools proposed in this manuscript, and the final conclusions will be presented in **Chapter 6**.

CHAPTER 2

SEGMENTATION OF GAUGINGS

This chapter is a slightly modified version of the article "Detection of Stage-Discharge Rating Shifts Using Gaugings: A Recursive Segmentation Procedure Accounting for Observational and Model Uncertainties" published in Water Resources Research [Darienzo et al., 2021], doi: https://doi.org/10.1029/2020WR028607.

Abstract

The stage-discharge rating curve is subject at many hydrometric stations to sudden changes (shifts) typically caused by morphogenic floods. We propose an original method for estimating shift times using the stage-discharge observations, also known as gaugings. This method is based on a recursive segmentation procedure that accounts for both gaugings and rating curve uncertainties through a Bayesian framework. It starts with the estimation of a baseline rating curve using all available gaugings. Then it computes the residuals between the gaugings and this rating curve with uncertainties. It proceeds with the segmentation of the time series of residuals through a multi change point Bayesian estimation accounting for residuals uncertainties. Once a first set of shift times is identified, the same procedure is recursively applied to each sub-period through a "top-down" approach searching for all effective shifts. The proposed method is illustrated using the Ardèche River at Meyras in France (a typical hydrometric site subject

23

to river bed degradation) and evaluated using several synthetic data sets for which the true shift times are known. The applications confirm the added value of the recursive segmentation compared with a "single-pass" approach and highlight the importance of properly accounting for uncertainties in the segmented data. The recursive procedure effectively disentangles rating changes from observational and rating curve uncertainties.

Plain Language Summary

For many hydrological and hydraulic issues, such as flood forecasting, a reliable river discharge estimate is needed. In general discharge is derived from the recorded water level (stage) through a stage-discharge relation (rating curve). This relation is calibrated using direct observations (gaugings). Unfortunately the rating curve is not only uncertain but it can also be subject to sudden changes or shifts due for example to intense floods that modify the river bed geometry. One solution to identify periods of rating curve stability is to apply a segmentation procedure to the gaugings. We propose in this paper an original recursive segmentation procedure that accounts for both gaugings and rating curve uncertainties.

2.1 Introduction

2.1.1 Rating curves

River discharge, or streamflow, is one of the most important variables in hydrology and hydraulics. Hydrometric data are essential for the calibration of hydrological models, flood forecasting and warning, engineering design (of dam and bridges for example) and policy decisions related to water resources and environmental management. However, streamflow time series are not direct observations as streamflow cannot generally be continuously measured in natural rivers. Instead, the water level (also called "stage") is continuously monitored. Streamflow time series is hence derived from rating curves [WMO, 2010; Rantz, 1982], hereafter called "RCs", which are models transforming an input stage into an output discharge. These models are estimated using occasional stage-discharge measurements (also known as gaugings) and hydraulic constraints. The physical relation between discharge and stage is determined by hydraulic controls, that is, physical characteristics of the river section or channel influencing the flow: geometry, friction, longitudinal slope, head losses, etc. A hydraulic analysis of the site, through field expertise or modelling, allows identifying the succession or addition of hydraulic controls as flow increases [Le Coz et al., 2014].

RCs are affected by many sources of uncertainty, including structural uncertainty (imperfection of the RC model), gaugings measurement uncertainty, and parametric uncertainty (estimation of RC parameters). Several methods for quantifying RC uncertainty have been developed as recently reviewed by Kiang et al. [2018]. Unfortunately, the stage-discharge relation can be unstable and affected by rating changes. When ignored, these changes may be the main source of RC uncertainty [Ibbitt and Pearson, 1987]. Concerning the causes of this instability, it is useful to distinguish between transient and sudden rating changes. Transient changes are caused by progressive phenomena [Herschy, 1998] such as hysteresis in unsteady flow during floods (rising limb and falling limb have different discharge values for the same stage), variable backwater due to unsteady downstream boundary conditions (e.g., stage controlled by a reservoir, sea tidal effect), growth and decay of aquatic vegetation, evolution of ice sheets covering cold-water rivers, river bed evolution due to sediment dynamics with progressive scour

Matteo Darienzo

and fill. On the other hand, sudden changes (shifts) are related to specific and occasional events such as morphogenic floods, dike breaks, dams built by swimmers or beavers, etc.

The next sections review the methods proposed in the literature to estimate the magnitude of rating changes and therefore to track the variability of RCs in time. The aforementioned transient and sudden changes require different approaches.

2.1.2 Detecting and modelling transient changes

Modelling transient changes requires dynamic approaches. Such methods have actually existed in the operational practice since the beginning of the 20th century at least, in the form of time-varying RCs accounting for gradual rating changes. Schmidt [2002] described the Stout's method (circa 1900) based on gradual daily shifts estimated from the gaugings. The same author also described the similar Bolster's method (circa 1910) which interpolates gaugings every day and develops parallel rating curves. Recently, Westerberg et al. [2011] and Guerrero et al. [2012] proposed to estimate RCs on moving temporal windows containing 30 successive gaugings. Morlot et al. [2014] proposed to compute as many RCs as there are gaugings and introduced the concept of RC aging: following an RC update, uncertainty increases with time according to a variographic analysis [Jalbert et al., 2011]. Reitan and Petersen-Øverleir [2011] developed a dynamic model based on time-varying RC parameters within a hierarchical Bayesian framework. Finally, in the specific context of sites affected by aquatic vegetation, Puechberty et al. [2017] proposed time-varying stage corrections and Perret et al. [2021] introduced the Bayesian estimation of a time-dependent rating curve model accounting for vegetation growth and decay, with year-specific parameters.

2.1.3 Detecting sudden changes

As rating changes often result from episodic morphogenic floods, models assuming sudden rating changes between stability periods are more widespread than dynamic models in the operational practice. This approach requires solving two main issues: detecting changes (which includes estimating shift times), and estimating the successive stable RCs with their associated uncertainties. In this paper we will focus on the first issue only. We refer the reader to

Mansanarez et al. [2019] for a review on the second issue.

Several methods exist for sudden rating change detection. The most common approach is arguably to use gaugings. For instance, an empirical rule [WMO, 2010] prescribes to start a new period (and hence a new RC) when a gauged discharge departs from the current RC by more than some predefined threshold, or when successive gauged discharges are systematically above or below the current RC. This rule varies across agencies and site conditions, for instance: ± 5 % of discharge or ± 0.6 cm (± 0.02 ft) in stage for low-flow controls for the USGS [Rantz, 1982]; ± 5 % of discharge for the Water Survey of Canada [Rainville et al., 2016]; ± 10 % of discharge and/or $\pm 2 - 3$ cm in stage in France [Puechberty et al., 2017]. While easy to apply, this approach is based on empirical rules and ignores both gaugings and RC uncertainties.

In addition, operational services monitor the evolution of the river bed elevation to detect a change in the corresponding RC parameter. They use field observations such as information about river works, gravel mining operations and bathymetry surveys. It is also possible to install submersible pressure transducers at various locations along the reach [Phillips and Eaton, 2009]. An observed drastic drop or raise in the stage record may indicate a sudden river bed change. Moreover, Łapuszek and Lenar-Matyas [2015] evaluated whether changes in the annual minimum stages may indicate changes of the river bed level. This method is useful to provide a trend of the river bed evolution, but due to its annual resolution it cannot precisely identify the dates of rating shifts. Alternatively, McMillan et al. [2010] proposed to arbitrarily select the 0.5-year return period discharge as a threshold triggering a new RC period.

Furthermore, some operational services perform correlation analyses with reference stable discharge time series (e.g., the output of a hydrological model, or a discharge time series from a stable and well gauged neighboring station). Changes in the correlation structure may be indicative of rating shifts.

Finally, a formal way to detect changes by using gaugings is to apply a segmentation procedure to the time series of residuals between the gaugings and a time-invariant RC in order to identify homogeneous families of gaugings, as done for instance by Morlot et al. [2014]. This

paper focuses on this approach.

2.1.4 Change point detection methods

The problem of finding abrupt changes in a time series is known in the literature as Change Point Detection (CPD). Reviews of the most representative methods have been proposed by many authors, such as Basseville and Nikiforov [1993]; Ducré-Robitaille et al. [2003]; Keogh et al. [2003]; Jandhyala et al. [2013]; Aminikhanghahi and Cook [2017].

A distinction can be made between single (sCPD) and multiple (mCPD) change point detection methods. sCPD methods are based on statistical tests questioning the existence of one single change affecting typically the mean or the median of the series, sometimes higher moments as well. The literature proposes several methods, e.g. likelihood-ratio tests [Hinkley, 1970; Chen et al., 2006; Chen and Gupta, 2012], non-parametric tests [Wilcoxon, 1945; Pettitt, 1979; Kruskal and Wallis, 1952; McGilchrist and Woodyer, 1975], "Standard Normal Homogeneity" tests Hawkins [1977]; Alexandersson [1986], and Bayesian procedures [Chernoff and Zacks, 1964; Lee and Heghinian, 1977; Booth and Smith, 1982; Perreault et al., 1999, 2000a,b].

Alternatively, mCPD methods look for multiple change points in the series. Unlike sCPD, mCPD is affected by a combinatorial challenge induced by the large number of possible change point positions. The Binary Segmentation or BS [Scott and Knott, 1974] recursively performs sCPD until no more changes are detected in any of the obtained segments. However this approach is prone to known issues such as premature termination (schematized in Figure 2.1a) and mislocated splits (Figure 2.1b). To overcome these issues, several options are available: e.g. the Circular BS method proposed by Olshen et al. [2004], sequential methods [Page, 1954; Hubert and Carbonnel, 1987; Hubert et al., 1989], Dynamic Programming [Auger and Lawrence, 1989; Killick et al., 2012], Bayesian inference [Green, 1995; Chib, 1998; Lavielle and Lebarbier, 2001] or Hidden Markov Models [Cappé et al., 2005; Luong et al., 2012].

However, these methods lack flexibility in the treatment of uncertainties affecting the segmented data. Indeed, the total uncertainty affecting RC residuals is induced by both gaugings and RC uncertainties. This uncertainty is not only potentially large, but it may
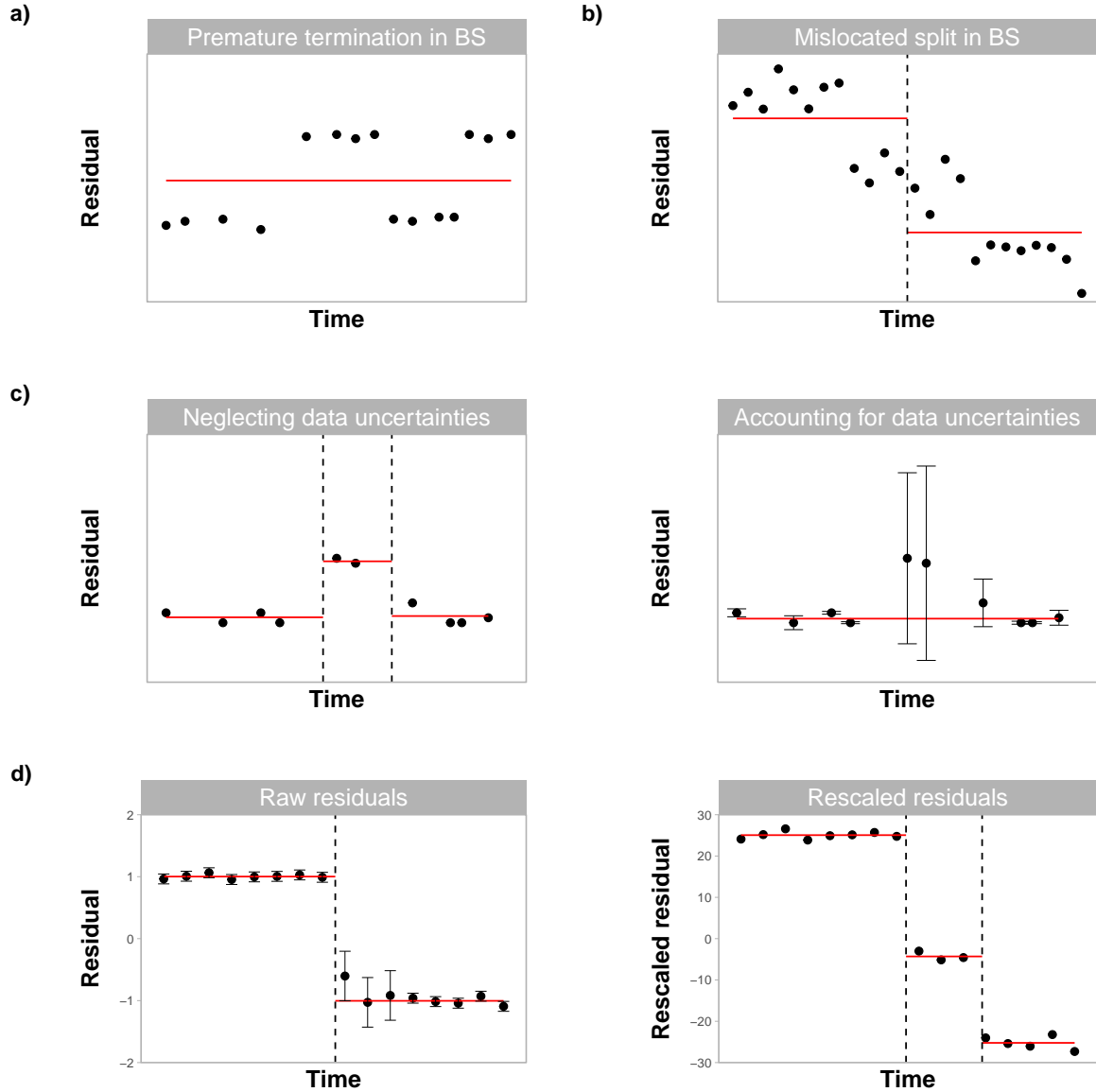
Figure 2.1: *Schematic illustration of typical segmentation pitfalls:*

(a) premature termination in Binary Segmentation: no single change point model provides a reasonable fit to the data and BS therefore stops at the first iteration, with no change detected;

(b) mislocated split in Binary Segmentation: optimal single change point is in the middle of a stable period;

(c) neglecting versus accounting for data uncertainties;

(d) artifact induced by residual rescaling: while raw residuals with standard deviation close to zero lead to rescaled residuals with high absolute values, highly uncertain residuals are sent to zero by the rescaling, thus creating a spurious period.

also strongly vary from point to point. This should be accounted for in the segmentation procedure, as illustrated in the conceptual example of Figure 2.1c: ignoring data uncertainty clearly suggests three periods, while recognizing that two points have a much larger uncertainty than the others suggests a single period may suffice. An option is to consider rescaled residuals instead of absolute residuals (e.g. dividing the absolute residuals by the standard deviation representing their uncertainty). However in some cases this rescaling might create spurious periods as illustrated in Figure 2.1d.

Furthermore, mCPD methods attempt to detect all changes in a given data set. In the context of RC shifts, this data set is derived using a baseline RC fitted to all gaugings, which may be a very poor representation of the stage-discharge relation. The large scatter and uncertainty of residuals may hide smaller changes that may be missed by such "single-pass" procedure. A recursive procedure, re-estimating the RC on each sub-period and deriving updated data sets of RC residuals, may hence be of interest.

Finally, the estimated change points provided by mCPD methods are not well-adapted to the context of RC shifts for the following reasons: (i) they are expressed in terms of position (i.e. observation index) rather than time, which is not ideal for irregular data such as gaugings; (ii) the uncertainty around the change point positions is rarely quantified. Nam et al. [2012] underlined the importance of accounting for the uncertainty of change point estimates. Estimating change points in terms of uncertain shift times would be useful to look for specific events that may have caused the change - e.g. a large flood that would typically occur *in between* gaugings.

2.1.5 Objectives of the paper

The main objective of this paper is to propose an original method for the detection of rating shifts through the segmentation of residuals between the gaugings and a baseline RC. The method must:

1. account for uncertainties in segmented data.

2. recursively re-estimate the baseline RC and apply the segmentation on each sub-period to reveal minor changes.

3. express change points in terms of time (rather than position), along with their uncertainty.

The structure of the paper can be summarized as follows. Section 2.2 describes the proposed method. In Section 2.3, this method is applied to a typical hydrometric station with the aims of illustrating the main properties of the method and introducing several possible variants. Section 2.4 then describes a more thorough evaluation of the method's performance based on synthetic data sets where change points are known. Section 2.5 discusses results and proposes future perspectives. Finally, Section 2.6 summarizes the main findings.

2.2 The proposed method for rating shift detection

2.2.1 Overview

Figure 2.2 illustrates in a schematic way the algorithm of the proposed method. The main steps are listed below and detailed in the next subsections.

1. Estimation of the baseline RC and its uncertainty using all available gaugings (Section 2.2.2).

2. Computation of the residuals between the gaugings and the baseline RC, and their uncertainties. (Section 2.2.3).

3. Multiple change point detection applied to the residuals time series (Section 2.2.4) and choice of the optimal number of change points (Section 2.2.5).

4. Shift times adjustment (Section 2.2.6).

5. "Top-down" recursion: re-apply steps 1-4 to each period until no more changes are detected (Section 2.2.7).

2.2.2 Estimation of the baseline rating curve

The first step of the proposed method is to estimate the baseline RC and its uncertainty using all gaugings. Since one of the basic objectives of this paper is to account for both gaugings and RC uncertainties, it is necessary to select an RC estimation method that provides quantitative uncertainties (see Kiang et al. [2018] for a review of such methods). In this paper the BaRatin method [Le Coz et al., 2014] is used for convenience. We refer to the aforementioned paper for a more detailed description and we stress that any other method could be used, as long as it provides the uncertainty around the RC.

2.2.3 Computation of residuals and their uncertainty

The residuals between the gaugings and the RC are defined as follows:
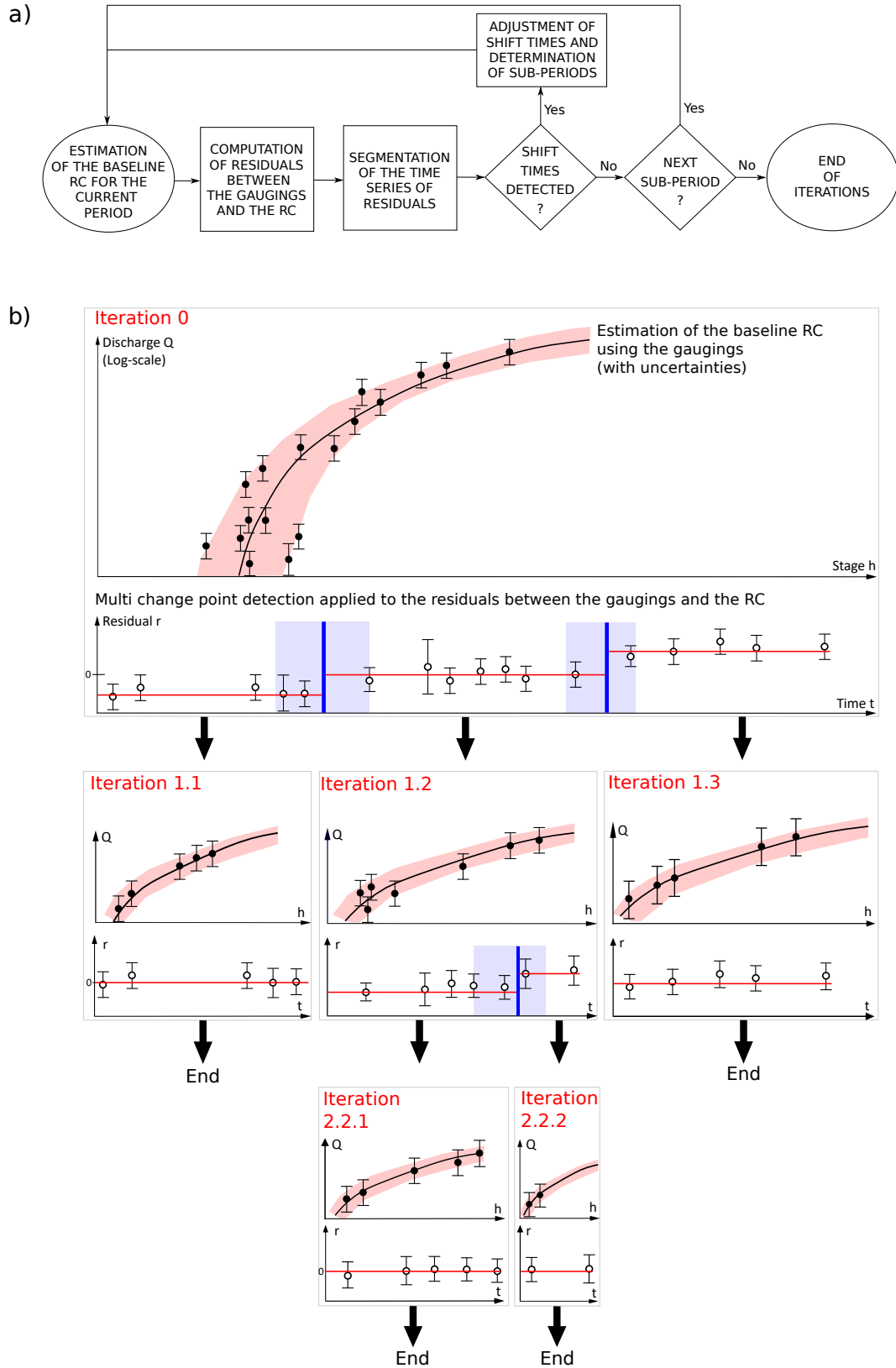
Figure 2.2: *a) Conceptual flowchart of the proposed algorithm. b) Schematic representation of the iterative procedure. Each iteration consists in the succession of Steps 1-4 described in Section 2.2. Colored ribbons and error bars represent 95% uncertainty intervals for RCs (pink), shift times (blue), gaugings (black dots) and residuals (empty dots).*

$$r_i = \widetilde{Q}_i - \widehat{Q}_i \quad i = 1, ..., N \tag{2.1}$$

where $\widetilde{Q}_i$ is the gauged discharge, $\widehat{Q}_i$ is the RC-estimated discharge and N is the number of gaugings. Each residual is affected by two sources of uncertainty. The first one is the measurement uncertainty affecting the observed discharge $\widetilde{Q}_i$, which does not depend on the RC method and should ideally be determined by an uncertainty analysis of the measurement process. Assuming zero-mean Gaussian measurement errors, this uncertainty can be quantified by the standard deviation $u_{\widetilde{Q}_i}$. By contrast, the uncertainty affecting the RC discharge $\widehat{Q}_i$ is obviously dependent on the RC method being used. The BaRatin method used in this paper assumes zero-mean Gaussian RC errors with standard deviation $u_{\widehat{Q}_i} = \gamma_1 + \gamma_2 \widehat{Q}_i$, where γ_1 and γ_2 are estimated as part of the RC estimation process. We reiterate that any other RC method could be used as long as it provides an uncertainty $u_{\widehat{Q}_i}$.

Further assuming that measurement and RC errors are independent, the combined standard uncertainty affecting residuals r_i is equal to:

$$u_{r_i} = \sqrt{u_{\widetilde{Q}_i}^2 + u_{\widehat{Q}_i}^2} \quad i = 1, \ldots, N \tag{2.2}$$

2.2.4 Segmentation model and Bayesian inference

The third step of the proposed method is the mCPD of the time series of residuals $(t_i, r_i)_{i=1...N}$ through the Bayesian estimation of a segmentation model.

2.2.4.1 General segmentation model

Generally speaking, a segmentation model can be viewed as a piece-wise constant model of the form:

$$r_i = \widehat{r}_i + \varepsilon_i \tag{2.3}$$

$$\widehat{r_i} = \begin{cases} \mu_1 & , \ t_1 \leq t_i < \tau_1 \\ \mu_2 & , \ \tau_1 \leq t_i < \tau_2 \\ \vdots & \\ \mu_K & , \ \tau_{K-1} \leq t_i \leq t_N \end{cases} \tag{2.4}$$

In Equation 2.4, K is the known number of segments; it will be selected based on a model-selection procedure described in the following section 2.2.5. The means μ_j of each segment j and the change point τ_j that separate segment j from segment $j+1$ are unknown and are grouped into the vector of inferred parameters $\boldsymbol{\theta} = (\mu_1, ..., \mu_K, \tau_1, ..., \tau_{K-1})$. The treatment of segmentation errors ε_i depends on how these errors are interpreted: it is a key focus of this paper, and two distinct approaches will be presented in the next section. Finally, it is noted that many segmentation models in the literature use the observation index i rather than the time t_i. We favor the latter option because it will allow expressing uncertainties on the change point in terms of time rather than position, which is particularly useful in the RC context where gaugings are performed irregularly.

2.2.4.2 Two approaches for describing segmentation errors

Segmentation errors ε_i are generally assumed to be realisations from a zero-mean Gaussian distribution. The two approaches considered here differ in the way they treat their standard deviation σ_i:

1. Type-1 approach: σ_i is assumed to be unknown but identical for all segmented data, i.e. $\sigma_i = \sigma$

2. Type-2 approach: σ_i is assumed to be known but to vary between segmented data, i.e. $\sigma_i = u_{r_i}$

Type-2 approach is particularly suitable for cases where the segmented data r_i are RC residuals (or more generally, residuals between a model and observations): indeed, Equation 2.2 provides the known standard deviation u_{r_i} to be used in this case. Type-1 approach is

arguably the most standard procedure, since it corresponds to the assumption made in standard regression models with homoscedastic errors. However, it ignores the uncertainty affecting the segmented data, despite the fact that it is known before applying the segmentation procedure.

2.2.4.3 Bayesian estimation

Assuming that segmentation errors ε_i are independent, the likelihood associated with the segmentation model can be written as follows:

$$
\begin{aligned}
\text{Type-1 approach: } & p\left(\boldsymbol{r}|\boldsymbol{\theta},\sigma\right) = \prod_{i=1}^{N} \phi\left(r_i|\widehat{r}_i(\boldsymbol{\theta}),\sigma\right) \\
\text{Type-2 approach: } & p\left(\boldsymbol{r}|\boldsymbol{\theta}\right) = \prod_{i=1}^{N} \phi\left(r_i|\widehat{r}_i(\boldsymbol{\theta}),u_{r_i}\right)
\end{aligned}
\tag{2.5}
$$

where $\phi\left(z|m,s\right)$ is the probability density function (pdf) of a Gaussian distribution with mean m and standard deviation s, evaluated at value z.

Bayesian inference requires specifying the prior distribution of parameters $(\boldsymbol{\theta},\sigma)$. Independent priors are specified for each inferred parameter. By default a uniform prior distribution is specified for each change point, $\tau_j \sim \mathcal{U}(t_1,t_N)$. Note that on top of this prior distribution, change points are also constrained by the relation $\tau_1 < \cdots < \tau_{K-1}$. An order-of-magnitude Gaussian distribution is specified for each segment mean, $\mu_j \sim \mathcal{N}(0,10^m)$; the value of m is case-specific and should reflect the expected order of magnitude of RC residuals, which in turn is specific to the studied catchment.

Bayes' theorem allows combining the information brought by the data through the likelihood with the prior information on the inferred parameters into a posterior distribution of the parameters, whose pdf is defined by:

$$
\begin{aligned}
\text{Type-1 approach: } & p\left(\boldsymbol{\theta},\sigma|\boldsymbol{r}\right) \propto p\left(\boldsymbol{r}|\boldsymbol{\theta},\sigma\right)p\left(\boldsymbol{\theta},\sigma\right) \\
\text{Type-2 approach: } & p\left(\boldsymbol{\theta}|\boldsymbol{r}\right) \propto p\left(\boldsymbol{r}|\boldsymbol{\theta}\right)p\left(\boldsymbol{\theta}\right)
\end{aligned}
\tag{2.6}
$$

A MCMC approach based on a multi-block Metropolis algorithm is used to explore this

multidimensional posterior distribution. The variance of each parameter jump distribution is also adapted during iterations in order to reach an user-defined acceptance rate. The implemented algorithm is detailed in Renard et al. [2006]. By default the first half of the simulations is ignored ("burned") and only the second half of simulated values is used for inference. MCMC convergence is assessed by visually inspecting trace plots and density plots (except in the synthetic case studies of Section 2.4 where this is not feasible given the large number of replications). In addition, the Potential Scale Reduction Factor Brooks and Gelman [1998] is computed for each parameter, verifying that it is smaller than 1.2.

Finally, to avoid short segments containing no observations, which may lead to an ill-posed inference, additional constraints can be enforced: a minimum number of points $N_{min} \geq 1$ for each segment and a minimum duration $d_{min} \geq 0$ between two consecutive change points. These constraints are case-specific and user-defined.

2.2.5 Choice of the optimal number of segments

The number of segments K is selected by minimizing the Deviance Information Criterion (DIC, Spiegelhalter et al. [2002]), in the formulation suggested by Pooley and Marion [2018]. The DIC is selected because it is adapted to the Bayesian estimation described in Section 2.2.4.3. We note that a maximum-likelihood estimation could also be used and possibly favored by some users. In this case, the DIC should be replaced by an alternative model-selection criterion such as the Akaike Information Criterion (AIC, Akaike [1974]), the Bayesian Information Criterion (BIC, Schwarz [1978]), or the Hannan-Quinn information Criterion (HQC, Hannan and Quinn [1979]).

Let $\boldsymbol{\Theta}$ denote the vector of all inferred parameters, i.e. $\boldsymbol{\Theta} = (\boldsymbol{\theta}, \sigma)$ for the type-1 approach ($N_{par} = 2K$) and $\boldsymbol{\Theta} = \boldsymbol{\theta}$ for the type-2 approach ($N_{par} = 2K - 1$). Moreover, let $D(\boldsymbol{\Theta})$ denote the deviance defined as $D(\boldsymbol{\Theta}) = -2 \ln(p(\boldsymbol{r}|\boldsymbol{\Theta}))$. The four criteria discussed above are computed as follows:

$$AIC = D(\widehat{\boldsymbol{\Theta}}) + 2N_{par}$$

$$HQC = D(\widehat{\boldsymbol{\Theta}}) + 2N_{par} \ln(\ln(N))$$

$$BIC = D(\widehat{\boldsymbol{\Theta}}) + N_{par} \ln(N)$$

$$DIC = \mathrm{E}\left[D(\boldsymbol{\Theta})\right] + \frac{1}{2}\mathrm{Var}\left[D(\boldsymbol{\Theta})\right]$$

(2.7)

In the first three criteria, $\widehat{\boldsymbol{\Theta}}$ is the maximum-likelihood parameter estimate. In the fourth criterion DIC, $\mathrm{E}\left[.\right]$ and $\mathrm{Var}\left[.\right]$ represent the posterior mean and variance, and the corresponding quantities can easily be computed using MCMC samples.

2.2.6 Adjustment of shift times

Bayesian estimation results provide the marginal posterior distribution of each inferred parameter. Rating shift times $\boldsymbol{s} = (s_1, \ldots, s_{K-1})$ can be obtained from the posterior distributions of parameters $\boldsymbol{\tau}$.

As illustrated in Figure 2.3, each posterior distribution provides a point estimate $\widehat{\tau}_j$ and a credibility interval CI_j. Typically, $\widehat{\tau}_j$ is the Maximum A Posteriori (MAP) estimate maximizing the posterior density. The interval CI_j can be explored to find a physically-justified shift time. The following three options can be considered for instance:

1. $s_j = \widehat{\tau}_j$ can be used as a default option.

2. If the stage record is available, s_j can be set to the time of the largest stage value within CI_j (cf. Figure 2.3), reasoning that a large flood is a likely cause of the shift.

3. s_j can also be set manually within CI_j using any other information on possible causes of the shift (e.g., gravel mining operations, beavers/swimmers dams, works in the river bed, earthquake).
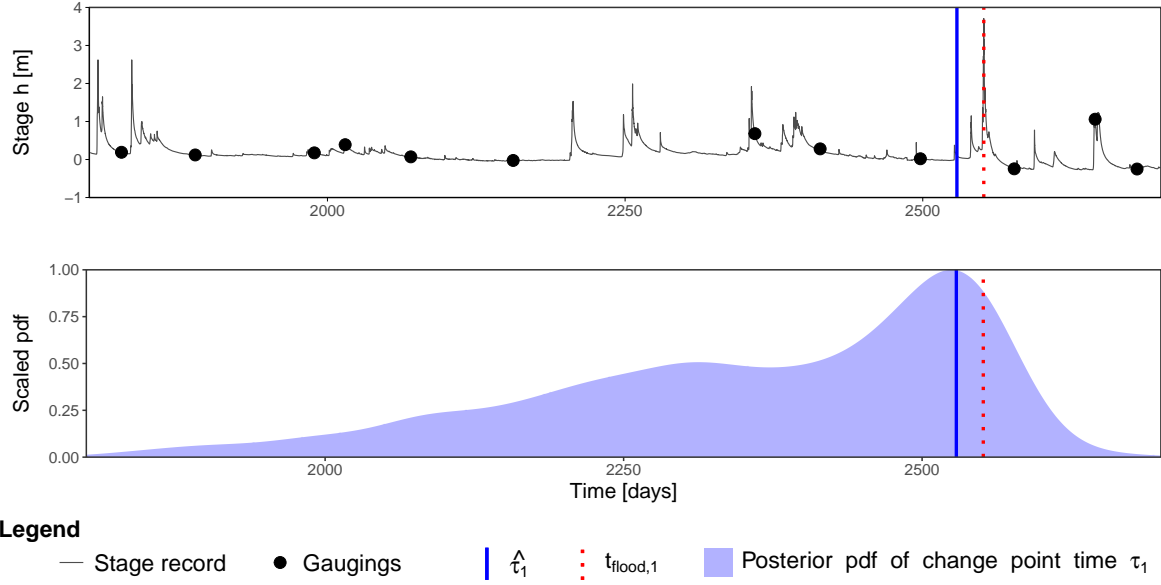
Figure 2.3: Example of shift time adjustment options. Instead of setting the shift time to the MAP estimate $\widehat{\tau}_1$, a better option may be to choose the time of the maximum stage $t_{flood,1}$ within CI_1.

2.2.7 Recursive segmentation

Once a first set of shift times has been identified, a recursive "top-down" procedure is performed (Figure 2.2). The segmentation procedure described in the previous sections (2.2.2 to 2.2.6) is recursively performed within each sub-period. At each iteration only the gaugings of the current sub-period are considered. The iterations stop when within all periods no more shift times are detected.

It may happen that at some iteration of the recursive segmentation only few gaugings are available. This may lead to challenging RC estimation and, if the BaRatin method is used, to challenging quantification of $u_{\widehat{Q}_i}$. When moving from one period to its sub-period, a better fit and hence a smaller standard deviation $u_{\widehat{Q}_i}$ is expected; thus a prior uniform distribution between zero and the posterior mean of the parent period is specified for $u_{\widehat{Q}_i}$.

2.3 Application to a real case study: the Ardèche River at Meyras, France

2.3.1 Presentation of the station

The Ardèche River at Meyras station is located in Mediterranean France, with a catchment area of 98 km². This station is characterized by a gravel bed degrading during each important flood. It has been already studied by Le Coz et al. [2014], Sikorska and Renard [2017] and Mansanarez et al. [2019]. They all proposed a three-control hydraulic configuration: a section control governed by a natural riffle for low flows, a main channel control for medium flows and one floodway channel control added to the main channel for very high flows. The stage record is available for the period between 07/11/2001 and 29/10/2018. Gaugings and comments about shift times have been provided by the hydrometric Service in charge of the station (UHPC Grand Delta).

2.3.2 Segmentation strategies

Several segmentation strategies are used in order to compare "single-pass" vs. recursive procedures and type-1 vs. type-2 treatment of segmentation errors:

A "Single-pass" mCPD method from the literature. The R function *cpt.mean* of the *changepoint* package Killick and Eckley [2014] is used with the following options: (i) maximum number of segments $K = 30$; (ii) change in the mean only; (iii) Binary Segmentation method Scott and Knott [1974]; (iv) Normal statistic test; (v) BIC selection of K; (vi) minimum number of data in a segment $N_{min} = 1$. Note that in this method, the segmentation model of Equation 2.4 is expressed in terms of observation index i rather than time t_i, and does not provide uncertainty on the change point. Consequently, each change point τ_k is assumed to be uniformly distributed between times t_{i_k} (the time associated with the $k - th$ detected change point) and t_{i_k-1}. The shift times are then adjusted (Section 2.2.6) on the largest stage value within this interval.

B "Single-pass" mCPD method proposed in this paper with a type-1 treatment of

segmentation errors (i.e., unknown but constant uncertainty). The following options are chosen: (i) maximum number of segments $K = 30$; (ii) DIC selection of K; (iii) minimum number of data in a segment $N_{min} = 1$; (iv) minimum duration of a segment $d_{min} = 0$ days. This approach is very similar to the previous Strategy A, except that the segmentation model of Equation 2.4 is expressed in terms of time t_i. Shift time adjustment is therefore applied by looking for the largest flood in the 95% credibility interval of the change point, as described in Section 2.2.6.

C Recursive mCPD method proposed in this paper with a type-1 treatment of segmentation errors (i.e., unknown but constant uncertainty). The maximum number of segments is now set to 5 because by using a recursive procedure, there is no requirement to find all changes during the first pass. All other options are identical to approach B.

D Recursive mCPD method proposed in this paper with a type-2 treatment of segmentation errors (i.e., known residuals uncertainties). All options are identical to approach C.

2.3.3 Results with Strategy D

Figure 2.4 shows the results of some significant steps of Strategy D. The structure and the enumeration of the iterations are schematised in Subfigure 2.4a. Seven shift times are detected in thirteen iterations. Panels (2.4b-2.4d) zoom to the intermediate results of iterations 0, 1.2, 1.3.

For each iteration Figure 2.4b shows the RC estimated using gaugings from the current period. At iteration 0 the baseline RC has a large uncertainty, confirming the presence of multiple stage-discharge relations for this data set. This uncertainty decreases in subsequent iterations, reflecting the fact that the RC is estimated using more homogeneous gaugings.

Figure 2.4c shows the evolution of four criteria (AIC, BIC, HQC and DIC) for the choice of the optimal segmentation (see Section 2.2.5). A similar behavior is observed between BIC, DIC and HQC, in particular between BIC and DIC. On the contrary AIC tends to favor a higher number of periods for the iterations shown in the figure and for other iterations (not shown).

Figure 2.4d shows the segmented residuals. These three iterations illustrate the added value
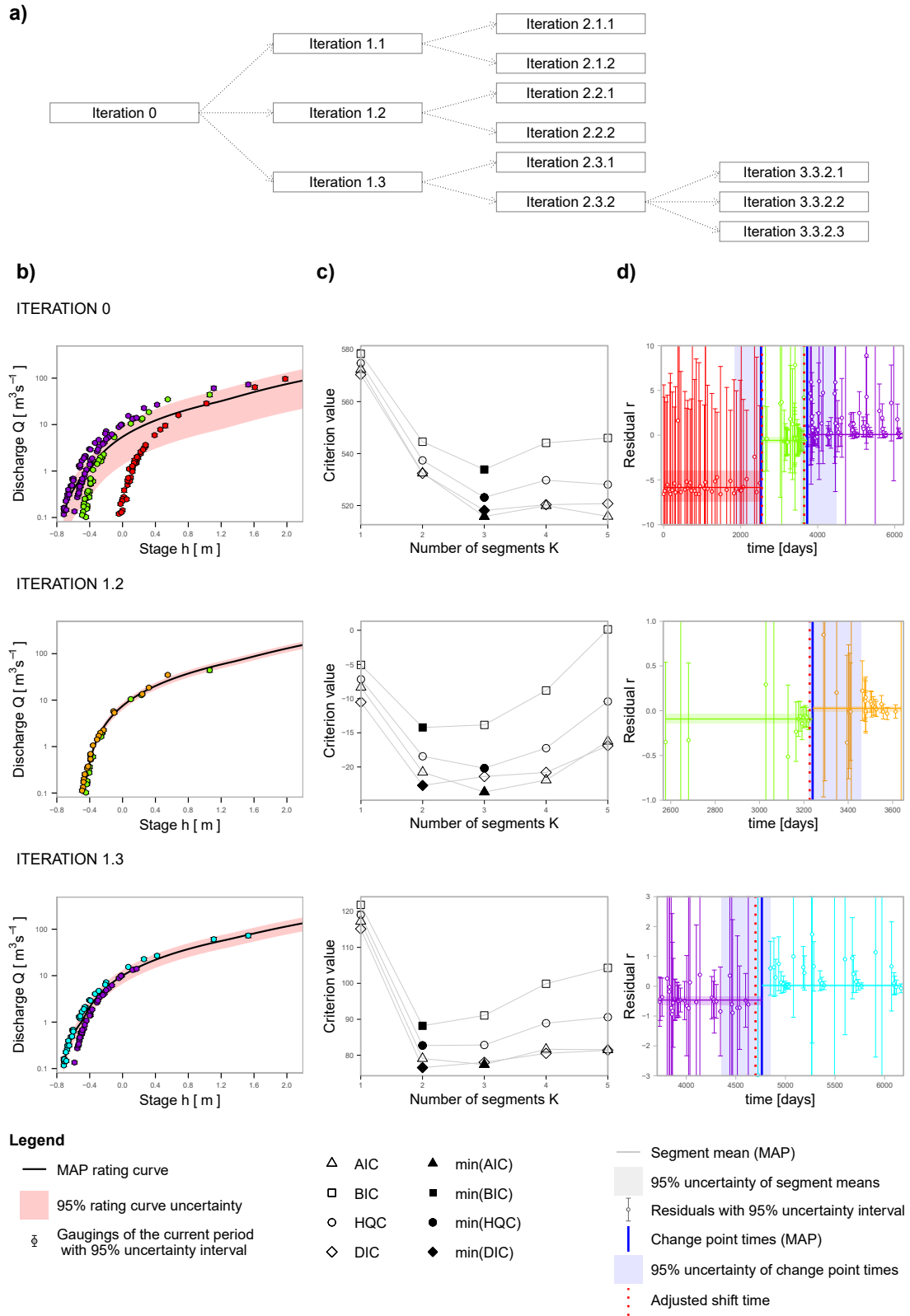
Figure 2.4: Strategy D applied to the gaugings of the Ardèche River at Meyras. Subfigure (a): structure of the recursion. Subfigures (b): baseline RC using the gaugings of the current period. Subfigures (c): evolution of four criteria for the selection the optimal segmentation applied to the residuals. Subfigures (d): results of the segmentation considering the lowest DIC.

of the "top-down" recursion: the large RC uncertainty at iteration 0 leads to the detection of two major shifts only; then iterations 1.2 and 1.3 lead to the detection of other minor shifts based on refined RCs. Iteration 1.3 also illustrates that, because of the uncertainty in the estimated change point location, the adjusted shift time (based on flood occurrence) may be far from the optimal time identified using gaugings only.

Finally, by the last iterations, segmentation errors (ε_i in Equation 2.3) do not generally exhibit any significant autocorrelation (not shown).

2.3.4   Comparison of Strategies A-D

The results of the four strategies are then summarized in Figure 2.5 in terms of detected shift times against the stage record. The official dates of RC updates are provided by the hydrometric Service SPC Grand Delta and are confirmed by the analysis proposed by Mansanarez et al. [2019]. Only Strategy D shows results similar to the official segmentation. However the official dates cannot be considered as a "truth" against which the performance of competing methods can be judged. Comparing the results of Strategies A-B-C-D may still be insightful.

The first striking observation is that the four Strategies lead to markedly different segmentations, in particular between Strategy D and Strategies A, B, C.

While both Strategies C and D are recursive, they lead to very different numbers of shifts (42 detected in 56 iterations vs. 7 detected in 13 iterations). This indicates that the treatment of segmentation errors (type-1 vs. type 2) is of prime importance.

Strategies A and B are both non-recursive, and differ in the following two aspects: Strategy A is index-based while B is time-based; they use a different criterion for selecting the number of shifts. Both strategies lead to very similar results in terms of number of shifts (27 vs. 29) and their location. The slight differences may be due to the stronger penalty term of the BIC or to Binary Segmentation issues as illustrated in Figure 2.1a-b.

Strategies A, B and C lead to many more change points than Strategy D. During the first
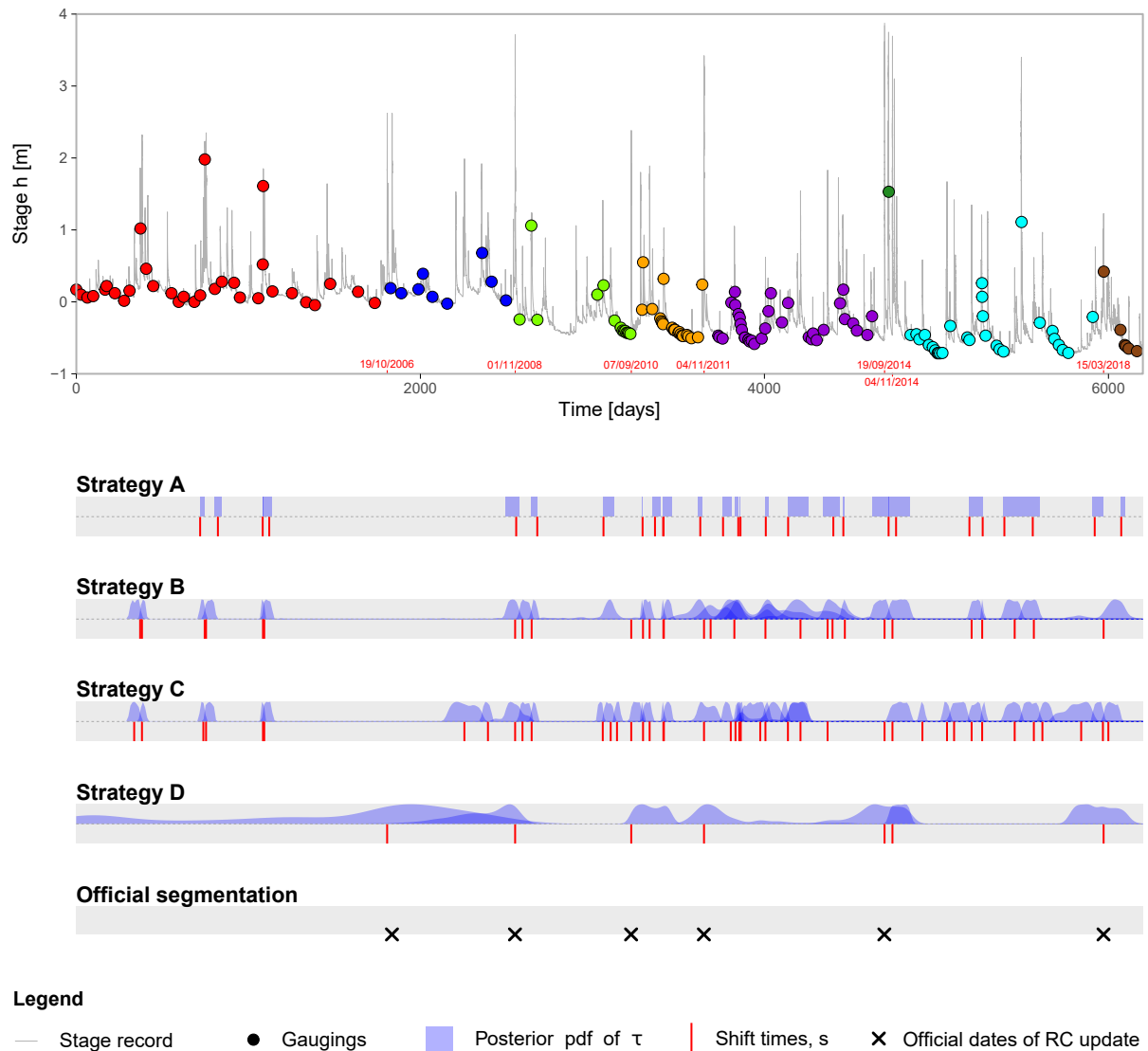
Figure 2.5: *Results of the segmentation procedure applied to gaugings of the Ardèche River at Meyras, France. Gaugings are plotted against the stage record with a different color for each period of RC stability identified by Strategy D. For each strategy, results are presented as posterior pdf of τ_j (blue ribbons) and adjusted shift times s_j (red segments).*

period (red gaugings) the detected shifts correspond to the largest gaugings. This might suggest that the shifts result from the much larger uncertainty affecting these residuals (which cannot be accommodated with the constant-sigma type-1 approach), rather than from a genuine change in the underlying RC. This evidences the problem illustrated in Figure 2.1c-d.

However the objective choice of the most efficient segmentation strategy is challenging without knowing the true shift times. In the next section, the model selection criteria and the segmentation strategies are compared based on synthetic data with known shift times and magnitudes, thus enabling a more objective evaluation of their performance.

2.4 Performance evaluation from simulated rating shifts

2.4.1 Generation of synthetic data

The generation of synthetic gauging data is based on the following steps (the corresponding R code is also provided as online material):

1. Select the length of the studied period $[0; T]$ (in years).

2. Shift times: generate inter-shift durations from an exponential distribution with rate λ_s (e.g. $\lambda_s = 1/5$ corresponds to 1 shift every 5 years on average); shift times are then derived as the cumulative sum of the inter-shift durations. The generation stops when the shift time exceeds T, leading to N_s shifts.

3. Shift magnitudes: it is assumed that RC shifts only affect the offset of the lower control (i.e. the b in equation $Q = a(h - b)^c$). Each shift magnitude $\delta b^{(i)}$ is generated from a Gaussian distribution with mean 0 and standard deviation σ_b. If there exists at least one shift, for each stable period j ($j \geq 2$), the offset parameter $b^{(j)}$ is hence equal to $b^{(j)} = b^{(1)} + \sum_{i=2}^{j} \delta b^{(i)}$.

4. Gauging times: use the same approach as for shift times, using a rate λ_g leading to N_g gaugings.

5. Gauging true discharge: for each gauging, the true discharge Q_i is generated by first sampling a non-exceedance probability p between 0 and 1, then transforming it into discharge using the quantile function of a LogNormal $\mathcal{LN}(\ln(50), 0.5)$ distribution. Probability p is sampled from a beta distribution $\mathcal{B}(0.1, 0.9)$ which is strongly skewed toward zero, mimicking the typical situation where gaugings are mostly performed during low flows.

6. Gauged stage: for each gauging, the stage h_i is computed by applying the inverse RC function to the true discharge Q_i.

7. Gauged discharge: for each gauging, the gauged discharge is obtained by adding a measurement error ξ_i to the true discharge Q_i. ξ_i is sampled from a Gaussian distribution with mean 0 and standard deviation $\rho_i \times Q_i$.

Table 2.1: Classes of simulation for the performance evaluation.

Class	Frequency of gaugings λ_g (year^{-1})	Frequency of shifts λ_s (year^{-1})	Mean number of gaugings/period λ_g/λ_s	Shift st.dev. σ_b (m)	Gauging error		Number of controls N_c
					Low flows $\rho_{LF}(\%)$	High flows $\rho_{HF}(\%)$	
1	2	1/5	10	0.5	2.5	5	1
2	4	1/5	20	0.5	2.5	5	1
3	7	1/5	35	0.5	2.5	5	1
4	10	1/5	50	0.1	2.5	5	1
5	10	1/5	50	0.3	2.5	5	1
6	10	1	10	0.5	2.5	5	1
7	10	1/2	20	0.5	2.5	5	1
8	10	1/5	50	0.5	2.5	5	1
9	10	1/5	50	0.5	10	15	1
10	10	1/5	50	0.5	2.5	5	3

2.4.2   Design of experiments

In order to assess how the properties of the data set impact the performances of the segmentation approaches, several classes of simulation are defined as described in Table 2.1. Each class is characterised by fixed values of the parameters described in Section 2.4.1. Comparing these classes allows assessing the impact of the following Properties:

- P1: number of hydraulic controls N_c (classes 8 and 10).

- P2: mean number of gaugings per period, which is equal to the ratio between the gaugings frequency λ_g and the shifts frequency λ_s (classes 1, 6, 2, 7, 3, 8), as suggested by Ibbitt and Pearson [1987].

- P3: uncertainty in gauged discharges as controlled by ρ_{LF} and ρ_{HF} (classes 8 and 9).

- P4: shift magnitude as controlled by σ_b (classes 4, 5 and 8).

For each class, 10 replications are generated, for a total of 100 simulations (some data sets are reported in Figure 2.6). To minimize computational cost all data sets are generated with a maximum number of 150 gaugings and a maximum number of 15 true shift times within a
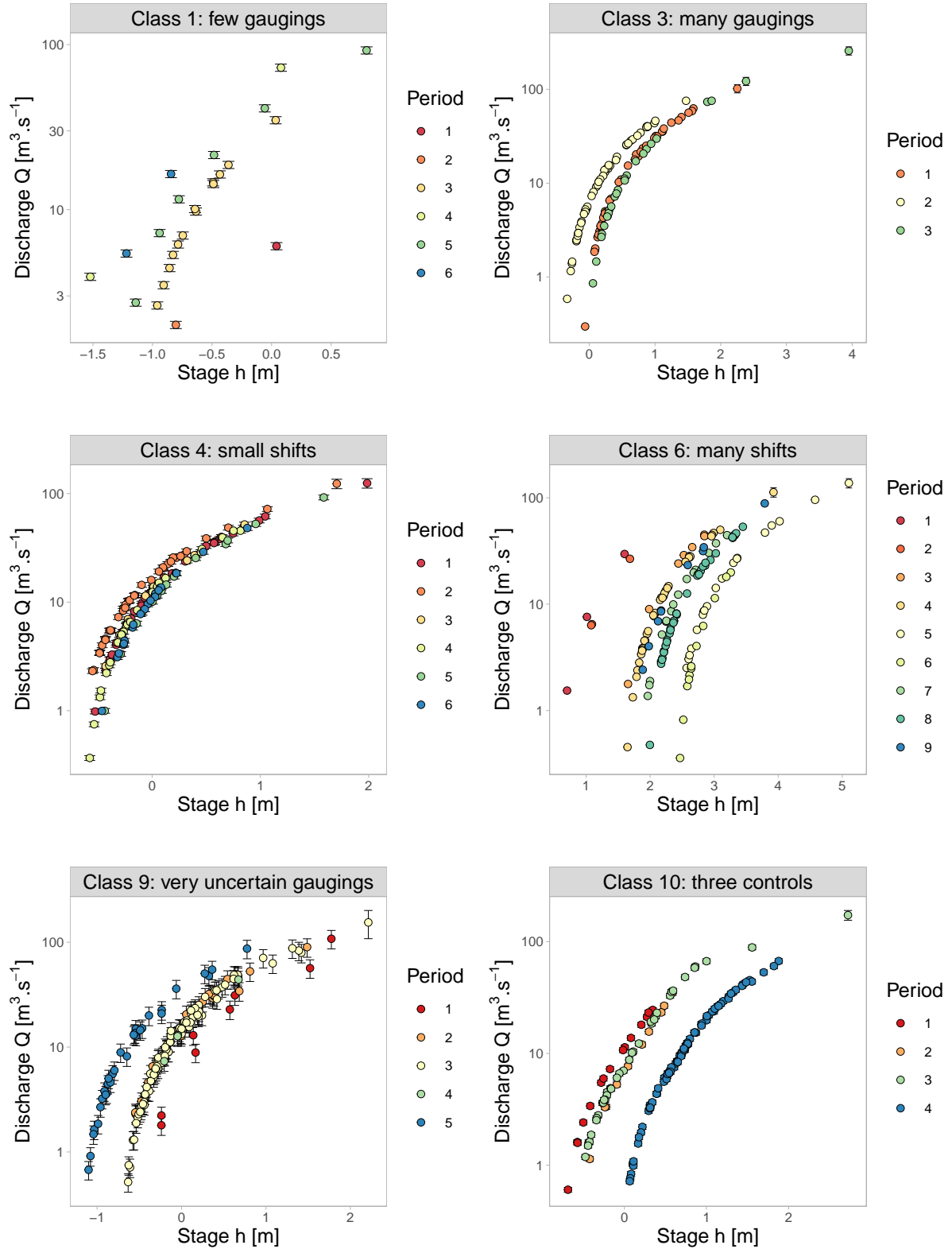
Figure 2.6: *Examples of synthetic data sets characterised by known rating shift times using parameters of Classes 1-3-4-6-9-10 defined in Table 2.1.*

period of 15 years. As an order of magnitude, the CPU time to apply approach C to one data set with 54 gaugings is around 50 minutes. This is to be multiplied by the number of data sets (100) times the number of approaches (4) or the number of criteria (4), which amounts to several days of effective running time.

The first experiment aims at comparing criteria AIC, BIC, DIC and HQC (see Section 2.2.5). To this aim, Strategy D is applied to all classes above.

The second experiment aims at comparing Strategies A, B, C and D. To this aim, all four Strategies are applied to the same 100 data sets of the first experiment. The stage record is not available for synthetic data sets, thus in Strategies B-C-D, the shift times are taken as the estimated parameters $\hat{\tau}_j$ (i.e., option 1 in Section 2.2.6). Since Strategy A provides the estimated change point as an observation index k (rather than a time), the shift time is taken as the middle of the interval $[t_{k-1}; t_k]$.

2.4.3 Metrics for performance evaluation

The performance evaluation uses some of the metrics proposed by Aminikhanghahi and Cook [2017]. At the end of the segmentation procedure each gauging is classified into one of TP, FN, FP, TN (see example in Figure 2.7), where:

- A gauging is classified TP (true positive) if it is the nearest neighbor of a true shift and this true shift is within the 95 % CI of an estimated shift.

- A gauging is classified FN (false negative) if it is the nearest neighbor of a true shift but this true shift is outside all 95 % CI of estimated shifts.

- A gauging is classified FP (false positive) if it is the nearest neighbor of an estimated shift but the 95 % CI of this estimated shift does not contain any true shift.

- Otherwise a gauging is classified TN (true negative).

- $N_g = n_{TP} + n_{FN} + n_{FP} + n_{TN}$
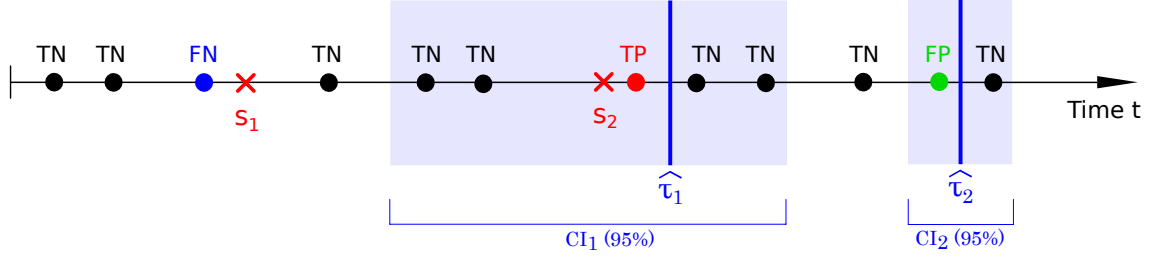
Figure 2.7: Schematic example of the gaugings classification into true positive (TP), false negative (FN), true negative (TN), false positive (FP) for the performance evaluation of the segmentation results. s_i represent the known shift times, while $\hat{\tau}_i$ are the change point estimates.

The Accuracy A is defined as the rate of correctly classified gaugings:

$$A = \frac{n_{TP} + n_{TN}}{N_g} \tag{2.8}$$

The Sensitivity S is maximal when no shift has been missed; low values hence correspond to under-segmentation:

$$S = \frac{n_{TP}}{n_{TP} + n_{FN}} \tag{2.9}$$

The Precision P is maximal when all detected shifts are real; low values hence correspond to over-segmentation:

$$P = \frac{n_{TP}}{n_{TP} + n_{FP}} \tag{2.10}$$

The $RMSE$ between the times of correctly-detected shifts s_i^{TP} and the times of corresponding true shifts $s_{k_i}^{true}$ is also computed:

$$RMSE = \sqrt{\sum_{i=1}^{n_{TP}} \frac{(s_i^{TP} - s_{k_i}^{true})^2}{n_{TP}}} \tag{2.11}$$

2.4.4   Results of the experiments

2.4.4.1   Comparison of criteria for choosing the number of change points

Figure 2.8 summarizes the results of the first experiment. Results reveal that:

- BIC and DIC on the one hand and AIC and HQC on the other hand lead to similar performance metrics.
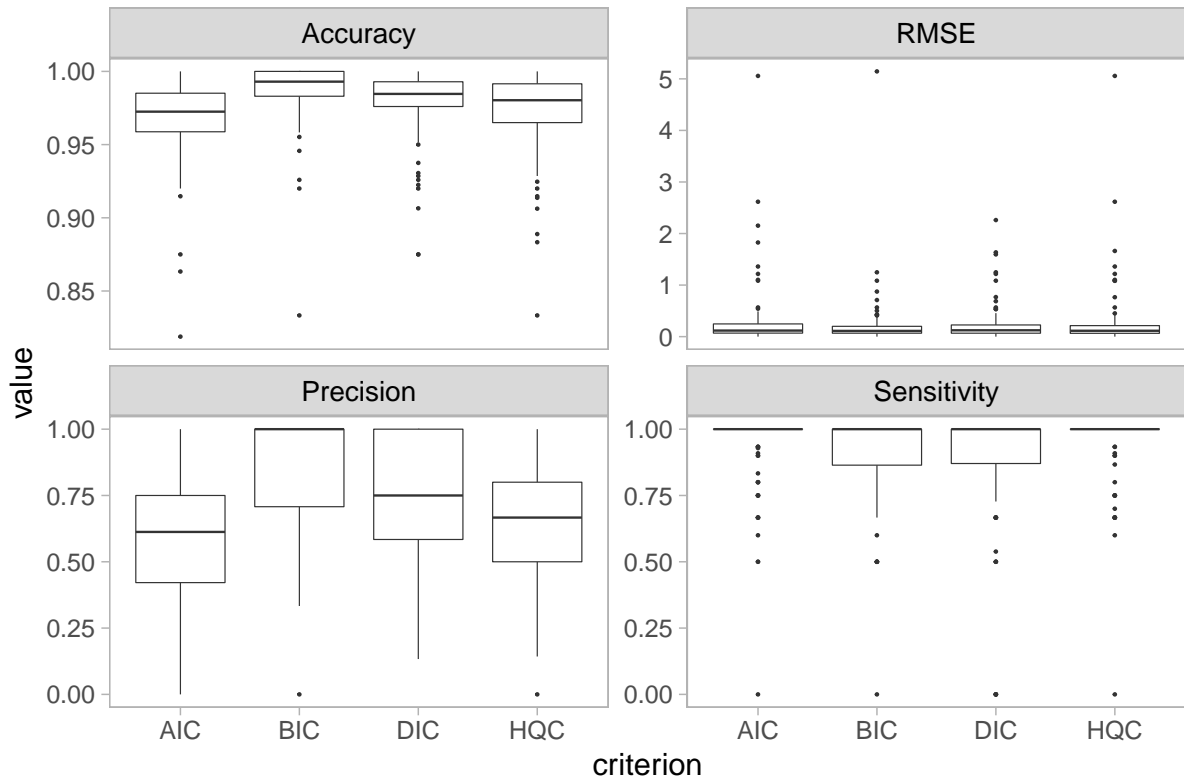
Figure 2.8: Results of the first experiment with Strategy D, comparing four criteria for the optimal choice of K and using all 100 simulated data sets.

- BIC has the highest Accuracy/Precision, closely followed by DIC, while AIC and HQC have the lowest. The same ranking holds for most simulation classes (not shown). AIC and HQC lead to a higher degree of over-segmentation with, on average, 125 % and 67 %, respectively, more detected shift times than there really are. On the contrary BIC and DIC over-estimate the number of shifts by only 13% and 40%, respectively.

- BIC and DIC sometimes miss a few shifts leading to lower values of Sensitivity than AIC and HQC.

These results indicate that AIC and HQC have a marked tendency to over-segmentation and should therefore be avoided. BIC and DIC have similar performances, and it is therefore sensible to select the one that is conceptually more adapted to the chosen inference paradigm. More specifically, BIC is solely based on the likelihood and is hence more adapted to maximum-likelihood estimation (despite what its name confusingly suggests). By contrast, DIC makes use of the whole posterior distribution and should therefore be favored in a Bayesian context such as the one adopted in this paper.

2.4.4.2 Comparison of segmentation strategies

Figure 2.9 summarizes the results of the second experiment. Strategies A, B, C, D are compared considering all simulations.

Strategy D is quite markedly the best-performing approach in terms of Accuracy, Precision and $RMSE$. On the contrary Strategy A is quite markedly the worst one, due to a strong tendency to over-detection. Its good Sensitivity means that it does not miss many changes, but this comes at the cost of detecting too many spurious ones.

Strategies C and D are both recursive procedures and both yield better results in terms of Accuracy, Precision and RMSE compared with the "single-pass" Strategies A and B, demonstrating the added value of the recursive approach. However Strategy D yields better results than Strategy C in terms of all metrics, emphasizing the added value of type-2 errors treatment.
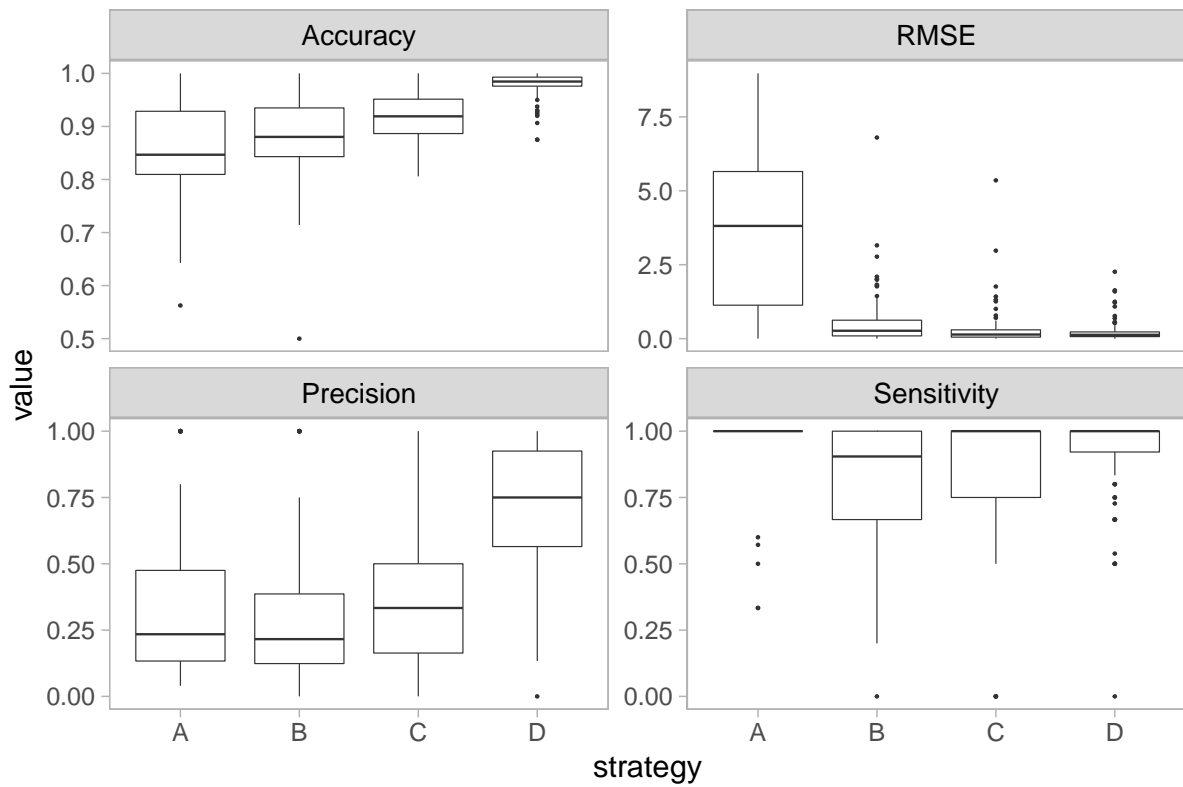
Figure 2.9: Results of the second experiment: comparison between the four strategies for the segmentation of residuals.

Finally, Strategies A and B are conceptually similar but, surprisingly, yield quite different results. Strategy B yields better results in terms of Accuracy and RMSE. In particular, the lower RMSE may be due to the added value of expressing change points in terms of time rather than position.

2.4.4.3 Factors influencing the method performance

Figure 2.10 focuses on the results of Strategy D and evaluates its performance for data sets with varied properties as described in Section 2.4.2.

The main factor affecting the performance of the segmentation is the mean number of gaugings per period. As expected, performance increases with this number, especially in terms of Accuracy and RMSE. Results suggest that 20 gaugings per period are sufficient to achieve a good-quality segmentation. For higher values the Accuracy seems to stabilize, while the RMSE continues decreasing, mainly because of the smaller inter-gauging interval. Performance markedly deteriorates with only 10 gaugings per period. This confirms that shifty curves require a high frequency of gaugings. Sensitivity sharply increases when moving from 10 to 20/35 gaugings per period. Then, for 50 gaugings per period, few particular realizations have Sensitivity=0 (since characterized by only one single small change which unfortunately has been missed). Instead, Precision is weakly influenced by the number of gaugings per period. However, with an average of 10 gaugings per period the segmentation detects some false shifts and Precision slightly decreases.

Other factors have a lower impact on performance. Different hydraulic configurations slightly influence the performance of the segmentation. More complex rating curves (with multiple controls) lead to a slight decrease in Accuracy and Precision and a slightly better Sensitivity. Surprisingly, increasing the gaugings uncertainty does not markedly impact performance. It leads to slightly lower but still very high values of Accuracy. It also leads to slightly lower Precision, and, surprisingly, to higher Sensitivity. The RMSE values remain very similar. Finally, increasing the shift magnitude does not markedly influence the performance. However, few simulations characterised by very small shifts show lower Accuracy.
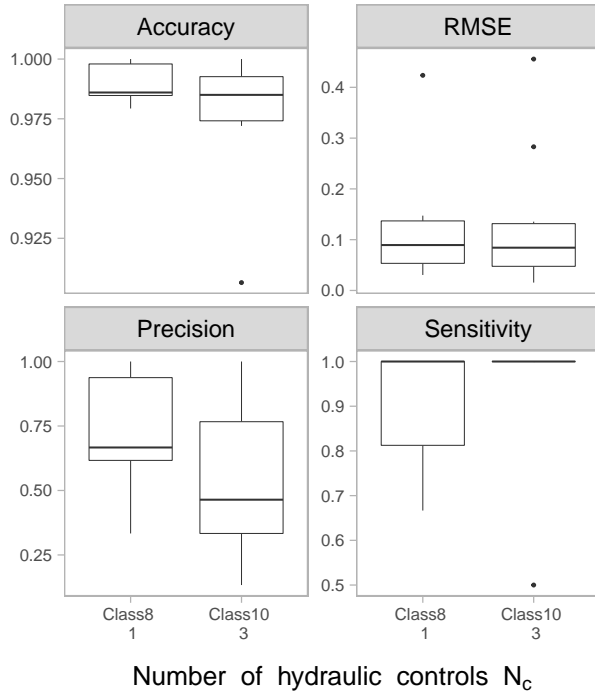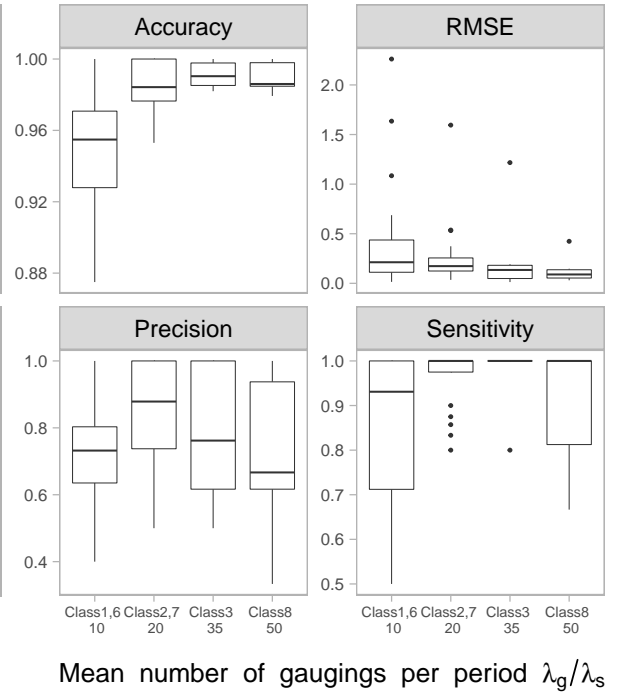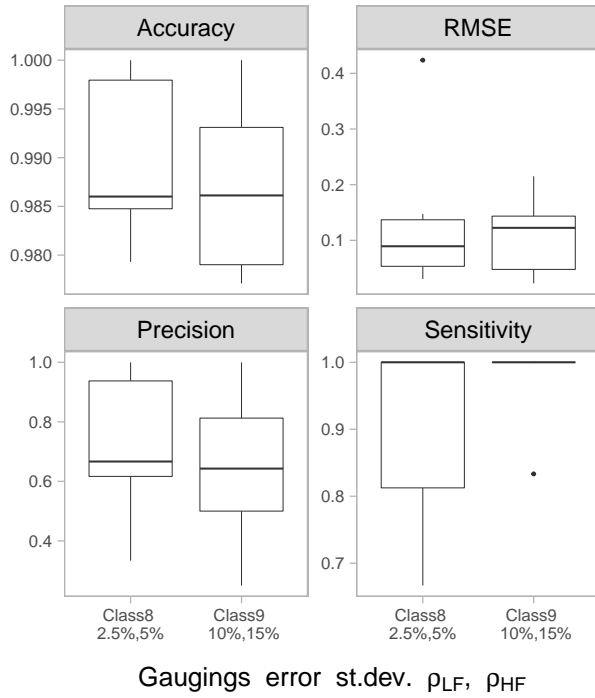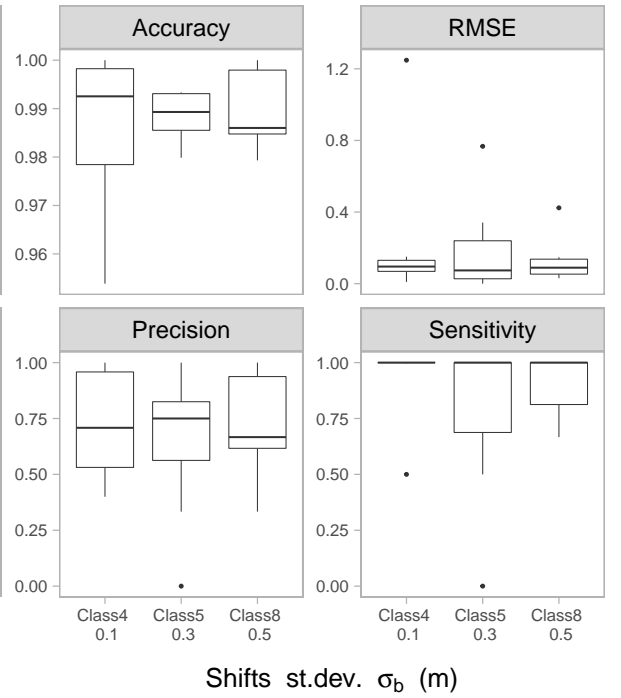
Figure 2.10: Results of the second experiment: impact of the four properties P1 to P4 on the performance metrics (Strategy D).

2.5 Discussion

2.5.1 Contributions to the operational practice and the scientific literature

The proposed method represents a more formal way to detect rating shifts using gaugings, compared to empirical rules commonly used in the operational practice [WMO, 2010]. A similar formalization objective was pursued by Morlot et al. [2014] who applied the Hubert segmentation method [Hubert et al., 1989] for segmenting the residuals between the gaugings and a baseline RC. Their method yielded satisfying results, even though it neglected the residuals' uncertainties. However, the synthetic simulations and the real case study proposed in this paper suggest that neglecting residuals' uncertainties may lead to over-segmentation.

The proposed method differs from the mCPD literature in its handling of shift times in two aspects: considering time rather than position and providing shift time uncertainty. Existing performance evaluation metrics proposed in the literature [Aminikhanghahi and Cook, 2017] were also adapted to account for shift times uncertainty while comparing the true shift times and the detected ones.

In addition to the segmentation procedure, this paper proposes a protocol for the generation of synthetic data sets of gaugings and shift times. This protocol is very useful to evaluate the performance of the segmentation method.

The case studies proposed in this paper indicate that the mean number of gaugings per period remarkably affects the performance of the segmentation: this is consistent with the observation of Ibbitt and Pearson [1987]. It is therefore important to consider this indicator when planning gauging campaigns or deriving gauging strategies. According to the simulations, the availability of 20 gaugings per period on average leads to an acceptable identification of rating shifts. On the contrary, less than 10 gaugings per period may lead to a poor segmentation. However, these numbers should be considered as rough orders of magnitudes rather than precise figures since not all existing hydraulic configurations, shift magnitudes and gaugings uncertainties have been

tested.

2.5.2 Current limitations

The method proposed in this paper is built on the main assumption that changes correspond to sudden shifts (as opposed to slower transient changes), which may be inadequate for phenomena such as vegetation growth and decay. The segmentation model proposed here is not designed to analyse a trend in the residuals. Dynamic approaches such as those discussed in the introduction Section 2.1.2 should instead be favored.

The case studies have illustrated the added value of expressing change points in terms of time (rather than position) and of adjusting the shift time by looking for some causative events within the uncertainty bound of the estimated change point, as described in Section 2.2.6. Nevertheless, this adjustment must be done with precaution. Determining the cause of a shift is a complex decision since several potential processes might be suspected (e.g., flood, gravel mining). This necessarily comes with a degree of expertise and subjectivity. For instance, how to separate the sudden shift created by a morphogenic flood from apparent shifts induced by transient phenomena such as vegetation, backwater, etc.? How to choose when a single shift may be attributed to several floods? Introducing some degree of expertise and subjectivity is not problematic in our opinion. It may even well improve an otherwise fully automated procedure.

2.5.3 Avenues for future work

The method proposed in this paper can, in principle, be used with any RC method that provides RC uncertainty. Results from various RC methods could be compared in future work to assess the extent to which the detected changes are robust with respect to the RC method.

The method is also based on the analysis of residuals computed with respect to discharge. They may be computed with respect to stage too, as suggested by Morlot et al. [2014]. It would therefore be of interest to modify the method to enable the use of stage residuals, and to evaluate whether it has an important impact on the detected changes. We note however that the treatment of stage residuals, and in particular of their uncertainty, is not straightforward.

This is because the equivalent of Equation 2.2 for stage is not immediately available and may require some additional error propagation.

More work could also be carried out to refine operational gauging strategies in the presence of shifty RCs. Many factors may affect the efficiency of the rating shift detection, in particular, the number of gaugings, their uncertainty and their location along the RC. A single gauging may be sufficient if it is precise and far away from the base RC. But in the case of minor shifts or very uncertain gaugings several gaugings may be required. Notice also that the gaugings for Meyras station (Section 2.3) have been performed for mostly all flow conditions. This leads to the estimation of relatively precise RCs. More uncertain RCs are likely to require more gaugings to detect a shift of a given magnitude.

The case studies have also evidenced that, among the proposed criteria for the choice of the optimal number of segments, the BIC and the DIC obtained the highest performance. However the segmentation appears sensitive to these criteria. Future work includes a more exhaustive comparison, as discussed by Buckland et al. [1997] and Burnham and Anderson [2004], by analysing the weight of each penalty term related to data fit and number of parameters.

The proposed method is also inherently limited by gaugings availability - no change can be detected in their absence. However, we stress that gaugings are not the only information available at hydrometric stations. The proposed tool may be complemented with other sources of information such as the stage record (e.g., by detecting a change in recession shapes or by deriving sediment transport estimates), other independent hydrologic data (e.g., correlation analysis with neighboring stations or with the output of a rainfall-runoff model) and direct observations (e.g., bathymetric surveys).

Finally, as a general perspective, the proposed method could probably be extended to other fields where a relationship between two variables, calibrated with uncertain data, is subject to sudden changes (e.g. relation turbidity vs. total suspended sediment concentration).

2.6 Conclusion

We propose a method for the detection of rating shifts using gaugings. The method applies a recursive segmentation procedure to the time series of residuals between the gaugings and a time-invariant baseline RC. Unlike other classical methods for the segmentation of residuals, the proposed method formally accounts for both gaugings and RC uncertainties through a Bayesian approach. It also expresses change points and their uncertainties in terms of time rather than position, which is of interest to search for specific events that may have caused the shift. It performs a "top-down" recursive procedure, progressively refining the RC estimation on homogeneous sub-periods and leading to the detection of minor shifts.

The method yielded encouraging results for the Ardèche River at Meyras, France, with the detection of effective rating shifts, in good agreement with the official dates of RC update. Accounting for the uncertainty in the change point times allowed identifying flood events as likely causes of the shifts. Furthermore a performance evaluation procedure based on synthetic gauging data sets for which the true shift times are known highlighted the added value of the recursive segmentation procedure and the importance of accounting for both gaugings and RC uncertainties. This approach yielded more accurate results than a "single-pass" strategy or a strategy assuming homoscedastic residuals.

CHAPTER 3

STAGE-RECESSION ANALYSIS

This chapter is written as an article to be submitted to a scientific journal with the title "Estimation of river bed evolution at hydrometric stations using stage-recessions".

Abstract

Tracking and estimating the evolution of the river geometry is particularly important at hydrometric stations where streamflow estimation is based on a stage-discharge relation. The evolution of the river bed (e.g. due to intense floods) may induce rating changes, which may undermine streamflow accuracy. We propose an original method for the detection and estimation of net variations in the river bed elevation after floods using the stage record only. The method is based on the fact that when streamflow tends towards zero, stage tends towards the mean elevation of the main channel bottom or, if it exists, the mean crest elevation of the low flow section control. The method comprises three main steps. Firstly, the stage-recessions are extracted from the stage record. Then all extracted recessions are estimated together in a unique regression model through a Bayesian pooling approach. Finally a segmentation procedure is applied to detect multiple step changes in specific parameters of this model. The method is applied to the Ardèche River at Meyras in France, a gravel bed river subject to intense floods causing episodic river bed shifts. The method yields encouraging results with the detection and

accurate estimation of major river bed shifts. Only some minor changes were more challenging to detect. The stage-based method complements more traditional approaches based on gaugings, and may enable a faster change detection.

3.1 Introduction

3.1.1 Stage-discharge rating shifts at hydrometric stations

Some hydrometric stations especially located in natural rivers are affected by changes in the stage-discharge **rating curve** (hereafter called **RC**), i.e. the relation used to estimate streamflow, Q, from the recorded water level, h (stage). These rating changes may undermine the accuracy of the streamflow estimates.

One of the causes of rating changes [Herschy, 1998; Mansanarez et al., 2019] is related to river morphodynamics. The geometry of the river cross-section is subject to changes governed by streamflow intensity and sediment transport processes that cause erosion and deposition [Coleman and Smart, 2011]. The intensity of these processes depends on many factors: geological and geotechnical properties (bed soil type, grain-size distribution, soil mechanical properties), catchment hydrology, channel sinuosity and geometry, vegetation cover, etc.

Some rivers are subject to sudden changes of river bed elevation during morphogenic floods, but are characterized by periods of stability between these events. Other rivers are characterized by a continuous evolution of the river bed geometry, especially sandy bed rivers [Jia et al., 2007; Wang and Xu, 2016] and rivers with dunes or alternated bars [Rodrigues et al., 2014].

The issue of sudden morphogenic changes is well known by the operational services and the decision makers in charge of an "unstable" station. Indeed, their main interest is to detect and estimate river bed changes after a flood event with the least possible delay.

3.1.2 Methods for estimating river bed evolution

Currently methods for monitoring the river bed evolution include bathymetry measurements, stage-discharge rating curves approaches and analysis of the stage record.

Bathymetry surveys provide a direct and relatively precise estimation of the river

bed geometry [Zhao and Zhang, 2008]. Nevertheless, these measurements are performed sporadically, usually during gaugings campaigns, and require important mobilization of staff and equipment. New techniques such as camera time lapse [Leduc et al., 2018] or Satellite-Derived Bathymetry [Legleiter and Overstreet, 2012] can also provide information on the river bed bathymetry. However, these techniques are restricted to large rivers in the absence of vegetation and under low turbidity conditions [Legleiter et al., 2011].

A standard method to estimate the evolution of the river bed elevation at hydrometric stations is based on gaugings and RC estimation [Rantz, 1982; WMO, 2010; Le Coz et al., 2018]. If the RC equation is a power law of type Equation 1.1, then the offset b is the parameter reflecting the river bed elevation. River bed changes can therefore be deduced by changes of parameter b over time. Note that the exact meaning of the expression "river bed elevation" depends on the type of control represented by Equation 1.1. For a channel control the offset b corresponds to the mean elevation of the controlling reach; alternatively, if low flows are controlled by a weir/natural riffle, the offset b denotes the mean crest elevation.

We propose in this paper an alternative method based on the stage record, which is continuously available at hydrometric stations and may represent a simple and useful information to detect the morphological changes and estimate the river bed elevation. Surprisingly, this option has not been thoroughly studied in the research literature, even though it is performed by many hydrometry operators who monitor visually the anomalies in the stage record.

Łapuszek [2003] suggested a method based on the assumption that the stage at low flows tends towards the river bed elevation as streamflow tends towards zero. Assuming that annual minimum stages are close to the river bed elevation, the author could thus study the long-term trends in river bed elevation. A limitation of this approach is that focusing on annual minimum stages restricts the detection of changes at an annual resolution. Consequently, the dates of the flood events responsible for morphological changes are difficult to identify. In addition, annual minimum stages might be far from the river bed elevation during wet years with no significant droughts. To overcome this issue, a recession analysis on the stage record may be of interest.

3.1.3 Recession analysis

The recession analysis is usually performed on streamflow. Two main issues are addressed in the literature: the extraction of the individual recessions and the estimation of the corresponding recession curves.

Many methods (both manual and automated) exist in the literature to separate streamflow recessions, as reviewed by Chapman [1999]; Tallaksen [1995]; Hall [1968]; Sujono et al. [2004]. In general, a recession period lasts as long as the streamflow does not rise. Vogel and Kroll [1996] proposed to start a recession period when a 3-day moving average begins to decrease and ends when it starts to increase. Other algorithms aim at separating the "storm runoff" caused by the flood event from the hydrograph [Chapman, 1999], in order to isolate the baseflow, i.e. the result of groundwater discharging into the stream. Some authors proposed to simply remove the initial portion of the recession period, e.g. the initial 30 % [Vogel and Kroll, 1996]. In addition to streamflow, other approaches use precipitation data to define periods not influenced by precipitation [Lang and Gille, 2006; Tallaksen, 1995]. Moreover, the recessions are also selected according to a minimum duration for the recession period, usually chosen between 4 and 10 days [Tallaksen, 1995].

The literature also proposes several methods for estimating the streamflow recession curves, as reviewed by Johnson and Dils [1956]; Tallaksen [1995]; Langbein [1938]; Lang and Gille [2006]; Dewandel et al. [2003]. Some methods aim at estimating the individual recession curves separately [Barnes, 1939]. Other methods aim at overcoming the high variability of the recession behavior through the estimation of a master recession curve [Toebes and Strang, 1964; Nathan and McMahon, 1990], obtained from various individual recessions. Moreover, Morlet et al. [1982] and Sujono et al. [2001] proposed a method for analysing the recession characteristics based on the wavelet transform.

The recession analysis is conceptually based on storage–outflow models in linear and non-linear forms [Brutsaert and Nieber, 1977]. The single linear reservoir is commonly used in engineering practice, in particular using the simple exponential Maillet's law [Tallaksen, 1995]:

Matteo Darienzo

$$Q(t) = Q_0 \, e^{-\Lambda \, t} \tag{3.1}$$

where:

- Q_0 is the initial flow of the recession period (at $t = 0$);

- $Q(t)$ is the flow after a recession time t;

- $\Lambda > 0$ is the recession rate.

Sometimes several exponential terms are distinctly visible [Barnes, 1939; Larue and Giret, 2004], denoting different streamflow origins: the rapid runoff due to fast flow after floods, the sub-surface flow and the very slow emptying of aquifers. By adding N_{exp} exponential terms, streamflow-recession can be seen as a superposed exponential function [Barnes, 1939]:

$$Q(t) = \sum_{i=1}^{N_{exp}} Q_i \, e^{-\Lambda_i \, t} \tag{3.2}$$

An alternative to the use of several exponential terms for modeling complex recessions is to use models based on non-linear reservoirs [Wittenberg, 1994; Toebes and Strang, 1964]: e.g. the double-exponential model [Horton, 1933] or the hyperbolic model [Werner and Sundquist, 1951; Drogue, 1972].

3.1.4 Objectives and structure of the paper

The objective of this manuscript is to propose a method for estimating the river bed evolution at hydrometric stations through the analysis of stage-recessions. In particular, the proposed method pursues the following specific objectives:

- overcome the annual resolution of the method proposed by Łapuszek [2003] by analysing all available recessions rather than annual minimum stages only;

- evaluate whether models proposed in the literature for streamflow-recessions can be applied to stage-recessions;

- build recession models that consider some parameters as common to all recessions (in the spirit of a "master curve" concept) and other parameters as specific to each recession;

- assess whether changes in the time series of the recession-specific parameters can indicate morphological changes.

The structure of the paper can be summarised as follows. Section 3.2 describes the proposed method for the recessions extraction, estimation and segmentation. Then Sections 3.3 applies the method to a well-documented case-study by evaluating different recession models. Section 3.4 proposes a discussion on the results and the future perspectives for this work, such as the real-time application. Finally, Section 3.5 summarises the main findings and conclusions.

3.2 The proposed method for river bed estimation using stage recessions

The proposed procedure for the stage-recession analysis is composed of three main steps, detailed in the following subsections:

Step 1: Extraction of the stage-recessions from the stage record.

Step 2: Estimation of the stage-recession curves in a unique model through a Bayesian approach.

Step 3: Segmentation of the time series of the recession-specific parameters estimates.

3.2.1 Step 1: Extraction of the stage-recessions

Let $\boldsymbol{h} = (h(t_1), ..., h(t_n))$ define the values of the stage record. Note that times t_i denote the absolute times at which stage is recorded. This is a slight abuse of notation since in recession equations, such as Equation 3.1- 3.2, t denotes the recession time, i.e. the time since the beginning of the recession. The proposed algorithm for the extraction of the recessions from the recorded stage time series $\boldsymbol{h}$ is based on the following steps:

1. Selection of all decreasing stage values $\boldsymbol{h_d}$ among $\boldsymbol{h}$ such that $h(t_i) < h(t_{i-1})$ (black and empty dots in Figure 3.1).

2. Definition of the continuous sequence $\boldsymbol{h_{rec}}$ from the values $\boldsymbol{h_d}$ such that every value $h(t_i)$ of the sequence is smaller than all the previous elements, $h(t_{i-1}), h(t_{i-2}), ...$ (black dots in Figure 3.1).

3. Separation of the recessions: a threshold parameter, χ, is used to separate one recession period (k) from the next one $(k+1)$. If:

$$[h_{rec}(t_i) - h_{rec}(t_{i-1})] > \chi \tag{3.3}$$

then the recession k ends at time t_{i-1} and a new recession $k+1$ starts at time t_i (see Figure 3.1).

4. Selection of the recessions that fulfill the following user-defined conditions:
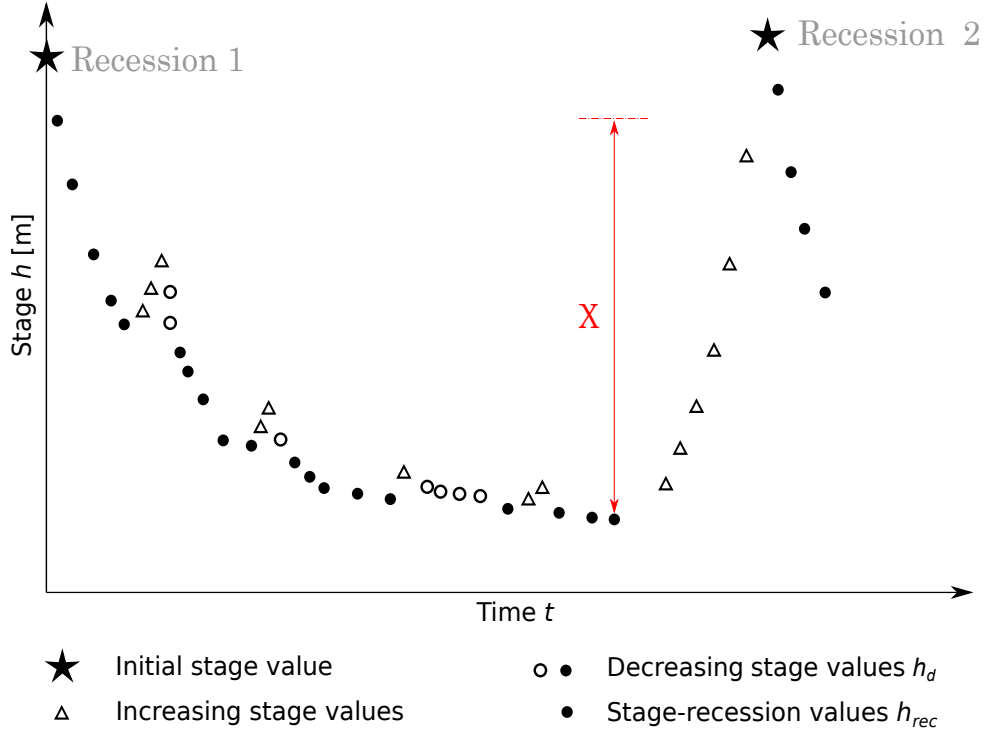
Figure 3.1: Schematic illustration of the recessions extraction method.

- a minimum number of stage data for each recession, e.g. $n_{min} = 10$;

- a minimum duration for the recession, e.g. $t_{min} = 10$ days.

Let N_{rec} denote the number of extracted recessions and N_k the number of stage values in the recession k. The total number of stage values in all recessions is therefore $N_{tot} = \sum_{k=1}^{N_{rec}} N_k$.

3.2.2 Step 2: Bayesian estimation of the stage-recessions

The second step of the proposed method is based on the estimation of a unique model for all recessions through a Bayesian pooling approach. We refer the reader to a similar approach described in Mansanarez et al. [2019].

3.2.2.1 The stage-recession model

As mentioned in the introduction, the simplest model for streamflow-recession is the single exponential function (Equation 3.1). Combining Equation 3.1 with the RC power law

Table 3.1: *Stage-recession models $h(t,k) = f(t,k|\boldsymbol{\theta_R})$ used in the paper, where t is the recession time, k is the recession index and $\boldsymbol{\theta_R}$ is the vector of model parameters.*

Stage-recession model			Stable parameters	Recession-specific parameters
	M1.	$h(t,k) = \alpha^{(k)} e^{-\lambda t} + \beta^{(k)}$	λ	α, β
Superposed-	M2.	$h(t,k) = \alpha_1^{(k)} e^{-\lambda_1 t} + \alpha_2 e^{-\lambda_2 t} + \beta^{(k)}$	$\lambda_1, \alpha_2, \lambda_2$	α_1, β
exponential	M3.	$h(t,k) = \alpha_1^{(k)} e^{-\lambda_1 t} + \alpha_2^{(k)} e^{-\lambda_2 t} + \beta^{(k)}$	λ_1, λ_2	$\alpha_1, \alpha_2, \beta$
[Barnes, 1939]	M4.	$h(t,k) = \alpha_1^{(k)} e^{-\lambda_1 t} + \alpha_2 e^{-\lambda_2 t} + \alpha_3 e^{-\lambda_3 t} + \beta^{(k)}$	$\alpha_2, \alpha_3, \lambda_1, \lambda_2, \lambda_3$	α_1, β
	M5.	$h(t,k) = \alpha_1^{(k)} e^{-\lambda_1 t} + \alpha_2^{(k)} e^{-\lambda_2 t} + \alpha_3 e^{-\lambda_3 t} + \beta^{(k)}$	$\alpha_3, \lambda_1, \lambda_2, \lambda_3$	$\alpha_1, \alpha_2, \beta$
Double-				
exponential	M6.	$h(t,k) = \alpha^{(k)} e^{-\lambda t^\eta} + \beta^{(k)}$	λ, η	α, β
[Horton, 1933]	M7.	$h(t,k) = \alpha^{(k)} e^{-\lambda^{(k)} t^\eta} + \beta^{(k)}$	η	α, λ, β
Hyperbola	M8.	$h(t,k) = \frac{\alpha^{(k)}}{(1+\lambda t)^\eta} + \beta^{(k)}$	λ, η	α, β
[Drogue, 1972]	M9.	$h(t,k) = \frac{\alpha^{(k)}}{(1+\lambda^{(k)} t)^\eta} + \beta^{(k)}$	η	α, λ, β

(Equation 1.1) gives the following stage-recession model:

$$h(t) = \left(\frac{Q_0}{a}\right)^{\frac{1}{c}} e^{-\frac{\Delta}{c}t} + b \tag{3.4}$$

Therefore, as for the streamflow-recession, the stage-recession can still be modelled with an exponential function with the unique difference that it does not tend to zero, but rather to the offset b.

Unfortunately, Equation 3.4 does not hold for more complex recession models and/or for a multi-control piecewise RC. Despite this, we postulate that models proposed in the literature for streamflow-recessions can reasonably be applied to stage-recessions by adding a parameter β representing the asymptotic stage.

In particular, nine different stage-recession models are proposed in this paper and reported in Table 3.1. They all use one or more parameters representing the initial stage (α_i), one or more parameters representing the recession rate (λ_i) and one parameter representing the asymptotic stage (β).

Model M1, representing a simple exponential behavior, is often used for studying the lowest part of the recession and may not be capable of describing the entire recession behavior. Instead,

all other models aim at describing the entire recession from the fast runoff to the slow emptying of the aquifer.

For this purpose models M2-M5 add to the simple exponential function few exponential terms based on the superposed-exponential concept (where $\lambda_i > \lambda_{i+1}$). In this paper we restrict to three exponential terms, but more terms may be added, keeping in mind that the additional flexibility comes at the cost of additional parameters.

On the other hand, models M6-M9 aim at describing the entire recession through the introduction of an additional parameter (η) acting on the shape of the recession.

Models M1-9 also differ in the choice of the common and recession-specific parameters. All models M1-5 assume a static λ_i, implying that the recession rates do not vary over recessions, and a recession-specific α_1, implying that the initial stage of the first exponential contribution (which describes the fast runoff) is specific to each recession, thus dependent on the high variability of flood peaks. Regarding the two-superposed-exponential models, M2-3, while M3 assumes a recession-specific initial stage α_2, M2 assumes the second exponential contribution is constant across recessions and the variability between recessions comes from the first exponential term only. Models M4-M5 add a static third exponential contribution to models M2-3, assuming that the aquifer emptying contribution is constant across recessions.

On the other hand, Models M6-9, which consider one single recession contribution, all assume a recession-specific initial stage α and a static shape parameter η. Finally, while models M6, M8 consider a static λ, implying that the recession rate does not vary over recessions, for models M7, M9 parameter λ is considered recession-specific.

For a given recession model, let $\boldsymbol{\theta_R}$ denote the inferred parameters of the recession model, comprising static $\boldsymbol{\theta_{static}}$ and recession-specific $\boldsymbol{\theta_{recession}}$ parameters.

3.2.2.2 Likelihood computation

Let t_i and k_i denote the time and the recession index, respectively, associated to the i-th recession stage value. Then, the observed stage value $\tilde{h}_i$ is written as the stage value predicted by the regression model $\hat{h}_i = f(t_i, k_i | \boldsymbol{\theta_R})$ plus a structural error and the observed stage error. Both types of error are assumed independent and Gaussian distributed with mean equals to zero and standard deviation equals to $\sigma_{R,i} = \gamma_{R1} + \gamma_{R2} \left(\hat{h}_i - min(\boldsymbol{h_{rec}}) \right)$ and to a given $u_{h,i}$, respectively. The vector of all inferred parameters is $\boldsymbol{\theta} = (\boldsymbol{\theta_R}, \gamma_{R1}, \gamma_{R2})$. The likelihood $\mathcal{L}$ of the N_{tot} observed stage recession values $\tilde{h}$ is:

$$\mathcal{L}\left(\tilde{\boldsymbol{h}} | \boldsymbol{\theta}, \boldsymbol{t}, \boldsymbol{k} \right) = \prod_{i=1}^{N_{tot}} p_{\mathrm{norm}} \left[\tilde{h}_i | f(t_i, k_i | \boldsymbol{\theta_R}), \sqrt{\sigma_{R,i}^2 + u_{h,i}^2} \right] \tag{3.5}$$

where $p_{\mathrm{norm}} \left[\tilde{h}_i | m, s \right]$ is the pdf of a gaussian distribution with mean m and standard deviation s at the observed stage value $\tilde{h}_i$.

The static recession parameters $\boldsymbol{\theta_{static}}$ appear in all N_{tot} terms of the product in Equation 3.5. Consequently, the information contained in all the recession observations is used to infer these static parameters. On the contrary, the recession-specific parameters $\boldsymbol{\theta_{recession}^{(k)}}$ only appear in the terms of the product involving observations from the $k - th$ recession.

3.2.2.3 Prior specification

Bayesian inference requires prior specification on parameters $\boldsymbol{\theta}$. The joint prior distribution is:

$$p(\boldsymbol{\theta}) = p(\gamma_{R1})\, p(\gamma_{R2})\, p(\boldsymbol{\theta_{static}})\, p(\boldsymbol{\theta_{recession}}) \tag{3.6}$$

Positive uniform distributions are assigned to the initial stage parameters: $\alpha \sim \mathcal{U}(0, 10^n)$, where n is the order of magnitude of the stage values. A uniform distribution is assigned to the asymptotic stage parameter: $\beta \sim \mathcal{U}(-10^n, +10^n)$. Log-normal priors are used for the recession rate parameters λ. It is convenient to specify this prior in terms of the more intuitive half-life τ (the time required for decreasing the initial stage by a factor of two), which is related to the rate parameter by:

$$\lambda = \frac{\ln 2}{\tau} \tag{3.7}$$

The log-normal prior on τ can be translated into a log-normal prior on λ whose logarithm has mean equal to $\ln(\ln 2) - \ln \tau$ and standard deviation equal to σ_{log}:

$$\lambda \sim \mathcal{LN}\left(\ln(\ln 2) - \ln \tau, \ \sigma_{log}\right) \tag{3.8}$$

A log-normal prior is also specified to the shape parameter $\eta \sim \mathcal{LN}(\ln 1, 1)$. For the structural error parameters a uniform prior is specified: $\gamma_{R1} \sim \mathcal{U}(0, 10^n)$ and $\gamma_{R2} \sim \mathcal{U}(0, 100)$,

3.2.2.4   Posterior distribution

Bayes' theorem combines likelihood with priors through:

$$\overbrace{p\left(\boldsymbol{\theta}|\tilde{\boldsymbol{h}}, \boldsymbol{t}, \boldsymbol{k}\right)}^{\text{posterior}} \propto \overbrace{\mathcal{L}\left(\tilde{\boldsymbol{h}}|\boldsymbol{\theta}, \boldsymbol{t}, \boldsymbol{k}\right)}^{\text{likelihood}} \overbrace{p\left(\boldsymbol{\theta}\right)}^{\text{prior}} \tag{3.9}$$

The multi-dimensional posterior distribution is explored with an adaptive block Metropolis sampler described in Renard et al. [2006]. The MCMC samples provide marginal and joint properties of parameters $\boldsymbol{\theta}$ (e.g. posterior mean, standard deviation, credibility interval) but also the most probable parameters values $\hat{\boldsymbol{\theta}}$ (maximum a posteriori) having the largest posterior pdf. MCMC convergence is visually checked through trace and density plots and by ensuring the Gelman factor [Brooks and Gelman, 1998] is smaller than 1.2. In this paper, 150,000 iterations are performed, but the first half of MCMC is discarded (burned). Finally, statistics are done considering one iteration every 100.

3.2.3   Third step: recessions segmentation

Once the recession model has been estimated, the temporal evolution of the recession-specific parameters $\boldsymbol{\theta_{recession}}$ is analysed. Particular attention is given to the evolution of the asymptotic stage parameter β, which corresponds to the elevation b of the lowest control.

A segmentation procedure is therefore applied to the series of the estimated asymptotic stages $\boldsymbol{\beta} = (\beta^{(1)}, ..., \beta^{(N_{rec})})$ searching for net shifts. Any segmentation method proposed in the

literature can be applied. In this paper the segmentation procedure developed by Darienzo et al. [2021] (Chapter 2) is used. It is a multi change point detection method based on a Bayesian approach and on a model selection criterion to choose the optimal number of change points, e.g. DIC [Gelman et al., 2004; Pooley and Marion, 2018]. This method is selected because it has the following properties:

- it accounts for the uncertainty affecting each estimated parameters (potentially variable from recession to recession);

- it expresses change points in terms of time (rather than position), which is convenient since the recessions are irregularly located along the time series. To this aim the time associated to each parameter $\beta^{(k)}$ is the time at which the corresponding recession begins.

- it provides an uncertainty on the detected shift times.

Finally, the method also provides the segments mean with uncertainty. They correspond to the estimation of the river bed elevation during each period of stability delimited by the shift times.

In the next section, the proposed stage recession analysis is applied to the Ardèche River at Meyras in France, a gravel bed river characterised by river bed degradation after episodic floods.

3.3 Application: Ardèche River at Meyras, France

3.3.1 Description of the station site

The Ardèche River at Meyras is located in a relatively small catchment (98 km^2). It is a gravel bed river degrading during each important flood resulting in vertical shifts in the stage record (as evidenced in Figure 3.2). Sikorska and Renard [2017] and Mansanarez et al. [2019] have exhaustively studied this station, proposing a three-controls hydraulic configuration: one rectangular weir section control activated at very low flows by a natural riffle, one main wide rectangular channel control activated at medium-high flows, and one wide rectangular floodway channel control added to the main channel control at very high flows. For this station the asymptotic stage of the stage-recession model, β, corresponds to the offset of the first control, b_1, i.e. the mean crest elevation of the natural riffle. The stage record is studied for the period between 07/11/2001 and 29/10/2018. Gaugings and comments about rating shift times have been provided by the hydrometric service, UHPC Grand Delta.

3.3.2 Step 1: Recessions extraction

Figure 3.2 illustrates the results of the first step of the proposed recession analysis by using, for comparison, three different reasonable values of the threshold parameter χ: 10, 30, 50 cm. All other options have been fixed to: $n_{min} = 10$ (to have enough points to estimate recession-specific parameters), $t_{min} = 10$ days (consistently with the literature). We also sub-sampled the stage time series to one value per day to reduce computational cost.

Figure 3.2 evidences the shifting of the low-stage recession levels, probably due to river bed erosion, confirming the interest of the proposed analysis to this station.

Moreover, using a low value of $\chi = 10$ cm leads to the extraction of a large number of recessions $N_{rec} = 130$. However, many of these recessions are very short (characterised by recession length between 10 and 30 days), with only 6 recessions reaching a length > 80 days. Higher values of χ lead to the extraction of fewer but much longer recessions. Since the main goal

Matteo Darienzo
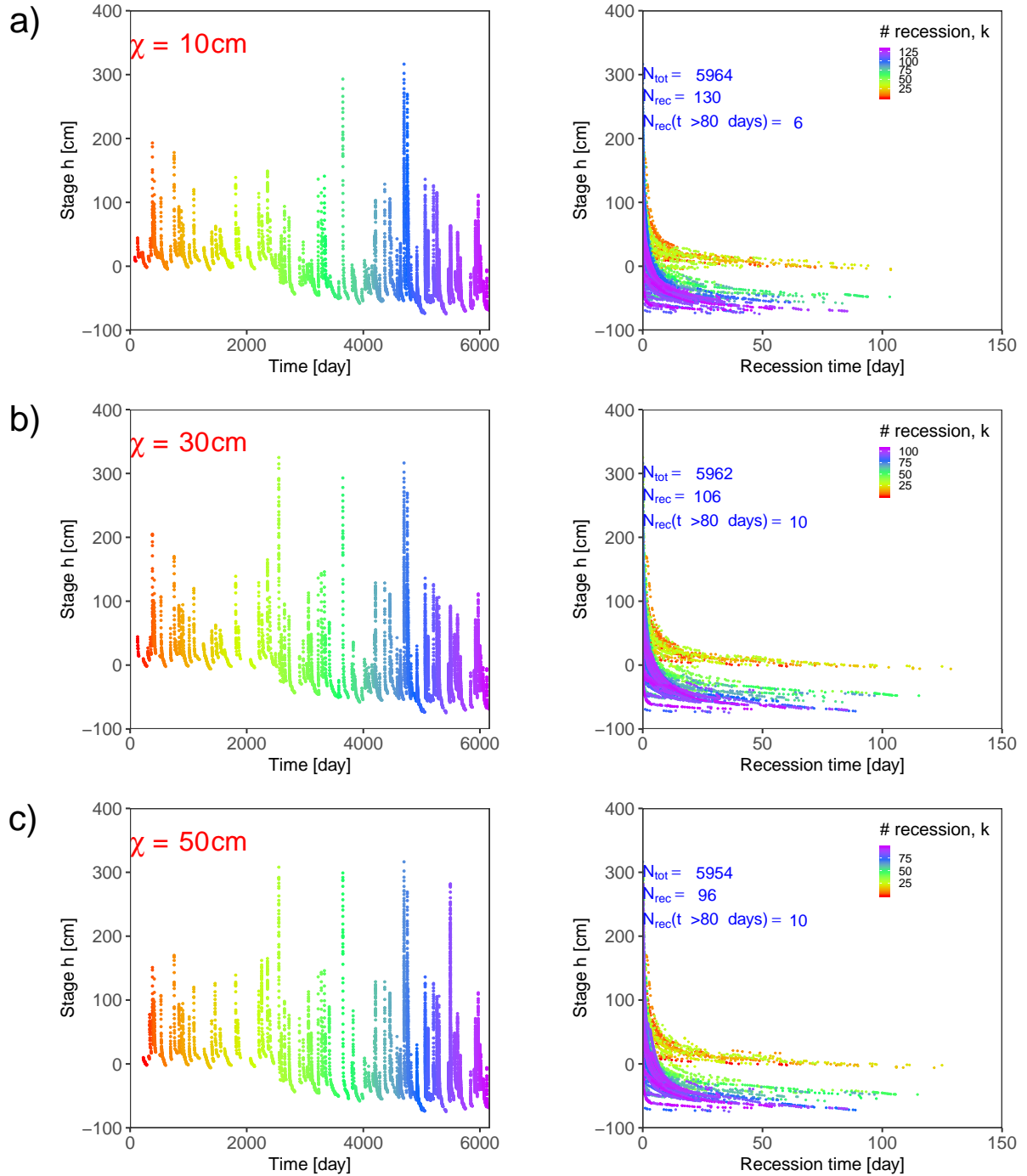
Figure 3.2: Results of the proposed recession extraction method applied to the Ardèche River at Meyras: the time series (on the left) and the overlapped recessions (on the right) extracted from the stage record with different values of the threshold parameter χ: a) $\chi = 10$ cm; b) $\chi = 30$ cm; c) $\chi = 50$ cm. A specific color is assigned to each extracted recession according to a rainbow gradient, going from the oldest recessions (in red) to the most recent ones (in violet).

of this work is the detection and estimation of shifts of the asymptotic stage, longer recessions are more suitable to the analysis, thus a reasonably high χ is here preferred.

3.3.3 Step 2: Recessions estimation

The second step consists of estimating the stage-recession models. For comparison purposes, all the recession models proposed in Table 3.1 are used for the recession data sets obtained with $\chi = 10, 30, 50$ cm. A standard deviation $u_{h,i} = 0.5$ cm is assigned to represent the uncertainty in all stage observations.

The priors for the inferred parameters for each model are specified as described in Section 3.2.2.3. Parameter λ is specified according to Equation 3.8. For all models having a single parameter λ we assume $\tau = 0.5$ days describing the fast runoff and $\sigma_{log} = 1$. For models M2-M5 we assume $\tau = 80$ days and $\sigma_{log} = 0.5$ for the slowest rate parameter (λ_2 for M2-M3, λ_3 for M4-M5) to describe the slow emptying of the aquifer. Finally, for models M4 and M5 we assume $\tau = 50$ days and $\sigma_{log} = 1$ for parameter λ_2 to describe the subsurface flow.

As an example, Figure 3.3a illustrates the results of the recession estimation using $\chi = 50$ cm and using models M1, M2, M4. For simplicity, only the MAP (maximum a posteriori) curves are plotted. As expected, results evidence that model M1 (one simple exponential term) does not fit well to the entire recession behavior. Instead, both model M2 and M4 (with two and three exponential terms, respectively) lead to quite similar curves and seem to better represent the fast runoff component as well as the slower components associated with low flow levels.

3.3.4 Step 3: Recessions segmentation

Figure 3.3b illustrates the results of the segmentation applied to the time series of the asymptotic stage parameter β (corresponding to the mean elevation of the low-flow control) for models M1, M2, M4. The minimum segment length has been fixed to 1 and the maximum number of change points has been fixed to 7. The results of the segmentation of β time series are also plotted against the stage record and the gaugings in Figure 3.3c.
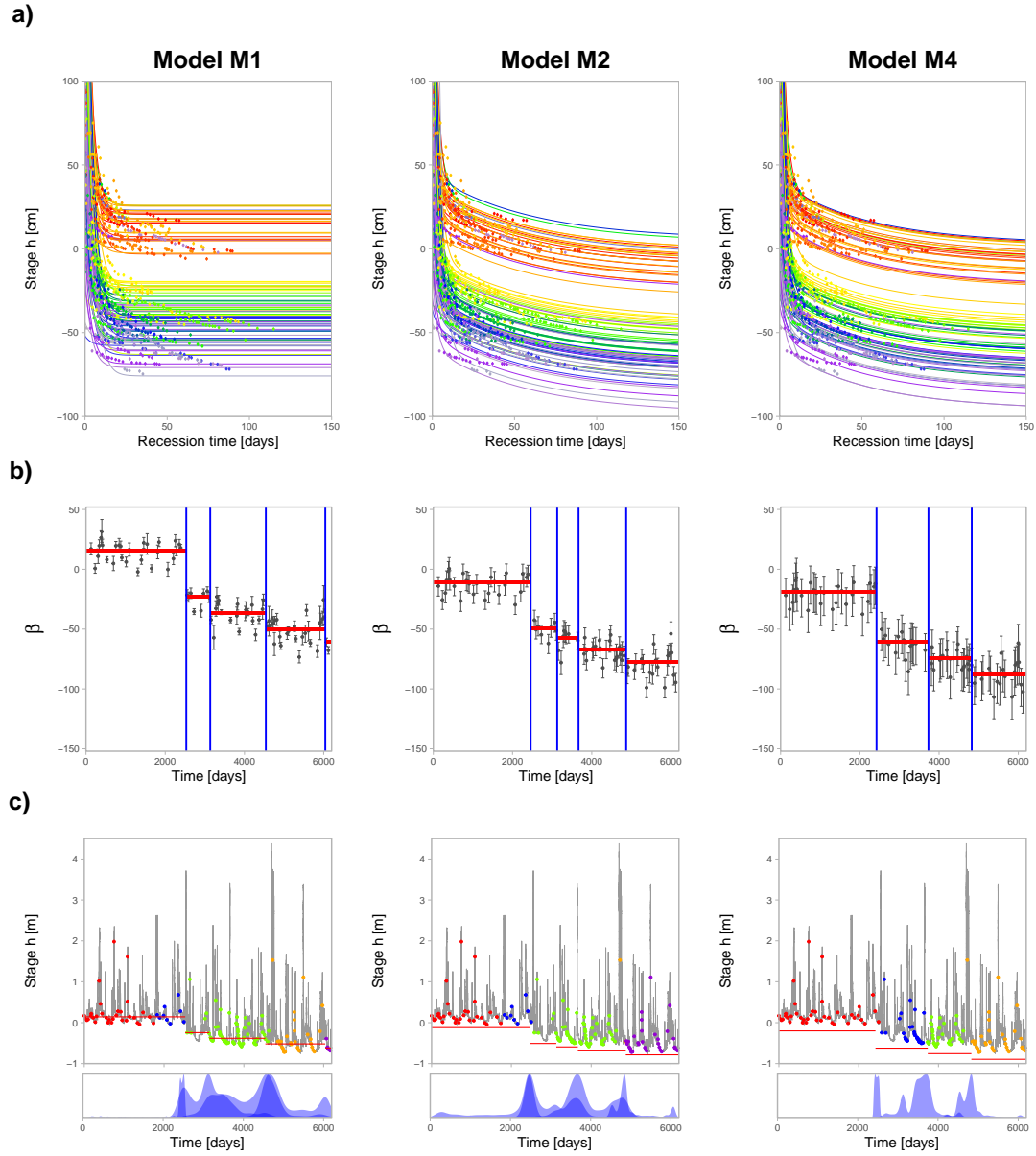
Figure 3.3: Results of the proposed method applied to the Ardèche River at Meyras by using = 50 cm and models M1, M2, M4 of Table 3.1: a) Estimation of the recession curves. b) Results of the segmentation applied to the time series of recession-specific parameter β. The horizontal red lines and the vertical blue lines are the most probable values of the segments mean and of the shift times, respectively. c) Gaugings, detected shifts and pdfs of the shift times plotted against the stage record.

Several step changes are found in the time series of parameter β, with results varying across the different recession models. This difference is in terms of number of detected changes (4 vs 4 vs 3 for models M1, M2, M4, respectively), their location and the estimated segments mean: with model M1, β represents a stage that is above the river bed elevation (notice the red segments in Figure 3.3c are above the minimum stage values in the stage record), while with model M4, β represents a stage that is much below the river bed elevation. With model M2, β corresponds more closely to the river bed elevation.

Finally, results reveal significant differences in the uncertainty of parameter β. While models M1 and M2 lead to similar and relatively small uncertainties of β, model M4 leads to much larger uncertainties (due to the additional parameters associated with the three superposed exponential terms).

As the true dates of river bed shift and the true values of river bed elevation are unknown, the choice of the most adapted model and χ value is challenging. This issue is addressed in the next section.

3.3.5   Sensitivity to the selected recession model

In order to select the most adapted model we propose two approaches:

- One general method applicable to all case studies and based on a model selection criterion.

- One method applicable to stations where information about past rating shifts is available, and based on the comparison between the shift times and magnitudes detected by the proposed method and those obtained by other methods (e.g. using the gaugings).

3.3.5.1   Using a model selection criterion

The recession models can be compared by means of the Deviance Information Criterion, which measures the trade-off between the fit and the number of parameters required to achieve it and which is well suited to the Bayesian framework adopted here (see Section 2.4.4.1). We use the version proposed by Pooley and Marion [2018] from the formulation of Gelman et al. [2004]

and based on the Deviance $D(\boldsymbol{\theta}) = -2 \ln{(p(\boldsymbol{h}|\boldsymbol{\theta}))}$, defined as:

$$DIC = \mathrm{E}\left[D(\boldsymbol{\theta})\right] + \frac{1}{2}\mathrm{Var}\left[D(\boldsymbol{\theta})\right] \qquad (3.10)$$

where $\mathrm{E}\left[.\right]$ and $\mathrm{Var}\left[.\right]$ represent the posterior mean and variance, computed using the MCMC samples. According to this criterion, the model to be chosen is the one with the lowest DIC.

Figure 3.4 illustrates the results for the Meyras case study by considering the different proposed models and the three different proposed values of parameter χ. Results reveal that while the ranking of the exponential models M1-M5 is sensitive to parameter χ (different χ values lead to different model rankings), models M6-M9 lead to similar DIC for all values of χ. Models that yielded the lowest DIC are M5, M9, independently on the values of χ, and M3 with $\chi = 30 - 50$ cm.

Another remarkable result from using models M2-M5 is that considering a recession-specific α_2 lowers the DIC (compare M3 vs. M2 and M5 vs. M4) with the exception for M2-M3 and $\chi = 10$. In a similar way, for models M6-M9 considering a recession-specific λ leads to a lower DIC.

Thus, if long recessions are available (as in this case study) the superposed exponential model with recession specific α_2 is preferred. On the contrary, for those case studies characterised by frequent floods thus with short recessions, the hyperbolic model with recession-specific λ, M9, may be preferred because not significantly depending on χ, thus on the length of the recessions.
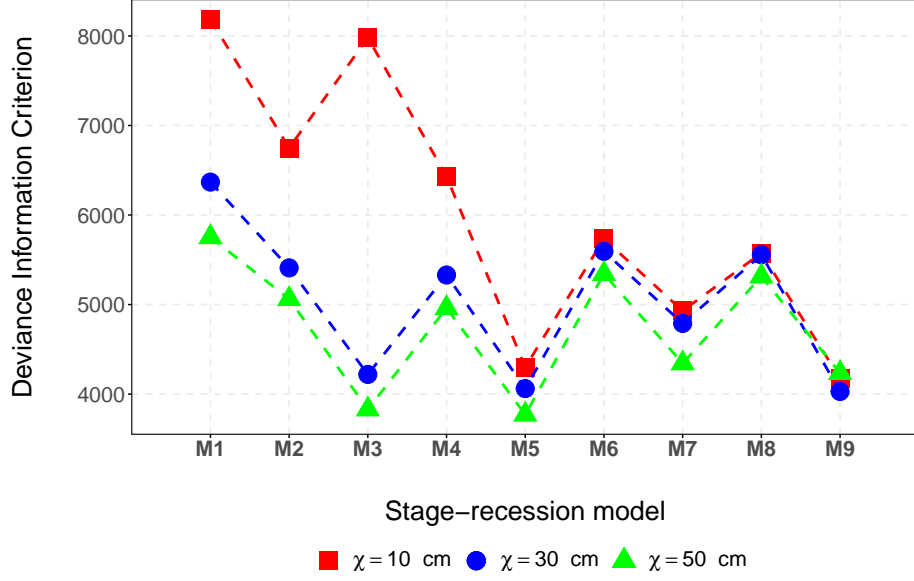
Figure 3.4: Values of DIC computed by using nine different recession models and three different values of extraction parameter χ.

3.3.5.2 Comparing the shift times and their magnitudes

In addition to using the DIC, comparing the segmentations obtained with different models and different values of χ can also be insightful.

Figure 3.5 evidences that increasing the value of χ (longer recessions) leads to slightly different segmentation for a given model. However it also shows that one shift time is detected by all models and by all χ values, and other two shift times by several models, which means that these three shifts are most likely three genuine shifts.

If additional information is available about the rating shift times from other methods (e.g. segmentation of the gaugings, or official dates of RC update) then the comparison can be even more exhaustive. In general we observe that models M1, M2, M4, M5 are the most consistent with the gauging segmentation (provided in Chapter 2), independently on the χ value, despite some of these models having a pretty high DIC. On the other hand, the models that yielded the less consistent segmentation independently on the χ values are models M6, M7, M8.
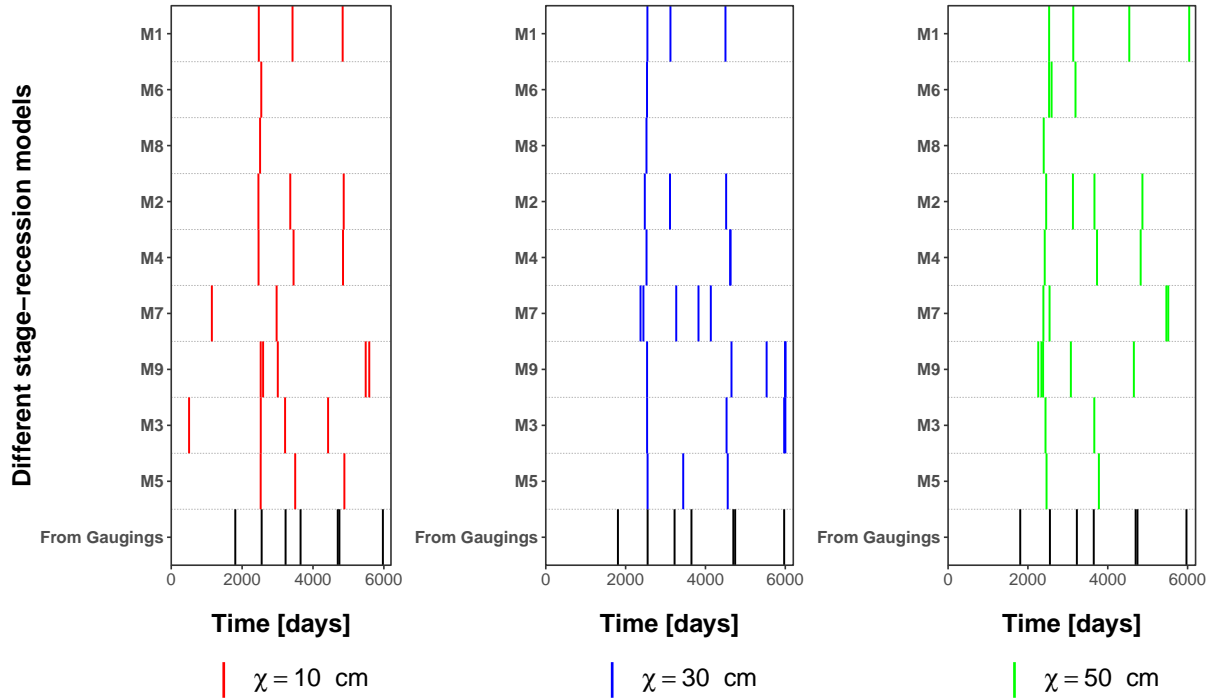
Figure 3.5: *Results of the segmentation in terms of shift times (only the most probable time values - maximum a posteriori - are plotted) yielded by using nine different recession models and three different values of extraction parameter χ. Also the shift times obtained from the gaugings [Darienzo et al., 2021] (Chapter 2) are plotted for comparison. Notice that the models have been ordered according to increasing values of DIC obtained with $\chi = 50$ cm.*
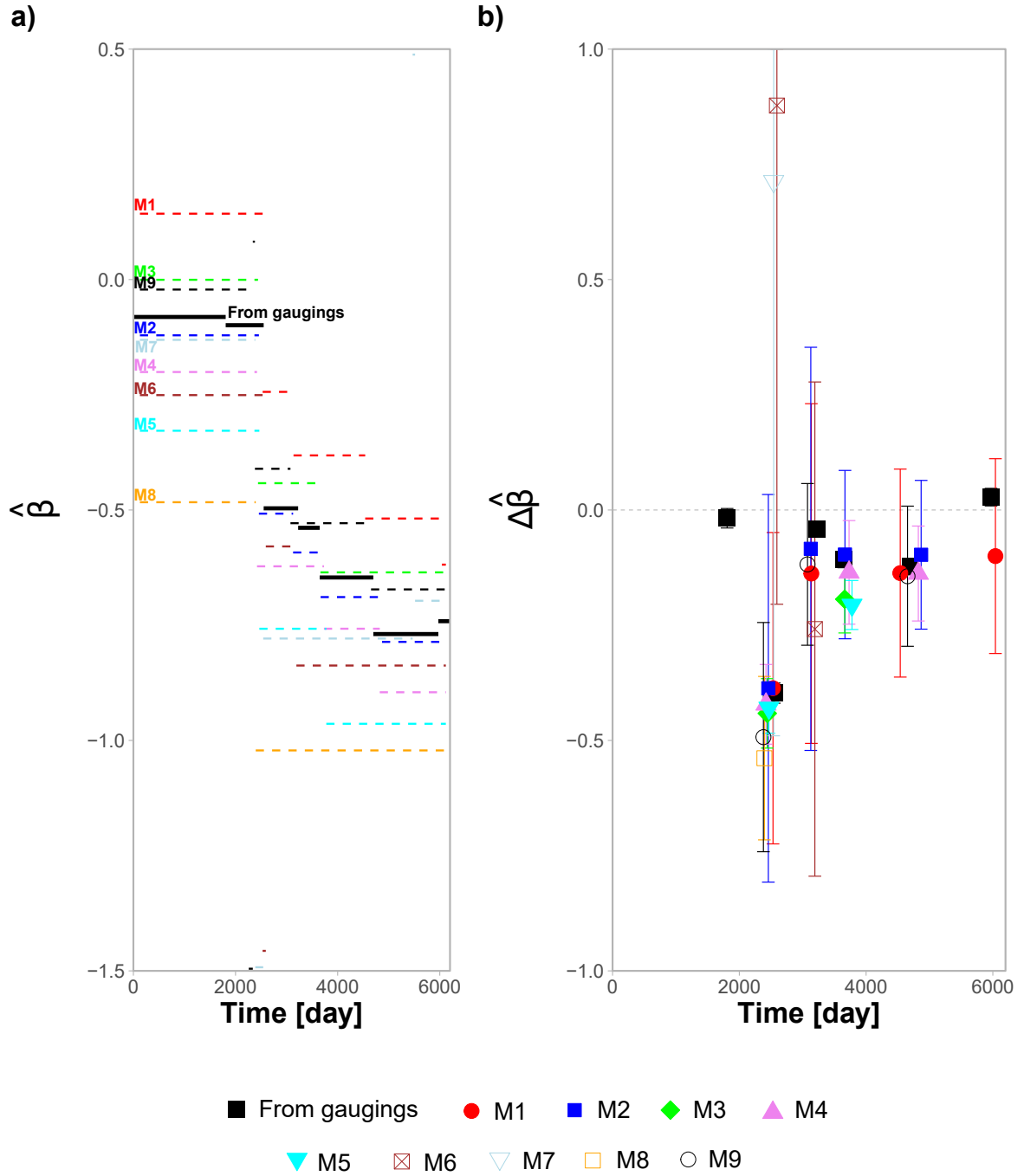
Figure 3.6: *Results of the segmentation in terms of estimated river bed elevation* $\hat{\beta}$ *(MAP) for each period delimited by the detected shift times (a) and of estimated shift* $\Delta\hat{\beta}$ *(b) for nine different stage-recession models and* $\chi = 50$ *cm. Also the estimated* b_1 *(MAP) and shifts* $\Delta\hat{b_1}$ *obtained from the gaugings [Darienzo et al., 2021; Mansanarez et al., 2019] are plotted for comparison. Error bars represent the 95% uncertainty interval of the shift estimates.*

Figure 3.6a compares the estimated $\hat{\beta}$ (MAP) for the nine models compared to parameter $\hat{b_1}$ (MAP) estimated by using the gaugings by means of the segmentation proposed by Darienzo et al. [2021] and the RCs estimation proposed by Mansanarez et al. [2019]. The estimation of $\hat{\beta}$ varies quite strongly with the model and is sometimes quite different from the one estimated with gaugings: models M1, M3 and M9 (especially model M1) tend to overestimate β, while models M2, M4 and M5 (especially M5) tend to underestimate it. Model M2 leads to β estimates very close to those obtained from gaugings.

Comparing the corresponding shift magnitudes is also insightful. Figure 3.6b shows the values of $\Delta\hat{\beta}$ (the differences between the consecutive $\hat{\beta}$ estimates (MAP)) and their uncertainty (the quadratic sum of the uncertainties of the two consecutive $\hat{\beta}$) for the nine models and $\chi = 50$ cm, which are compared to the shift estimates $\Delta\hat{b_1}$ obtained from the gaugings.

Results reveal that all models lead to shift estimates similar to those obtained by using the gaugings, with the exception of models M6, M7 which lead to some unrealistic (and highly uncertain) shift estimates. This interesting result suggests that reasonably estimating shift magnitudes is possible even when the estimation of the absolute river bed elevation is inaccurate. Moreover, the two shifts (the first and the last one) detected by the gaugings and missed by almost all models appear to be very small (of the order of 2 cm).

Finally, an interesting observation from this comparison with gauging-based segmentation results is that recession models ranking quite poorly in terms of DIC (Figure 3.4) can still estimate shift times and amplitudes quite acceptably (e.g. M2 and even M1). The only models that lead to consistent results both in terms of DIC and comparison with gaugings are models M5 (with $\chi = 10 - 30$ cm) and M9 (with $\chi = 50$ cm).

3.4 Discussion

3.4.1 Limitations

The recession extraction results have shown for some models a high sensitivity of the threshold parameter χ. A reasonably high value of the threshold parameter χ for the recession extraction is in general recommended, to ensure the availability of quite long recessions. However, even with a high value of χ, obtaining recessions long enough may be challenging for those catchments characterised by frequent floods. For such catchments the shift detection and estimation may be challenging.

The recession models considered in this paper are adapted to undisturbed natural systems but may not be adapted when low flows are affected by other processes: e.g. gravel mining operations, beavers/swimmers dams.

This paper is limited to river bed vertical instability. However, the shape of the river cross-section can change horizontally or vertically [Łapuszek, 2003] and the horizontal instability implies change in the width. Moreover, the method is geared toward change in low flow controls, and it's unlikely that changes in e.g. floodways of high-flow channels can be detected from the stage record.

Finally, the proposed stage-recession analysis needs to be tested for stations subject to frequent floods, or for stations located at sandy bed rivers subject to a continuous evolution of the river bed. For sandy bed rivers the segmentation step should be replaced by some form of trend analysis.

3.4.2 Perspective: real-time stage-recession analysis

A stage-recession analysis may be able to detect and estimate a RC change even before any gauging is performed, which is of interest to manage the RC in "real time". Indeed, the real-time application of the proposed recession analysis is a promising perspective of this work.

Note that the expression "real time" refers to the attempt to use the continuously incoming stage data to make decision about the RC, but it does not imply a notion of quickness. The estimation of the river bed already a few days after a flood may be very useful to provide fast information about river bed shifts and update the RC. While the retrospective analysis of the stage-recessions is characterised by the availability of all entire recession data sets, the real-time recession analysis sequentially adds the incoming stage values to the current recession.

The real-time application firstly requires the retrospective analysis of all past recessions in order to estimate the static parameters of the considered recession model. This can be done through the method described in Section 3.2. Then, the real-time estimation of the current recession can be performed in a sequential way by adding at each time step the incoming stage and updating the recession estimation. The recession estimation can be done through the same Bayesian regression approach but using the data of the current recession only and by considering as priors for parameters $\boldsymbol{\theta_{static}}$ the corresponding posteriors obtained from the retrospective analysis.

Figure 3.7 shows an example of real-time re-analysis for the Meyras case study by using model M2 and $\chi = 50$ cm. The considered real-time window comprises the recession period that follows the morphogenic flood at day 2550 (see the stage record of Figure 3.3) for which a net shift was observed. Model M2 detects a shift after only nearly 6 days and the shift is confirmed at all subsequent time steps.

These first results are encouraging but further work is necessary to test the real-time ability to accurately detect and estimate existing shifts and to avoid detecting shifts that do not exist.
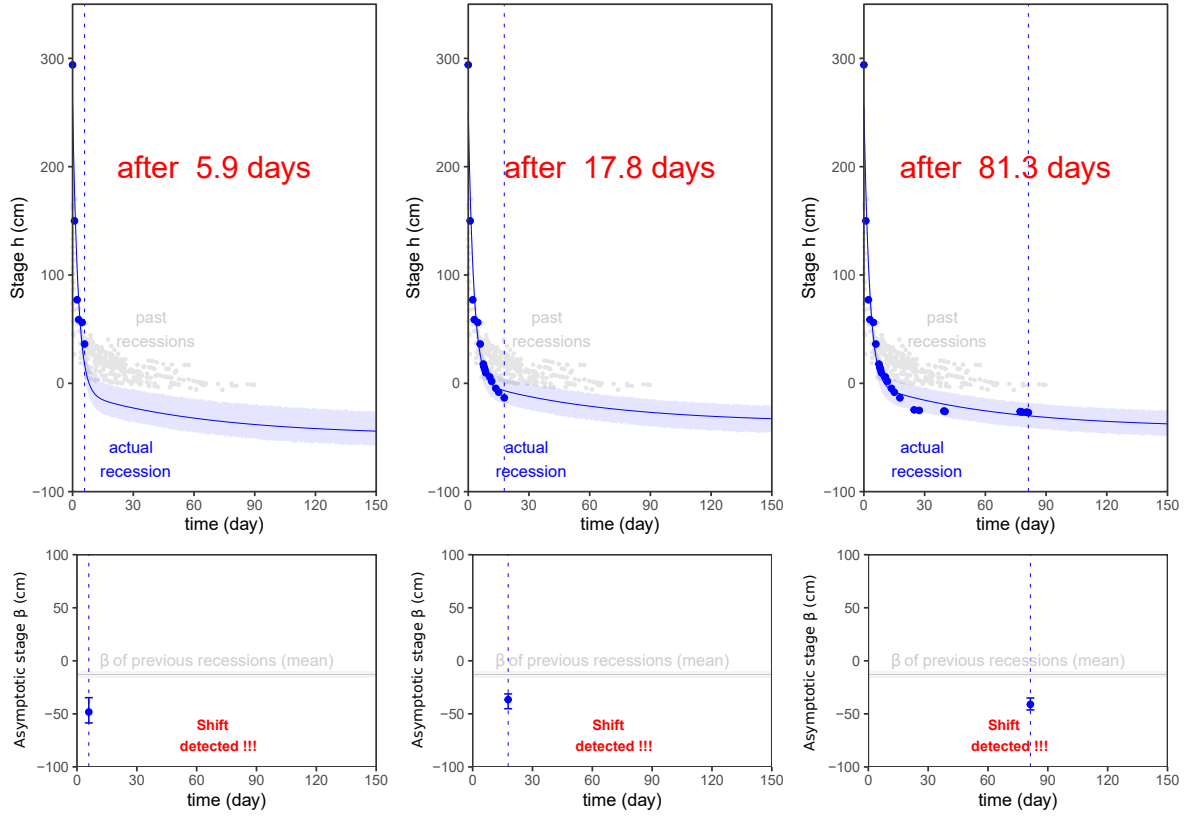
Figure 3.7: Results of the real time application by using model M2 and $\chi = 50$ cm and for three different real-time iterations: $t = 5.9 - 17.8 - 81.3$ days after the flood peak. The current recession estimation is illustrated in blue in the top panels and the asymptotic stage estimation β in the bottom panels. Also the past recessions are plotted in gray for comparison. The gray horizontal line and the gray ribbon represent the mean and the uncertainty interval (at 95 %), respectively, of the β estimates of all past recessions.

3.5   Conclusion

The proposed method for detecting river bed changes and estimating their evolution using the stage record is based on a stage-recession analysis and on the assumption that stage tends to the river bed as streamflow tends to zero.

The method consists of three main steps. It starts with the extraction of all available recessions from the stage record. It proceeds with the estimation of a unique model for all recessions through a Bayesian approach distinguishing recession-specific parameters and common parameters. Among the recession-specific parameters the asymptotic stage corresponds to the river bed elevation. Finally, the method applies a segmentation procedure to the series of the asymptotic stage parameter of all recessions. If some step changes are detected it provides the river bed change estimates with quantitative uncertainty.

The method yielded encouraging results with the detection and estimation of major river bed changes for the Ardèche River at Meyras in France. These changes can be detected quite accurately, even when the absolute river bed elevations cannot. Some recession models ranked poorly in terms of DIC but were still capable of detecting and estimating changes. Future perspectives include the application of the proposed recession analysis to the real-time context. The prediction of changes in the river bed elevation may be possible a few days after the flood.

CHAPTER 4

FAST DETECTION OF POTENTIAL RATING SHIFTS BASED ON
THE STAGE RECORD AND BEDLOAD ASSESSMENT

4.1 Introduction

4.1.1 General principle

As already discussed in previous chapters, one frequent cause of rating changes at the hydrometric stations is river bed morphological changes. Erosion and deposition are mainly due to the sediment transport induced by intense floods. During these events the RC may become obsolete and the estimation of streamflow inaccurate. For this reason, station managers and flood forecasting services may want to quickly detect potential morphological changes during and after the floods.

However, gaugings and bathymetry surveys are rarely performed during floods because of the difficulty and danger of accessing the site. Thus gauging-based methods such as the one proposed in Chapter 2 are not suitable for the fast detection of rating changes. Also the recession analysis proposed in Chapter 3 is not adequate during floods since it applies to recession periods only. Sometimes non-contact techniques, such as radar or imagery techniques, are deployed during floods for fast detection but they cannot be generalized, thus we cannot only rely on them. The stage record $h(t)$ is in fact the only information always available, including during floods, to detect and estimate morphological changes (as long as the recording

instrument is not damaged by the flood).

One possible way of using the stage data for the fast detection of a potential change is based on the fact that a minimum water depth is needed to trigger bedload, hence a potential morphological change (c.f. critical threshold for incipient motion [Meyer-Peter and Müller, 1948; Buffington and Montgomery, 1997; Perret, 2017]). Thus, the morphogenic flood can be defined as the period of the stage record characterised by values larger than a triggering stage. Moreover, the volume of transported sediments, and therefore the potential for morphological change, increase with the duration and the intensity of the flood.

The change detected by simply considering the exceedance of a critical stage value merely represents a potential change. Indeed, it may happen that both scour and fill processes occur during floods [Laronne et al., 1994] or that bedload transport is at equilibrium so that no net changes (significant difference before and after the flood) really occur. Furthermore the consolidation degree of bed material may change in time. Thus, two floods with the same intensity and duration may cause different morphological changes, depending on upstream sediment sources and local conditions.

From an operational point of view a potential change requires increasing the uncertainty around the parameters of the RC, with longer and more intense floods leading to a larger uncertainty increase. By contrast, methods using gaugings or stage-recessions (see previous chapters) aim at detecting effective changes and re-estimating these RC parameters, thus modifying not only their variance but also their mean value.

There is the need to develop a tool for detecting potential changes and to calibrate it against the historic morphological changes of the station assuming that the dynamics of the causal processes do not vary over time. The proposed approach is developed by borrowing ideas from river sediment transport modelling.

4.1.2   Sediment transport modelling

River sediments are heterogeneous aggregates of minerals, organic matter and biological matter. Their density and grain-size distribution strongly influence the processes of erosion and deposition. The sediment transport is initiated when the bed shear stress τ_b exerted by the water exceeds a critical value τ_c [Meyer-Peter and Müller, 1948]. Under the assumptions of wide rectangular channel and uniform flow conditions the shear stress condition can be re-expressed in terms of water depth y, with the triggering depth y_c being a function of the characteristic sediment diameter, the water and the sediment densities, the river bed longitudinal slope and the critical shear stress [Shields, 1936].

Once the critical shear stress is defined, there exist many semi-empirical formulas (e.g. Meyer-Peter and Müller [1948]; Engelund and Hansen [1967]; Camenen [2007]; van Rijn [1984]) to estimate the sediments flux as reviewed and compared by Davies et al. [1997]; Camenen and Larroudé [2003] for instrumented rivers. These formulas make various assumptions on where this flux comes from (e.g. bed load flux for well-sorted fine gravel).

4.1.3   Sediment transport models as proxys for potential changes

Sediment transport models need to be calibrated using measurements of transported fluxes which, unfortunately, are not available in general at hydrometric stations (especially during floods). Therefore it is not possible to use these models to precisely predict the volume of transported sediment.

However, we postulate that these models can still provide a valid information on the dynamics of transport (not the fluxes themselves), which we consider as a proxy for potential change. We also postulate that this proxy model, to be related to morphological changes, should compute the cumulative volume of transported sediments, rather than the instantaneous flux. This proxy model first has to be calibrated in retrospective mode, using previously detected changes identified by other methods: e.g. the segmentation of gauging residuals proposed in Chapter 2 or the stage-recession analysis proposed in Chapter 3. This calibration can be based on the

principle that all past flood-induced changes should be detected by the proxy model.

4.1.4 Objectives and structure of the chapter

The main goal of this work is to propose a sediment transport proxy analysis for the fast detection of potential morphological changes at hydrometric stations during floods. The proposed method must be:

- calibrated without the use of sediment transport measurements, but by using only information widely available at hydrometric stations: past rating changes and the stage record;

- suitable for a real-time application, when the managers of a station may want to quickly detect a potential morphological change.

The structure of this chapter can be summarised as follows. Section 4.2 describes the steps of the proposed method for the sediment transport proxy analysis. Section 4.3 then presents and discusses the results of its application to the Ardèche River at Meyras in France. Then limitations and possible improvements are discussed in Section 4.4. Finally Section 4.5 summarises the main findings of the study.

4.2 The proposed sediment transport proxy analysis

4.2.1 Overview

The method is based on a retrospective analysis of the stage record and on documented rating shifts. It starts with the selection of the reference morphogenic events from the information available from the station history. Then it applies a sediment transport model to the stage record in order to reproduce the reference morphogenic events and to identify all other potential morphogenic events. It finally establishes a relation between the cumulative sediment transport and the associated potential rating shift to be used in real time. All steps are described in the following subsections.

4.2.2 Information available from the station history

In order to calibrate the proposed method, some information from the station history is required, and more specifically the following two sets of data:

1. the set of the effective flood-induced shifts, leading to the reference shift times $\boldsymbol{t_{ref}}$.

2. the set of the associated shift estimates. Usually the shifts affect the offset of the lowest control. We therefore use the notation $\boldsymbol{\Delta b}$.

As regards the set of $\boldsymbol{t_{ref}}$, one can use the methods proposed in the literature (see Chapter 2) or the methods proposed in the previous chapters to detect effective rating shifts. However, only the morphological changes caused by sediment dynamics should be included, and hence there may be more $\boldsymbol{\Delta b}$'s related to other processes (e.g. gravel mining). Since the causes of the rating shifts are in general challenging to determine, if no additional information is available, then we suggest to apply the simple following rule: if the reference shift time refers to a flood then the rating shift is kept because most probably due to the sediment dynamics. On the contrary if it refers to a period of low flows it is discarded because probably caused by other processes.

As regards the shift estimates $\boldsymbol{\Delta b}$, they can be obtained from the RCs established for each period delimited by the times $\boldsymbol{t_{ref}}$. To this aim, several methods are proposed in the literature

(as reviewed by Kiang et al. [2018]). We use in this manuscript the BaRatin-SPD method proposed by Mansanarez et al. [2019] because of its ability to estimate RCs also for periods characterised by few or no gaugings. Alternatively, in the absence of gaugings the recession analysis proposed in Chapter 3 can be used too. Then, if we consider a single-control hydraulic configuration $a\left(h - b^{(k)}\right)^c$ valid for the period k before a flood peak $t_{ref}^{(k)}$ where the offset b represents the mean elevation of the channel bed, the control becomes $a\left(h - b^{(k+1)}\right)^c$ after the flood, with the shift of parameter b:

$$\Delta b^{(k)} = b^{(k+1)} - b^{(k)} \sim \mathcal{N}\left(\mu_b^{(k+1)} - \mu_b^{(k)}; \sqrt{\left(\sigma_b^{(k+1)}\right)^2 + \left(\sigma_b^{(k)}\right)^2}\right) \qquad (4.1)$$

where μ_b indicates the estimated value of b and σ_b its uncertainty. In the Bayesian context they correspond to the mean and the standard deviation of the posterior distribution of parameter b, respectively. Notice that Equation 4.1 can be generalised to more complex hydraulic configurations.

4.2.3 Estimation of the triggering stage and detection of all potential morphogenic events

The basic principle of the proposed method is that a minimum water depth is needed to trigger a potential morphological change. More precisely, the sediment transport is initiated when the bed shear stress at time t, $\tau_b(t)$, exerted by the water exceeds a critical value τ_c. In a wide rectangular channel in uniform flow conditions this relation can be written as:

$$\tau_b(t) = \rho \, g \, y(t) \, S_0 \; > \; \tau_c \qquad (4.2)$$

where:

- $\rho = 1000$ kg/m3 is the water density;

- $g = 9.81$ m/s^2 is the gravity acceleration;

- S_0 is the river bed longitudinal slope (whose approximated value can be obtained from a hydraulic modelling or topographical survey, e.g. 0.005);

- $y(t)$ is the water depth at time t, which is not known directly but can be obtained from the stage record through the hydrometric relation: $y(t) = h(t) - b(t)$.

For non-cohesive sediments this condition is in general made dimensionless [Shields, 1936]:

$$\tau_b^*(t) = \frac{\tau_b(t)}{(\rho_s - \rho) \, g \, d} > \tau_c^* \tag{4.3}$$

where:

- $\rho_s = 2650$ kg/m^3 is the usual quartz-rich sediment density;

- d is the median or other characteristic diameter of sediments. Even though its value is difficult to estimate without specific grain size measurements, its order of magnitude (e.g. $d = 0.05$ m) can be evaluated from prior knowledge on the site and/or photos;

- τ_c^* is the dimensionless critical bed shear stress with typical value within the range $[0.03; 0.09]$ [Buffington and Montgomery, 1997; Soulsby, 1997] according to grain size, slope, friction, hiding/exposure etc. It can be set to the traditional value for gravels, 0.047 [Meyer-Peter and Müller, 1948].

The triggering stage $h_c(t)$ can be obtained by combining Equation 4.2 and Equation 4.3:

$$h_c(t) = \tau_c^* \frac{\rho_s - \rho}{\rho} \frac{d}{S_0} + b(t) \tag{4.4}$$

All parameters of Equation 4.4 can be set to their predefined values, except for parameters d and S_0, which are strongly site-specific and may be affected by much larger uncertainty (if no specific surveys are performed). Therefore, the method needs to compute the triggering stage $h_c(t)$ by calibrating the value of the fraction d/S_0 (hereafter called ϕ) such that all the stage peaks corresponding to the reference times $\boldsymbol{t_{ref}}$ are above $h_c(t)$. To this aim, we propose two main steps:

1. Class the N reference events (with reference shift times $\boldsymbol{t_{ref}}$) with respect to the maximum stage: $h_{max}^{(1)} < h_{max}^{(2)} < ... < h_{max}^{(N)}$.

2. Fix a value of ϕ such that the obtained $h_c < h_{max}^{(1)}$.

Unfortunately, while parameter b is known for each period delimited by the reference shift times $\boldsymbol{t_{ref}}$ (see previous step), the evolution of $b(t)$ during the floods is unknown and challenging to determine. If no precise information is available, a linear interpolation can be applied to solve this discontinuity (see example in Figure 4.1). Considering the event k we first compute $h_c^{(k)}$ for the period before the flood and $h_c^{(k+1)}$ for the period after. Then the linear
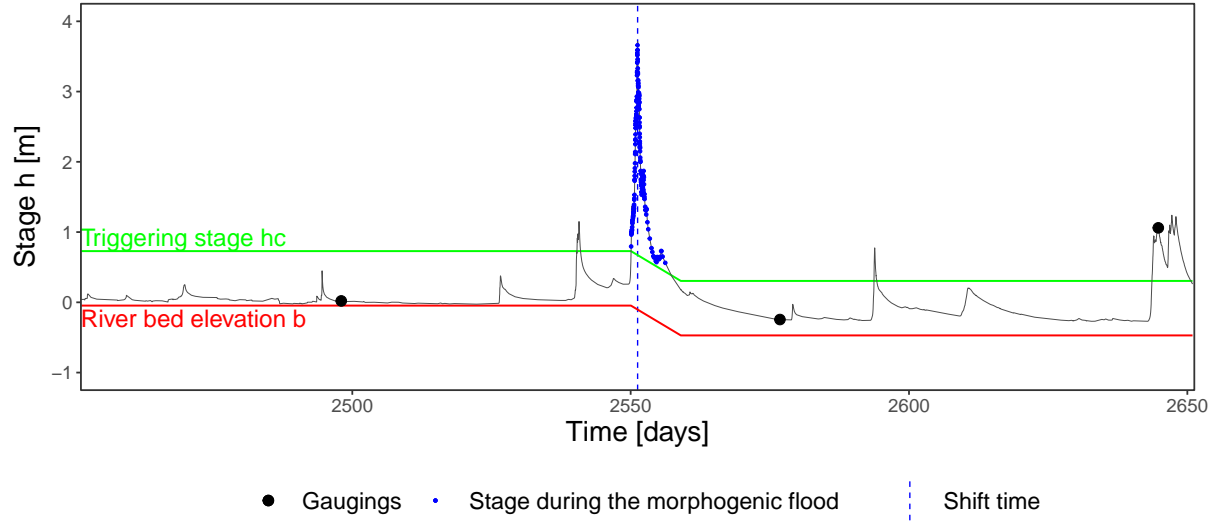
Figure 4.1: Linear interpolation of the river bed elevation b during a morphogenic flood event.

interpolation is computed starting from time $t_{in}^{(k)}$ (the first time before the flood peak stage exceeds the threshold $h_c^{(k)}$) until the time $t_f^{(k)}$ (when stage goes below the threshold $h_c^{(k+1)}$ for the first time after the flood peak).

The application of Equation 4.4 to the stage record determines the set of all potential morphogenic events. Then, the peak of these detected events define the times of the potential flood-induced shifts, $\boldsymbol{t_{pot}}$. Notice that the impossibility of verifying and estimating the corresponding shifts makes them potential shifts only.

4.2.4 Computation of the sediment transport

In addition to the potential shift times detection, the analysis may also provide an estimate on the variance of the associated shifts $\boldsymbol{\Delta b}$ by establishing a relation between the cumulative volume of sediment V at the end of each event and the associated shift magnitude Δb.

Several models have been proposed in the literature to estimate the sediment discharge per unit of width $q_s(t)$ expressed in m^2/s. We selected the widely used model for bed load proposed

by Meyer-Peter and Müller [1948]:

$$q_s(t) = \begin{cases} 8\sqrt{\frac{\rho_s - \rho}{\rho} g \, d^3} \, [\tau_b^*(t) - \tau_c^*]^{1.5} & , \quad \tau_b^*(t) > \tau_c^* \\ 0 & , \quad \tau_b^*(t) \leq \tau_c^* \end{cases} \qquad (4.5)$$

By substituting Equations 4.3-4.4 in Equation 4.5, the bed load equation becomes:

$$q_s(t) = \begin{cases} \psi \, [h(t) - h_c(t)]^{1.5} & , \quad h(t) > h_c(t) \\ 0 & , \quad h(t) \leq h_c(t) \end{cases} \qquad (4.6)$$

where coefficient ψ is equal to $\psi = 8\sqrt{\frac{\rho_s - \rho}{\rho} g \, d^3} \left(\frac{S_0}{d} \frac{\rho}{\rho_s - \rho} \right)^{1.5}$. All parameters included in ψ are fixed to generic values, except for the ratio S_0/d which has been calibrated as described in Section 4.2.3.

The cumulative volume of mobilised material $V^{(k)}$ expressed in m^3 computed from the beginning $t_{in}^{(k)}$ to the end $t_f^{(k)}$ of the morphogenic event k is:

$$V^{(k)} = \sum_{t=t_{in}^{(k)}}^{t_f^{(k)}} q_s(t) \, B \, \Delta t \qquad (4.7)$$

where B is the average active channel width at the hydrometric station.

4.2.5 Estimation of the uncertainty on the potential shifts

The principle behind the relation $\Delta b \leftrightarrow V$ is that the larger the volume of transported sediment during a flood is, the larger the associated potential shift is or at least larger is its uncertainty. When the volume V is small, the change cannot be large, but when V increases, it has the potential for being larger. The variance of Δb is expected to increase with V. Moreover, the shift can be positive (sediment deposition, hence river bed raise) or negative (erosion, hence river bed lowering). Therefore to fit the set of $(V^{(k)}, \Delta b^{(k)})$ pairs we propose the following probabilistic assumption:

$$\Delta b^{(k)} \sim \mathcal{N}(\mu^{(k)}, \sigma^{(k)}) \qquad (4.8)$$

with:

$$\begin{cases} \mu^{(k)} = 0 \\ \sigma^{(k)} = \sqrt{\left(\sigma_{\Delta b}^{(k)}\right)^2 + \left(\xi \, V^{(k)}\right)^2} \end{cases} \tag{4.9}$$

where $\sigma_{\Delta b}^{(k)}$ is the standard deviation representing the uncertainty in the shift $\Delta b^{(k)}$ (Equation 4.1) and ξ is a positive parameter that is estimated though a Bayesian-MCMC approach described in Renard et al. [2006] and in Chapters 2-3. Poorly-informative prior is specified for ξ (e.g. $\xi \sim \mathcal{U}(0,1)$).

In real time, starting from the beginning of the morphogenic event, the uncertainty of RC parameter $b^{(k)}$ can be updated by accounting for the standard deviation $\xi(V)$ of the potential shift. In a Bayesian context the prior distribution of parameter $b^{(k)}$ can be updated (e.g. assuming a Gaussian distribution) as follows:

$$b(t) \sim \mathcal{N}\left(\mu_b^{(k)}; \sqrt{\left(\sigma_b^{(k)}\right)^2 + \left(\xi \, V^{(k)}(t)\right)^2}\right) \tag{4.10}$$

To illustrate the method in the next section the proposed sediment transport analysis is applied to the case study of the Ardèche River at Meyras, France (also treated in Chapters 1 and 2).

4.3   Application to the Ardèche River at Meyras, France

4.3.1   Information from the station history

For the Meyras station, as described in the previous chapters, a documented knowledge on the hydraulic configuration, the stage record, the gaugings and the official dates of RC update is available for the period between 07/11/2001 and 29/10/2018 [Sikorska and Renard, 2017; Mansanarez et al., 2019].

Moreover, some effective rating shifts for the studied period are proposed in the previous chapters of this manuscript by the analysis of the gaugings (Chapter 2) and by the analysis of the stage-recessions (Chapter 3). The combined results are illustrated by vertical dotted lines in Figure 4.2. All detected rating shifts refer to flooding events and can thus be related to sediment transport dynamics, leading to the set of reference morphogenic events with peak times $\boldsymbol{t_{ref}}$. By analysing the gaugings for this station, Mansanarez et al. [2019] found that the rating shifts affect in particular the elevation of the low flow riffle control (b_1) and the mean elevation of the main channel (b_2). The riffle width and channel width and slope (and consequently, parameters a_1 and a_2) as well as the floodplain control are assumed stable.

The BaRatin-SPD method [Mansanarez et al., 2019] is used to estimate parameters b_1 and b_2 (illustrated by the horizontal segments in Figure 4.2 and by the boxplots in Figure 4.3) for each period delimited by $\boldsymbol{t_{ref}}$. Notice that the uncertainty on the parameters b_1 and b_2 is larger for period 6. This is because only one high-flow gauging (the green dot in Figure 4.2) is available for this period.

4.3.2   Estimation of the triggering stage and detection of all potential shift times

The detection of all potential morphological shifts is based on the selection of the events exceeding the triggering stage h_c, which is estimated through Equation 4.4. As explained in Section 4.2.3 the parameter that needs to be "calibrated" is $\phi = d/S_0$. By observing the
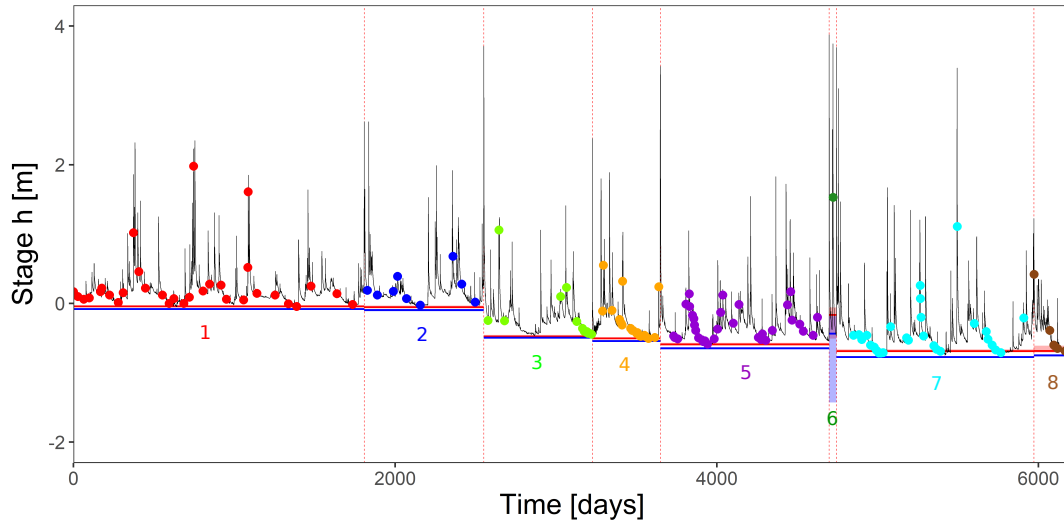
Figure 4.2: Stage record of the Ardèche River at Meyras (France) for the period 07/11/2001 - 29/10/2018 illustrating the combined results of the detection of effective rating shifts through the segmentation of gaugings and the recession analysis on the stage record. Moreover the RC parameters b_1 and b_2 are estimated through the BaRatin-Stage-Period-Discharge analysis [Mansanarez et al., 2019] and are illustrated (posterior mean value and 95% uncertainty) with blue and red segments and ribbons, respectively, for each reference stable period (whose index is indicated below the segments).
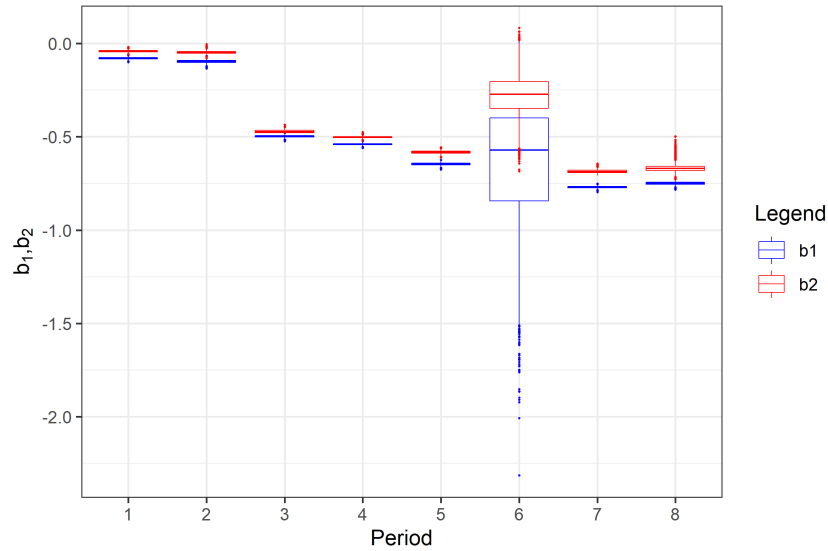
Figure 4.3: Posterior boxplots of the RC parameters b_1 and b_2 estimated for each reference stable periods of the Ardèche River at Meyras (France) for the period 07/11/2001 - 29/10/2018 through the BaRatin-Stage-Period-Discharge analysis [Mansanarez et al., 2019].
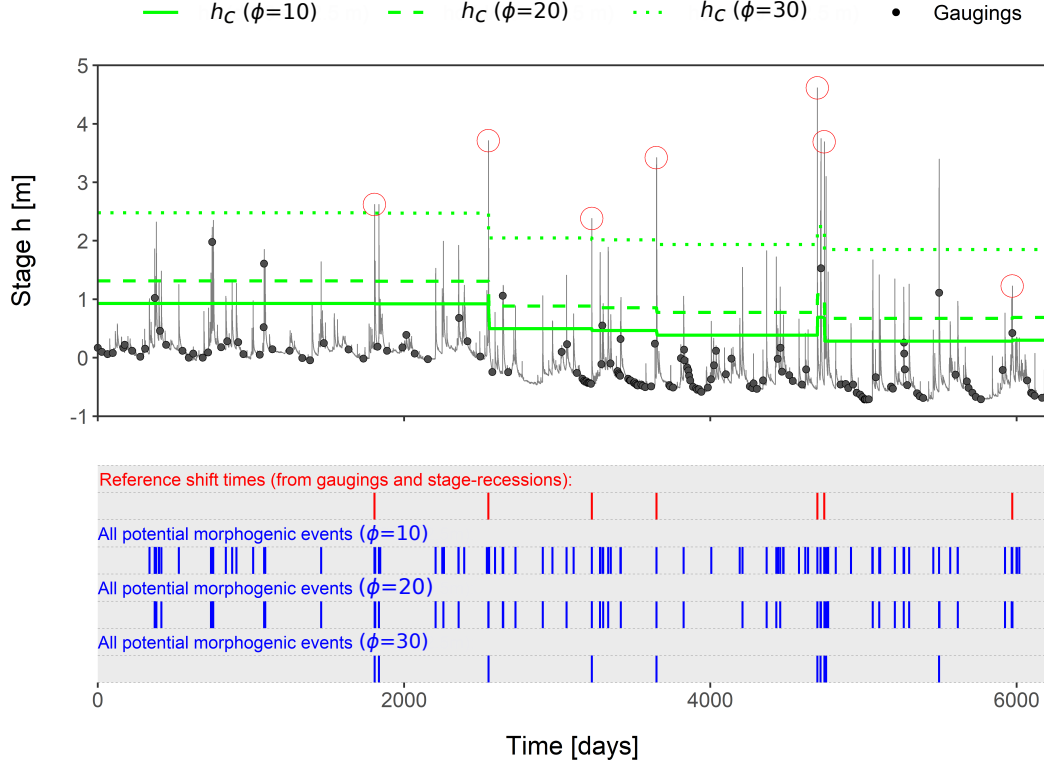
Figure 4.4: Results of the detection of all potential rating shifts t_{pot} caused by sediment dynamics for the Ardèche River at Meyras station. Three different values of $\phi = d/S_0$ are used and compared against the reference shift times t_{ref} (shown on stage record by red open dots).

topography and the available photos of the station, the longitudinal slope may take values $S_0 = 0.005 \pm 0.002$. The river bed material is composed of coarse gravel material, with characteristic diameter roughly estimated around $d = 0.10 \pm 0.05$ m. Using a Monte-Carlo propagation of uncertainty, this gives $\phi = 20.9 \pm 14.7$ m.

Due to the large uncertainty on parameter ϕ three different values of ϕ in this interval are tested: $\phi_1 = 10$, $\phi_2 = 20$, $\phi_3 = 30$. The results are illustrated in Figure 4.4. The three sets of potential morphogenic events, characterised by different values of ϕ and by $h(t) > h_c(t)$, and whose peaks define the potential shift times $\boldsymbol{t_{pot}}$, are represented by blue segments. These sets of potentials shift times can be compared with the reference shift times $\boldsymbol{t_{ref}}$ (red segments) and the corresponding peak values (circles).

The choice of the proper value of ϕ can be done through the two steps described in Section 4.2.3. In particular, Figure 4.4 shows that, while the set of shift times $\boldsymbol{t_{pot}}$ obtained with $\phi = 30$ misses one of the reference shift times (the last one), both $\phi = 10$ and $\phi = 20$ lead to set t_{pot} including all $\boldsymbol{t_{ref}}$. The choice between $\phi = 10$ and $\phi = 20$ is subjective, though. However we may want that the cumulative volume of bed load for the period when $h(t) > h_c$ is large enough. If for example we take ϕ such that $h_c = h_{max}^{(1)}$, the bed load would occur for a too short time (equal to zero) to induce a river bed shift. With $\phi = 20$, h_c is still too much close to $h_{max}^{(1)}$. However, if we take $\phi = 10$ too many potential shifts are detected. Instead, using $\phi = 15$ can be considered as a good trade-off between detecting all reference events and detecting other potentials shifts. Thus, $\phi = 15$ is selected for this application.

4.3.3 Relation between shift Δb and sediments volume V

The cumulative volumes of sediment V for each potential morphogenic event have been computed by using Equation 4.7 and by fixing $\phi = 15$ and $B = 15$ m. They are plotted with blue bars in Figure 4.5. Several potential events have a large volume but are not associated with any reference events (whose peaks are identified with circles in the figure), e.g. the volume at $t = 5500$ is larger than the volumes of events 1, 3, 6. This suggests that no change occurred despite the large transported volume. The sediment dynamics can be very different during each event leading to different responses: the alternation of scour and fill processes may cause net shift very close to zero at the end of the flood.

Then, the volumes V of the reference events are used as calibration data for the relations $\Delta b_1 \leftrightarrow V$ and $\Delta b_2 \leftrightarrow V$. Each reference event has been selected as the largest flood within the uncertainty interval of the shift time obtained by the segmentation of gaugings (see Chapter 2). It may happen that several floods are included within this interval and they are probably contributing to the rating shift. Therefore we propose that some very close events (separated by maximum 100 days, the order of magnitude of the shift times uncertainty) are merged in unique events (see ribbons in pink in Figure 4.5). Notice in particular that reference events 5 and 6 have been merged in a unique event. The effective shifts Δb_1 and Δb_2 associated to each $\boldsymbol{t_{ref}}$ are then estimated through Equation 4.1 and used as calibration data for the relations $\Delta b_1 \leftrightarrow V$ and $\Delta b_2 \leftrightarrow V$ illustrated in Figure 4.6.
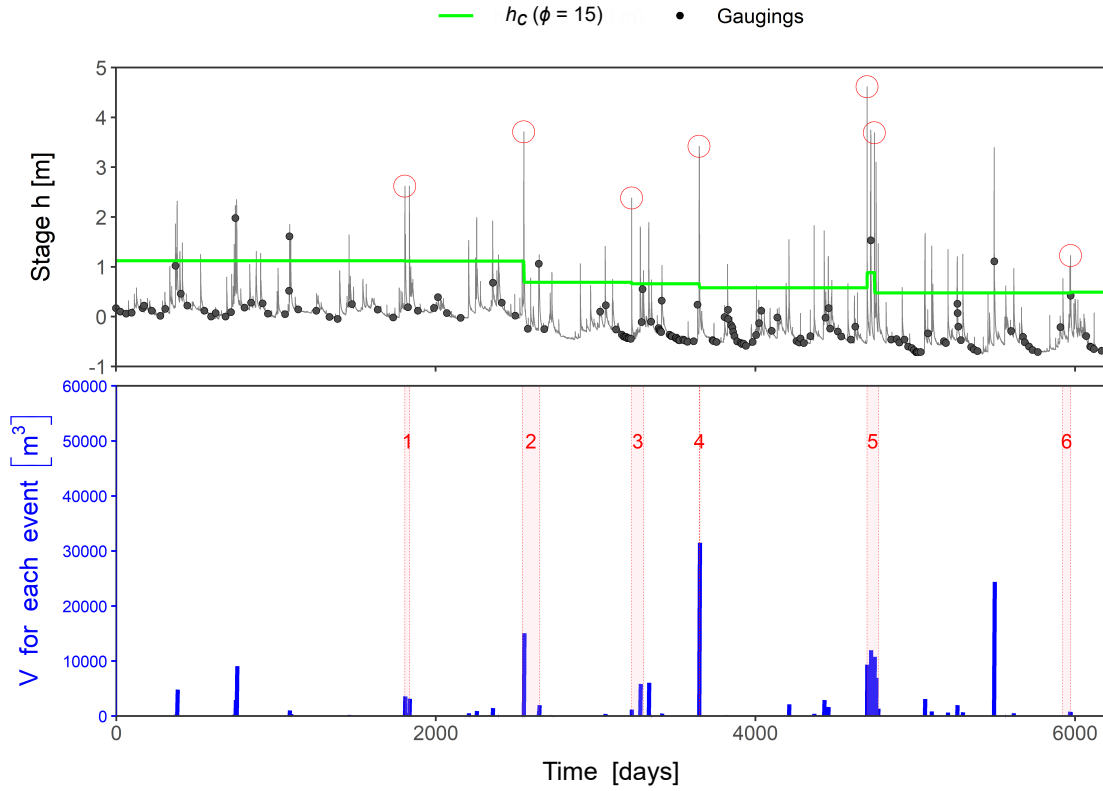
Figure 4.5: Results of the estimation of the cumulative volume of transported sediments after each potential morphogenic event for the Ardèche River at Meyras, France.

The two relations are very similar since parameters b_1 and b_2 are found to change in a similar way at this station. Results reveal that for high volumes the potential shift is estimated at about $\pm$ 1 m, which sounds reasonable. An application in real time of this relation during a flood event is proposed in Chapter 5.
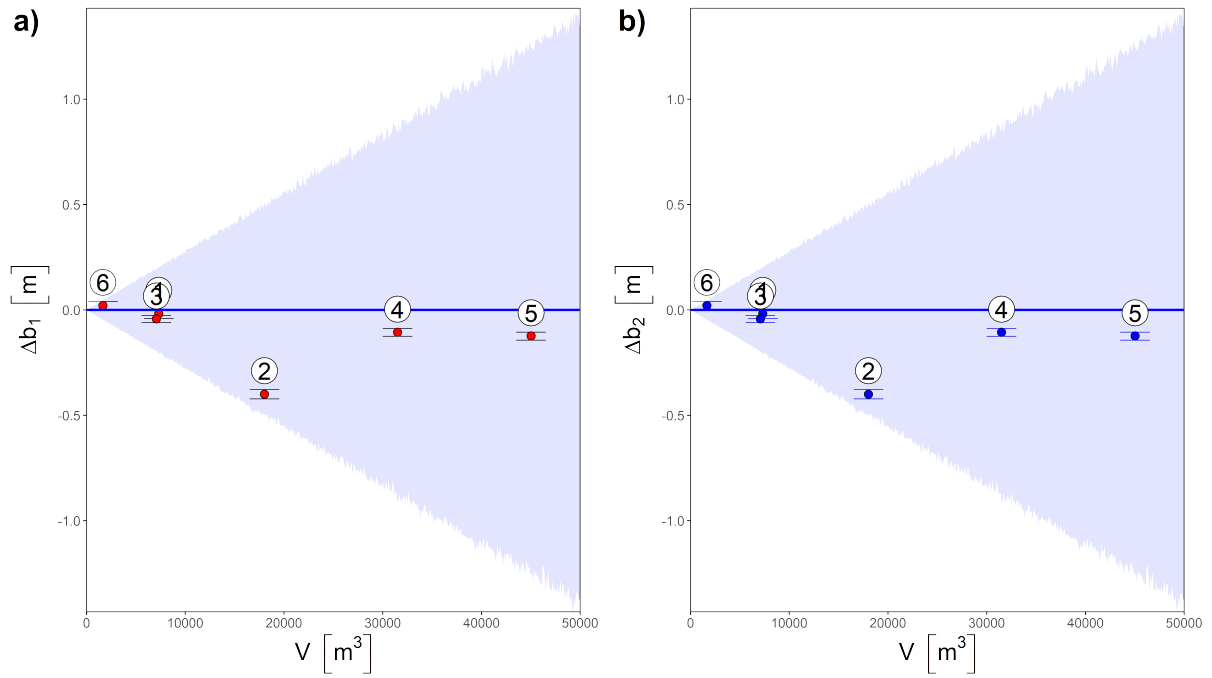
Figure 4.6: Relation $\Delta b_1 \leftrightarrow V$ (a) and $\Delta b_2 \leftrightarrow V$ (b) for the Ardèche River at Meyras, France. Calibration data are the estimated Δb and V for each reference morphogenic event. The number above the calibration data represent the index of the reference event. The blue line represents the maximum a posteriori and the blue ribbon illustrates the total uncertainty at 95 %.

4.4 Discussion

4.4.1 Main limitations

The applicability of the approach may be restricted to gravel bed rivers. Indeed, for sandy rivers the estimated triggering water depth may be extremely small which may lead to the continuous detection of potential shifts. The proposed method should still be applicable but using sediment transport models more suitable to sand granulometry [e.g. Engelund and Hansen, 1967] instead of the one proposed by Meyer-Peter and Müller [1948]. However the formulation proposed by Engelund and Hansen [1967] (frequently used for fine sediments) does not include any thresholds for incipient motion. A dynamic modelling of the stage-discharge relation may be necessary in this case.

Moreover, the calibration of the triggering stage is based on the assumption that all reference shift times are correctly identified. However this assumption may be wrong, if a shift is missed or attributed to the incorrect flood, or if a shift that doesn't exist is detected. The impact that this issue may have on the results needs to be studied.

Another issue is that the method excludes the breathing phenomena of scour and fill that may occur during floods. To properly study these events a solution may be to apply theoretical sediment transport modelling under unsteady flow and unsteady sediment transport conditions [Davies and Griffiths, 1996]. However this requires experimental surveys on the sediment size distribution and on the time-scale of bed deformation. Notice also that during floods the variation of the river bed may be complex and may affect not only parameter b of the low controls but also the width of the control or the channel slope, hence parameter a (see the example in Figure 4.7 of the braided Wairau river at Barnetts Bank in New zealand). However, detecting in real time changes in the parameter a, based on the stage record only, may be challenging. On the other hand, photos or videos might be enough for this purpose, since a change in the width should be easier to observe visually than a bed change.

Another possible issue is related to the merging of multiple morphogenic events. The choice
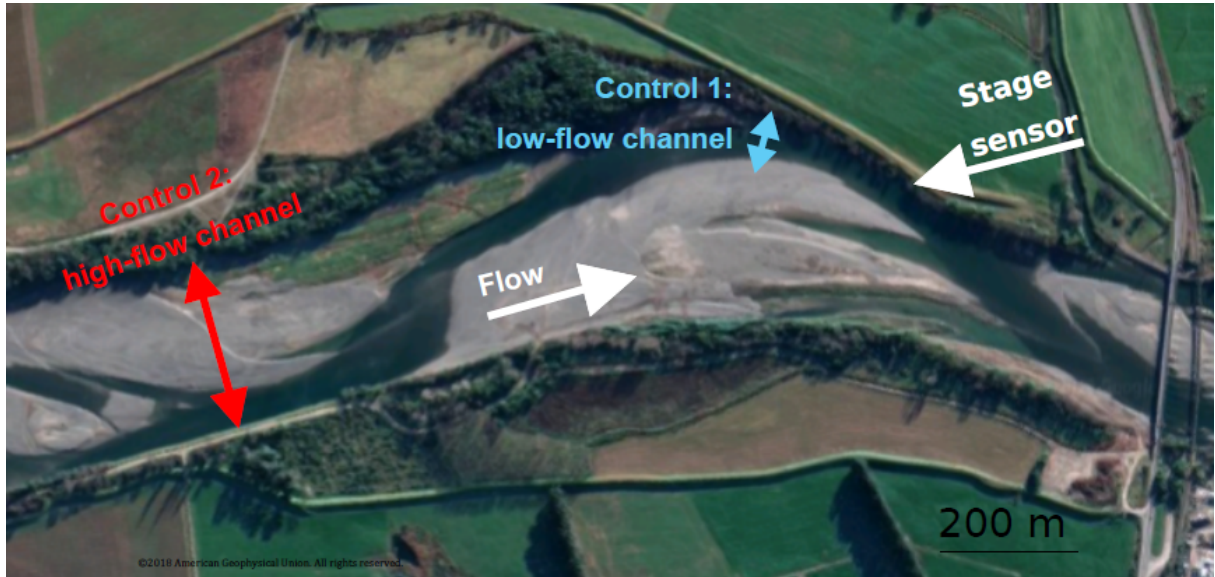
Figure 4.7: Aerial view of the Wairau River at Barnetts Bank in New zealand (taken from Mansanarez et al. [2019]): a braided gravel bed river subject to very frequent floods causing frequent sudden modification of elevation and width of the lowest control.

of the maximum inter-event time-lag for merging the events (e.g. 100 days for Meyras) is quite subjective and case-specific. Further work is necessary to improve this step. A solution may be to merge the events there are located within the uncertainty interval (e.g. at 95 %) of the shift times obtained from the gaugings segmentation (see Chapter 2).

Moreover, the relations $\Delta b \leftrightarrow V$, by using the model described by Equations 4.8-4.9 with mean equals to zero and standard deviation increasing proportionally with V, successfully yielded the estimation of the uncertainty on the potential rating shift during floods. However, we could also use a linear or proportional model which would provide the trend and the direction of the morphological evolution (e.g. raising or lowering of the bed elevation).

Finally, the assumption of constant channel longitudinal slope S_0 and of constant characteristic diameter d (hence constant ϕ) may be too strong in some cases. A sensitiviy analysis could be done in the future to assess whether this assumption has an impact on the results or not.

4.4.2   Use of the method for retrospective purposes

Notice that the objective of this chapter is the fast detection and estimation of potential rating shifts in the real time context. However, the station managers may be also interested in the retrospective detection of all past potential rating shifts in order to re-calibrate the RC for each stable period and reconstruct the historic streamflow time series. Working with many near-zero potential changes is not useful and creates practical problems. Filtering out such minor potential changes would therefore be valuable.

In fact, the condition $h(t) > h_c(t)$ does not imply that a net morphological change occurred but only that the bed sediment transport is initiated. A minimum volume of transported sediments (V_{min}) from the beginning of the event may be necessary to result in a net morphological change, justifying an update of the RC. Moreover an armouring phenomenon of the river bed may occur. Sediment transport can start well beyond the triggering stage and suddenly mobilise a lot of material.

The minimum volume of transported sediments V_{min} (necessary for a morphological change) can be estimated as the minimum volume among the reference events. Then, the manager may decide to select among all the potential events only those ones characterised by $V \geq V_{min}$.

4.4.3   Other perspectives

Perspectives of the proposed sediment transport proxy analysis include the tests on more challenging stations: in particular rivers with sandy bed and continuous bed evolution, and rivers characterised by frequent floods. The method to be validated should also be tested on a station where sediment transport measurements are available.

Finally, the calibration of the triggering stage and the sediment transport, thus the detection and the estimation of potential shifts, may be performed through a Bayesian method, using a binary detection index I, where $I = 0$ if the potential shift is not part of the reference shifts and $I = 1$ if it is. This approach may allow a more formal inclusion of the prior knowledge on d/S_0

and may provide uncertainty on the estimates of the cumulative volumes V that is otherwise ignored. Further work is necessary to test its feasibility and its added value.

4.5   Conclusion

The method proposed in this chapter for the fast detection of potential shifts uses the stage record and a proxy sediment transport analysis.

The method is based on the exceedance of a triggering stage. Computing this threshold requires calibrating a parameter in retrospective such that the triggering stage is exceeded by all the reference morphogenic floods detected by other methods (e.g. segmentation of gaugings and stage-recession analysis). The method yielded encouraging results for the Ardèche River at Meyras confirming all reference effective shifts. Several other potential morphogenic events have been identified.

The analysis then proceeds by establishing a relation between the cumulative volume of transported sediments during the flood and the associated potential rating shift. This relation provides quantitative information on the uncertainty of the shift, which can be used in a real time context. The application on the Meyras case study shows that the method provides a realistic relation between transported volume and potential change.

CHAPTER 5 ⎯⎯⎯⎯⎯⎯⎯⎯⎯⎯⎯⎯⎯⎯⎯⎯⎯⎯⎯⎯⎯⎯⎯

⎯⎯⎯⎯⎯⎯⎯⎯⎯⎯⎯⎯⎯⎯⎯ THE REAL-TIME APPLICATION

5.1 Introduction

5.1.1 Retrospective vs Real-time analysis

As expressed in the general introduction, it is sometimes necessary to detect and estimate rating shifts with the least possible delay in order to obtain more reliable streamflow data which may lead to more informed decisions, for example for the following applications:

- during a flood event for forecasters, a poorly-estimated streamflow assimilated into a flood forecasting modeling chain may compromise its reliability;

- during drought the decision-makers (Water Authorities) must know the streamflow each day in order to be able to take orders regulating the use of water resources;

- the minimum environmental flow downstream of a hydroelectric facility or a nuclear power plant must be respected continuously, hence known at all times. Upstream streamflow is also required in real time for optimizing the production and the safety of the facility.

It is important to draw a clear distinction between real-time and retrospective analyses.

The retrospective analysis is the study of the past hydrometric data (e.g. gaugings, stage record) which are fully available. In this context there is no need to detect a rating shift right

after its occurrence. A shift can be detected with a delay of one year for example and then it is possible to search back for the event most probably associated with the shift (e.g. the most intense flood). The detection of rating shifts and the periods of RC stability delimited by the shift times may then lead to the re-construction of the past hydrograph, which is essential for several purposes such as flood frequency analysis and design flood maps, or to simply classify the stations into "stable" and "unstable" categories [Morlot et al., 2014] in order to give priority to the unstable stations when planning gauging campaigns.

On the contrary, the real-time analysis is based on the analysis of any data or information available in real time to detect a shift while it is occurring or at least as soon as possible after its occurrence. Real-time analysis should be applicable before any field intervention has been performed. Therefore the real-time analysis cannot only rely on the segmentation of gaugings (Chapter 2) and the stage-recession analysis proposed in Chapter 3 can be applied only when the stage is located in a recession period. During a morphogenic flood the real-time application should use all kind of information, however uncertain it may be, to suspect a potential shift. The sediment transport proxy analysis proposed in Chapter 4 is a solution to achieve this, but other tools may be explored.

5.1.2 Solutions proposed in the literature and main difficulties

Unfortunately, while for the retrospective analysis several methods have been proposed in the literature (see the introduction of the previous chapters), less information is available on the management of rating curves in real time, and as far as we know, no formalised and automated methods have been proposed for this purpose.

The necessity of solving this issue is mentioned by Kiang et al. [2018], Mansanarez et al. [2019], Le Coz et al. [2017], Puechberty et al. [2017], but they do not propose any general protocol. In the operational practice, each hydrometric service makes use of expertise and available shift detection tools but especially of good sense for taking decisions and actions about the suspicion of a rating shift. A real-time quality check of gaugings and RC is performed but this remains very empirical, with very little automated procedure to help the operator to detect and estimate a potential shift during its occurrence.

The national (French) hydrometry quality plan [Puechberty et al., 2017] proposes to analyze the streamflow consistency with another neighboring station to detect a discrepancy either with upstream-downstream linear regression (on stage or on streamflow). Alternatively a correlation analysis can be performed between the estimated streamflow and the output of a hydrological model [Garçon, 1996], looking for discrepancies in the correlation [Puechberty et al., 2017; Lucas, 2018].

However, the basic principle discussed in this chapter is that if we succeed in providing a warning about a potential rating shift to the operator and to quantify its uncertainty in real time this would be already an important step forward. However, these estimates will necessary come with large uncertainties, and they do not intend to replace a new field measurement (e.g gauging, bathymetry) to decrease this uncertainty.

5.1.3 Outline of a real-time procedure

The functioning of such a real-time application should basically be structured around one or more methods for the detection and estimation of rating shifts and one method for the RC estimation with uncertainty. All of the traditional and emerging methods for detecting/estimating rating shifts (including the three methods proposed in the previous chapters) can be used. These tools should first be tested retrospectively by detecting all past shifts before their application in real time.

The time step of the real-time application depends on the incoming stage frequency. However many time steps may be needed before being able to detect and estimate an **effective rating shift**, i.e. a shift for which the magnitude can be estimated. In the meantime, we may want to use some tools (e.g. the sediment transport proxy analysis proposed in Chapter 4) to detect the shift as quickly as possible, thus a **potential shift**, for which the objective is to estimate its uncertainty, as opposed to its precise magnitude.
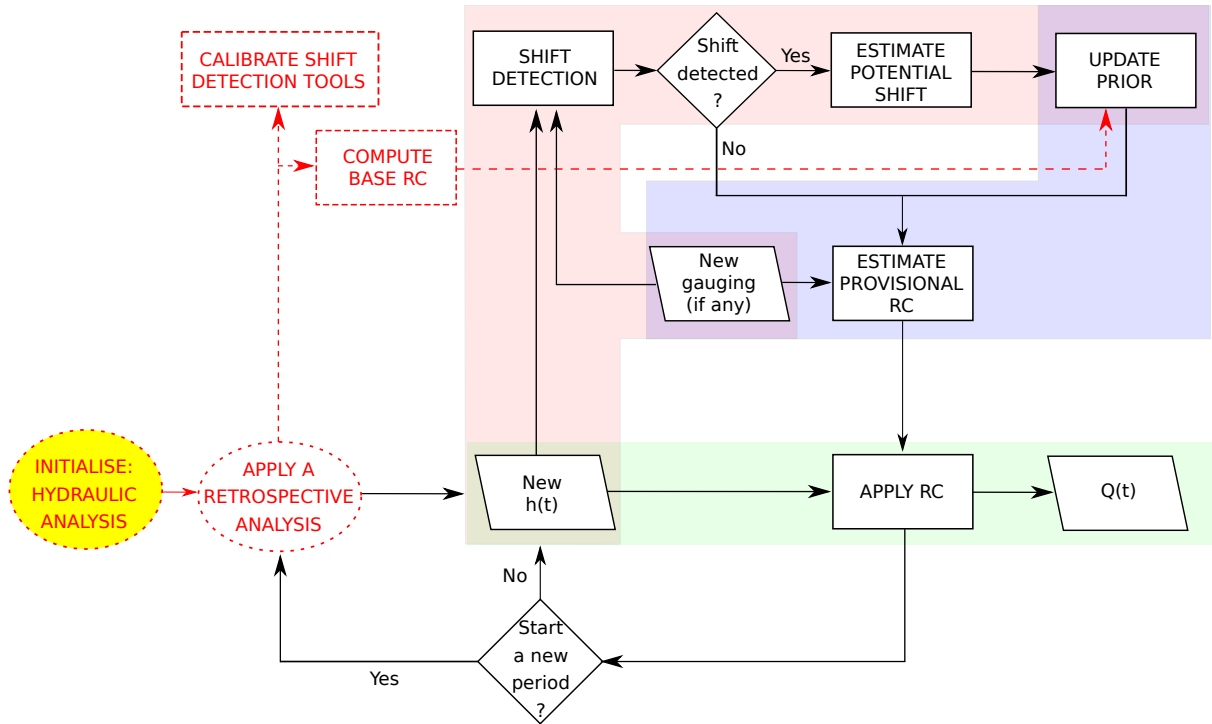
Figure 5.1: General workflow of the proposed real-time application. The area in green denotes the rating curve; the area in red denotes the shift detection tools; the area in blue denotes the updating of the provisional RC.

Let **"provisional period"** denote the period elapsed between the detection of a potential shift and its confirmation or rejection (in general, only the new gaugings or bathymetry measurements are trustworthy enough to end a provisional period and start a new stable period).

During the provisional period all intermediate estimated RCs are hereafter called **"provisional RC"** because their validity is temporary and need then to be re-estimated retrospectively once an effective rating shift is detected. The provisional RCs represent the correction of the reference RC hereafter called **"base RC"** which is the valid RC for the current period until a new effective shift is detected.

The scheme in Figure 5.1 illustrates the general functioning of the proposed real-time application. Briefly, the application performs a retrospective analysis on the entire past available period in order to calibrate the tools used for rating shift detection and to estimate the initial base RC. Then, the real-time iterations are based on the frequency of the incoming new stage data $h(t)$. At each time step t the application investigates on the existence of a

potential or an effective rating shift, and possibly estimates its magnitude and updates the prior knowledge on RC parameters. The iteration ends with the estimation of the provisional RC and the current provisional discharge estimate $Q(t)$ with uncertainty. Finally if the rating shift is confirmed the provisional RC becomes the new base RC and a new period of RC validity begins.

5.1.4   Objectives and structure of the chapter

We propose in this chapter an original protocol for the real-time management of RCs and the streamflow estimation especially during the provisional period for stations affected by sudden rating shifts. We propose to combine the tools for the fast detection of potential rating shifts and the tools for the detection of effective ones. This real-time framework is applied to a real-time re-analysis to one known morphogenic flood event on the Ardèche River at Meyras which aims at providing a proof-of-concept demo application. Sub-objectives include setting up the analysis chain, illustrating several situations that can be encountered in practice (in terms of available information and possible decisions) and gaining a first experience on what such a real-time procedure might look like in practice, including foreseeable challenges.

Section 5.2 describes each step of the real-time application. Section 5.3 shows the results of a prototype of the proposed real-time application on one flood event. Section 5.4 discusses the results of this demo along with the main limitations and the avenues for future work. Section 5.5 summarises the main findings of the proposed real-time application.

5.2 The proposed real-time application

The steps of the proposed general method for the real-time management of unstable RCs are schematized in Figure 5.1 and detailed in the following subsections.

5.2.1 Initialisation: hydraulic analysis

The application starts at time t_0 by performing the hydraulic analysis of the station to get some knowledge on the hydraulic and geometric properties of the river stretch: the average geometry of the cross and longitudinal sections; the roughness and composition of the bed material, the number, the type and the succession of the elementary hydraulic controls defining the RC model.

5.2.2 Retrospective analysis

After the hydraulic analysis and before starting the real-time iterations, a retrospective analysis is performed on the entire past period searching for all past rating shifts (and hence identifying all periods of RC stability), with three main objectives:

- Identify the type and the causes of the past rating shifts and the identification of the most unstable RC parameters. This is important for the selection of adequate tools for the rating shift detection and estimation in real time.

- Calibrate the tools for the shift detection and estimation to be used in real time.

- Estimate the "base RC" at the initial time t_0 of the real time application. To this aim we could use one of the methods proposed in the literature for the estimation of RC with uncertainty [Kiang et al., 2018] applied to the last stable period before t_0. However the "stage-period-discharge" method proposed by Mansanarez et al. [2019] is preferred since it allows the transfer of information across the periods through the common RC parameters, which is particularly important for periods with very few gaugings.

As will be explained in Section 5.2.8, this retrospective analysis is also performed every time that the beginning of a new stable period is declared.

5.2.3   Incoming stage data

While for the retrospective analysis the entire data sets of past gaugings and stage record are available, in the real time iterations the input data are unending sequence of high-frequency stage observations and low-frequency gaugings. Since the detection tools developed and used in this manuscript for fast detection of potential rating shifts are mostly based on the stage record, the real-time step Δt is adapted to the frequency of the incoming stage (e.g. 15 minutes). In this manuscript the stage data are assumed not affected by any instrumental error, but this assumption is discussed in Section 5.4.2.

5.2.4   Shift detection

Once the new stage data have been received, the application proceeds by investigating the RC stability at time t. To this aim the proposed application makes use of all available tools for rating shift detection and estimation. By default these tools are kept on stand-by until some predefined threshold is exceeded or some conditions are met. In this manuscript three tools are used:

- During floods, when the stage exceeds the triggering stage for incipient motion (see Chapter 4) the tool based on the sediment transport proxy analysis is activated and a potential rating shift is detected.

- During stage recessions, after a few consecutive days of recession, the tool based on the stage-recession analysis is activated. As described in Chapter 3, this analysis allows detecting a shift but also estimating its magnitude.

- If a new gauging is performed between two time steps then it is added to the gaugings data set of the base RC and used as input for the detection of effective rating shifts, as described in Chapter 2.

We stress that any rating shift detection tool and on-site information on the shift (photos, witnesses) can be used at this step.

5.2.5 Shift estimation

If no rating shifts have been detected using the available tools at time t then the priors for the RC parameters are not updated and the base RC is kept invariant. On the contrary, if a rating shift has been detected the validity of the current base RC is ended and a provisional period begins. In this case the real-time application proceeds with the estimation of the shift magnitude, when it is possible.

As regards the stage-recession analysis, if a shift is detected, the time series of the asymptotic stages β is segmented by applying the segmentation model with 2 predefined segments: one segment for the past recessions (which belong to the stable period before the shift) and one segment for the ongoing recession, thus with only one point (which belongs to the provisional period during/after the shift), with uncertainties. The difference between the two segment means is used to estimate the shift of the RC parameter b (offset of the low flow control) at time t obtained from the recession analysis:

$$\Delta b_{rec}(t) \sim \mathcal{N} \left(\mu_\beta(t) - \mu_\beta^*, \sqrt{(\sigma_\beta(t))^2 + \left(\sigma_\beta^*\right)^2} \right) \tag{5.1}$$

where $\mu_\beta(t)$ and μ_β^* indicates the mean of the estimated parameter β for the current provisional period at time t and for the past stable period, respectively, while $\sigma_\beta(t)$ and σ_β^* are their standard deviation.

The sediment transport proxy analysis leads to the estimation of potential shift of parameter b at time t, by using the relation between the cumulative sediments volume and the magnitude of the potential shift (as described in Chapter 4):

$$\Delta b_{ST}(t) \sim \mathcal{N} \left(0 \; ; \; \xi \, V(t) \right) \tag{5.2}$$

where the mean of the shift is zero (corresponding to a potential change), unlike in Equation 5.1, and the standard deviation is proportional to the cumulative sediment volume $V(t)$ computed from the beginning of the flood event t_{in} to time t.

As regards the segmentation of gaugings, the inclusion of a new gauging does not directly

provide the estimate of a shift of a specific RC parameter. The rating shift can be estimated only after the estimation of the provisional RC (where the new gauging is used as calibration data) by comparing the RC parameters of the past base RC and those of the actual provisional RC.

Finally, it may happen that at time t more than one tool lead to the estimation of the rating shift (e.g. $\Delta b_{ST}(t)$ from the sediment transport proxy analysis, $\Delta b_{rec}(t)$ from the stage-recession analysis). In this manuscript the combined shift estimate $\Delta b(t)$ is equal to the shift estimate having the smallest standard deviation, but alternative choices are discussed in Section 5.4.3.2.

5.2.6 Update of RC priors and RC estimation

The RC estimation is here performed through a Bayesian approach, which requires the gaugings and the prior distributions of the RC parameters and provides their posterior distributions. In the real-time context at time t we could have the four main following situations:

1. No detected shift and no new gaugings: the RC priors are taken equal to the posteriors of the current base RC, thus in fact the estimated RC is equal to the base RC.

2. No detected shift and a new gauging: BaRatin method [Le Coz et al., 2014] is used for the RC estimation by using the new gauging and transferring information (on the RC parameters) from the base RC through the prior specification.

3. Shift detected by the gauging segmentation: in this case we enter in a provisional period and the validity of the base RC is ended. All the past gaugings now belong to the past base RC. Only the new gauging is used to estimate the provisional RC at time t. The BaRatin-SPD developed by Mansanarez et al. [2019] can be used to allow the transfer of the information on the parameters in common between the past base RC and the current provisional period. Assumptions on the stable and unstable RC parameters are necessary: e.g. all parameters remain unchanged except for parameter b of the low flow control. Since no estimate on Δb is available a weakly informative prior is specified for b.

4. Shift detected and estimated (e.g. using the tool based on the stage-recession analysis or on the sediment transport proxy analysis): the prior on the corresponding unstable RC

parameter (e.g. $b(t)$) needs to be updated as:

$$b(t) \sim \mathcal{N}\left(\mu_b^* + \mu_{\Delta b}(t); \sqrt{\left(\sigma_b^*\right)^2 + \left(\sigma_{\Delta b}(t)\right)^2}\right) \qquad (5.3)$$

where μ_b^* and σ_b^* are the posterior mean and posterior standard deviation, respectively, of parameter b from the base RC right before the beginning of the provisional period, and $\mu_{\Delta b}(t)$ and $\sigma_{\Delta b}(t)$ are the mean and the standard deviation, respectively, of the shift estimate $\Delta b(t)$ during the provisional period at time t. If there are not new gaugings then the RC estimation is done through prior propagation, otherwise it is performed by using the BaRatin method.

5.2.7   Discharge computation

The new RC is used to compute the discharge $Q(t)$ (the main output of each time iteration). This is a standard RC procedure in hydrometry and leads to the most probable value of $Q(t)$ (MAP) and its uncertainty [Le Coz et al., 2014].

5.2.8   Start of a new stable period

At the end of the real-time iteration, after having provided the provisional RC and the value of discharge at time t, we need to decide whether or not a new stable period starts after this iteration. Considering the situations described in the previous step:

- For situations 1 nd 2, the stable period is still ongoing.

- For situations 3 and 4, the provisional RC becomes the new base RC only if there are new gaugings. In this case a new retrospective analysis is performed with the addition of the newly detected shift information to update the calibration of the tools for rating shift detection. When there are no new gaugings the provisional period proceeds.

The next section illustrates a prototype of the proposed real-time method applied to the case study of the Ardèche River at Meyras in France during one flood event.

5.3 Application to the Ardèche River at Meyras: a demo

5.3.1 Overview of the application

A real-time re-analysis is applied to one morphogenic flood event at the Meyras station on the Ardèche River (France). The hydraulic analysis and the retrospective analysis are performed at time t_0. A truly real-time context is studied, by fully ignoring any data that would not be available at time t_0. The retrospective analysis detects and estimates all past rating shifts in order to calibrate the shift detection tools and estimate the stable RC at t_0. Next, the crucial real-time conditions for the studied event are:

- A first period where the RC is stable and equal to the base RC (no shifts are detected).

- The occurrence of a morphogenic flood inducing a potential rating shift. The sediment transport proxy model proposed in Chapter 4 is used to provide an estimate on the potential shift uncertainty. Consequently the RC uncertainty increases as the cumulative volume of transported sediments increases.

- A recession period after the flood peak. The stage-recession analysis proposed in Chapter 3 is used. The longer the recession period, the more precise the estimation of the asymptotic stage becomes, and consequently the RC uncertainty may be refined with time.

- Finally the arrival of new gaugings may confirm or dismiss the rating shift previously detected. The segmentation procedure applied to gaugings and proposed in Chapter 2 is used to this aim. If the shift is confirmed, then a new RC stable period begins.

Figure 5.2 illustrates the selected period for the analysis, subdivided in two parts by the initialization time t_0: the retrospective analysis and the real-time analysis. t_0 is chosen such that the RC stability is ensured: no floods located nearby, no new gaugings since the previous stage data and a very low stage value.

5.3.2 The retrospective analysis

The retrospective analysis has been performed on the stage record and the gaugings preceding t_0. The results are summarised in Figure 5.3.
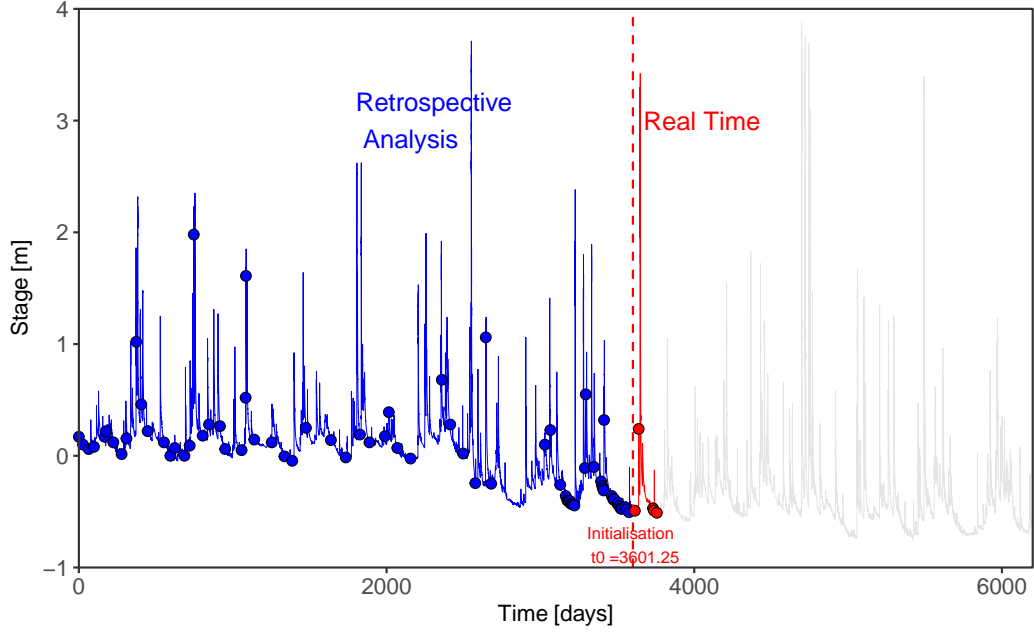
Figure 5.2: Selection of the period for the real-time analysis (in red) as well as for the retrospective analysis (in blue) applied to the Ardèche River at Meyras. The real-time initialisation of the application is indicated by the time t_0. Points on the stage record indicate the gaugings.

The stage-recession analysis is here performed using the model and the parameter χ that lead to the most accurate estimation of shift times and magnitudes for the application of Chapter 3: M2 (two superposed exponential terms and one asymptotic stage parameter), $\chi = 50$ cm and all other options for the stage-recession extraction used in the application of Chapter 3. Then, the posterior distributions of the common parameters of the stage-recession model will be used as priors for the recession estimation during the real-time iterations, as described in Section 3.4.2 of Chapter 3.

The combined results of the segmentation of gaugings and of the stage-recession analysis are used to define the four RC stable periods of the retrospective period. A BaRatin-SPD analysis [Mansanarez et al., 2019] is performed to estimate the RC for each period (Figure 5.4a). Figure 5.4b also shows the boxplots of the estimation of RC parameters b_1 (mean elevation of the natural riffle) and b_2 (mean elevation of the main channel bed), assumed to be the only two unstable parameters for this case study.
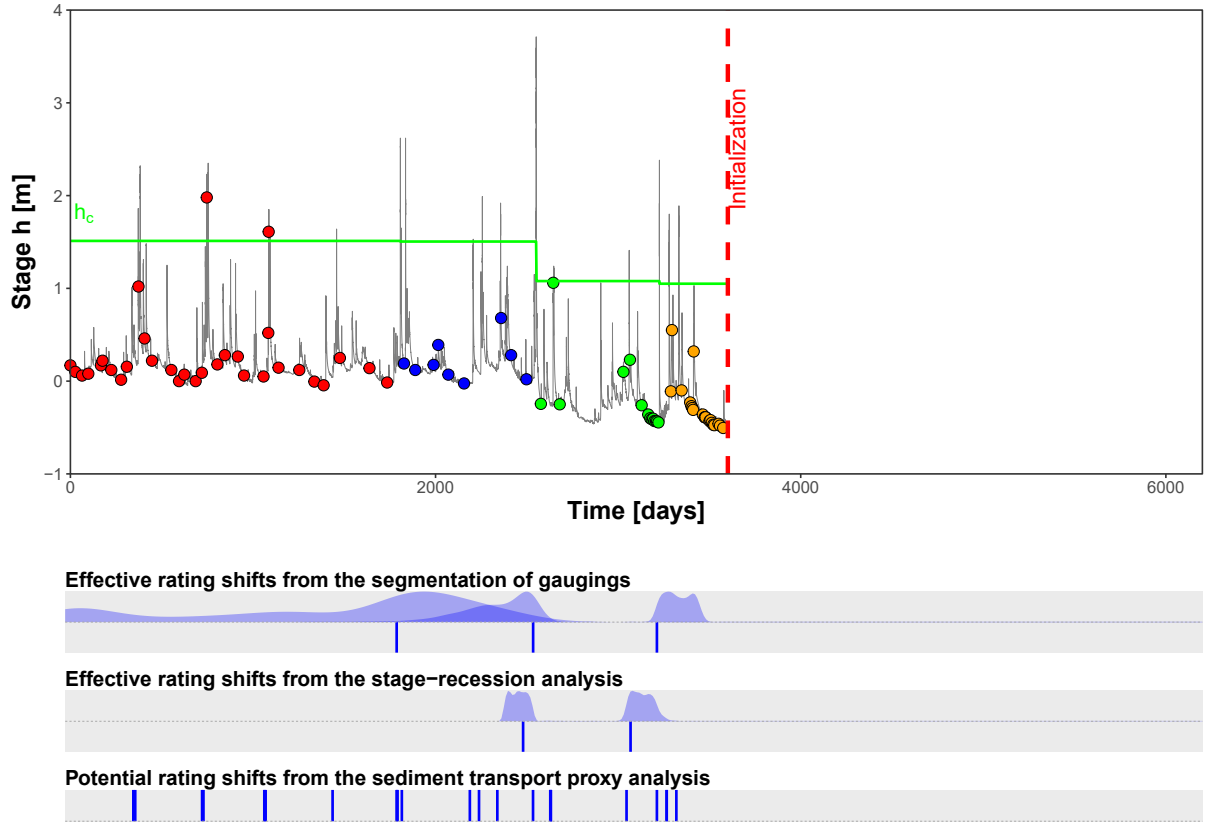
Figure 5.3: Results of the retrospective analysis applied to the Ardèche River at Meyras in terms of the detected shift times (and their pdfs). Three tools have been used: the segmentation of gaugings, the stage-recession analysis for detecting effective rating shifts and the sediment transport proxy analysis for detecting potential rating shifts.

These combined results are then used to calibrate the sediment transport proxy analysis. Firstly, the triggering stage h_c is computed and reported in green in Figure 5.3. This leads to the detection of several other potential rating shifts. Secondly the sediment transport, and in particular its cumulative volume, is computed. A relation between the cumulative volume of sediments transported during the morphogenic event and the associated potential rating shifts Δb_1 and Δb_2 is then established (as described in Chapter 4) and shown in Figure 5.5. At this stage, only three calibration data $(V, \Delta b)$ are available.

Finally, the BaRatin-SPD analysis [Mansanarez et al., 2019] also provides the estimate of the stable rating curve (base RC) preceding the initialisation and still valid at time t_0. The initial conditions of the real-time application, including the data and the RC of the last stable
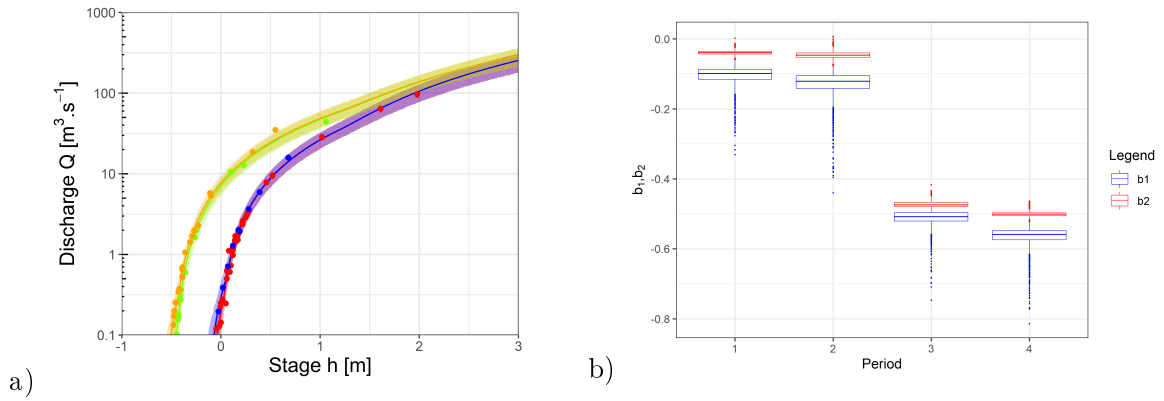
Figure 5.4: a) Estimation of the RC for each of the four past stable periods using BaRatin-SPD [Mansanarez et al., 2019]. Colors correspond to Figure 5.3. b) Boxplots of RC parameters b_1 and b_2 for each period.
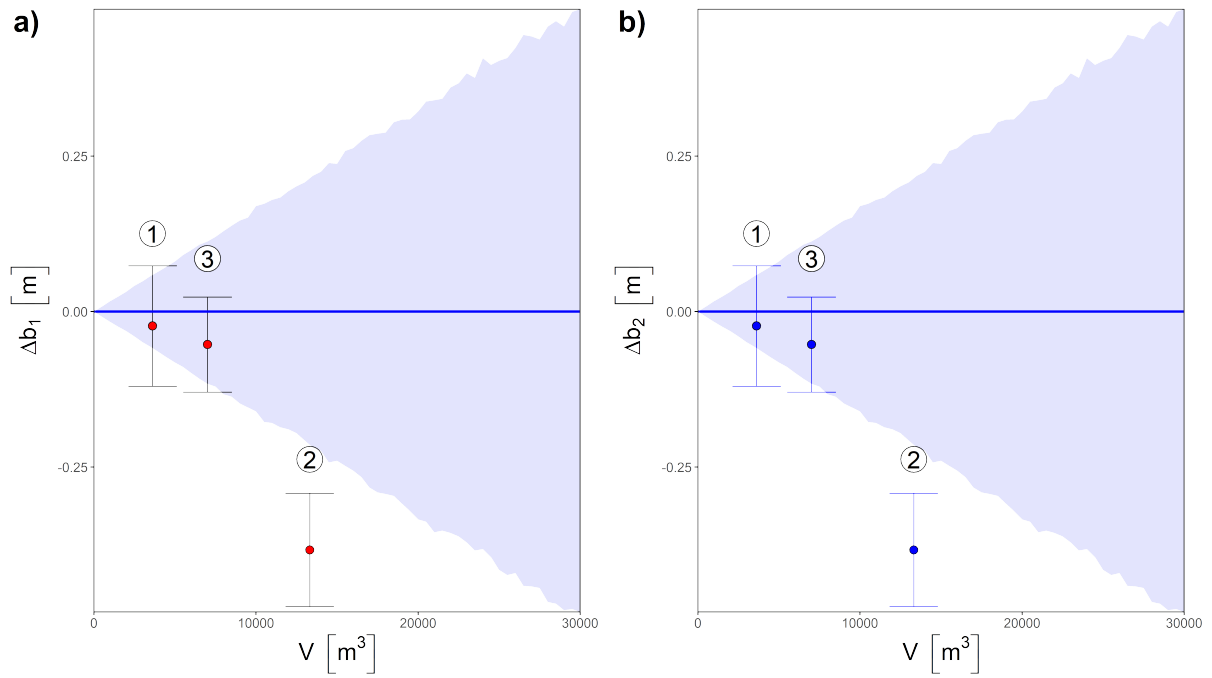
Figure 5.5: Results of the retrospective sediment transport analysis applied to the Ardèche River at Meyras: relation between the cumulative sediments volume V and the rating shifts Δb_1 and Δb_2. The blue ribbon illustrates the total 95 % uncertainty interval for the shift. The number above the points indicate the indexes of the reference morphogenic events.

period, are illustrated in Figure 5.6.

More specifically, Figure 5.6A reports the discharge time series $Q(t)$ with uncertainty and the stage record $h(t)$ for the last stable period preceding the initial time t_0 (indicated with a vertical red line). Also the past gaugings are shown by dots and the triggering stage h_c for the detection of morphological shifts (see Chapter 4) is reported against the stage record (by green dashed line).

Figure 5.6B shows the current base RC with total uncertainty valid at time t_0. The intersection of the two dashed black segments indicates the current position along the RC.

Figure 5.6D shows a very schematic representation of the river cross-section in order to visualize the current hydraulic conditions. Elevation z indicates the elevation with respect to the zero of the stage recording instrument. Water flowing through the river is represented in light-blue (however time t_0 is characterised by very low-flow conditions thus the water table is very close to the main channel bed). The triggering stage h_c is also represented.

Finally Figure 5.6C represents the shift detection toolbox, where the results of the three tools proposed in this manuscript for rating shift detection are presented. For each tool, on the top-right corner of the plot, a traffic light is used to indicate whether the tool is activated or not. In particular, the light is:

- **green:** the tool is on stand-by;

- **yellow:** the tool is activated but no rating shift is detected

- **red:** the tool is activated and a rating shift is detected

The proposed application makes use of (from top to bottom of Figure 5.6C):

- the segmentation of the residuals between the gaugings and the base RC (procedure described in Chapter 2). If no new gauging is performed then no rating shift warning is provided by this tool keeping the light on "green". For the next time iterations every time that a new gauging is performed, its residual with respect to the base RC (with uncertainty) is then computed and plotted here and the light is turned on "yellow". The

segmentation procedure is then applied to the time series of the residuals looking for one shift. The mean of the residuals is reported by the horizontal red segment.

- The sediment transport proxy analysis (see details in Chapter 4). If the current stage is below the triggering stage h_c no potential rating shifts are detected by this tool and the light is kept on "green". The volume of transported sediments V in this case is equal to zero. Instead, when the actual stage exceeds the triggering stage h_c, the light is turned on "red" warning for a potential rating shift. The sediment transport volume is in this case larger than zero and the relation in Figure 5.5 is used to estimate the uncertainty of the potential shifts $\Delta b1$ and $\Delta b2$, thus to increase the uncertainty on corresponding RC parameters.

- the stage-recession analysis (Chapter 3). If the current stage is not in a recession period then no warning for rating shift is provided by this tool, keeping the light on green. Instead, when the current stage is located in a recession period then the new stage data is plotted and the light is turned on "yellow". If the number of the stage-recession data and the duration of the recession period are larger then the minimum number N_{min} and minimum duration t_{min}, respectively, then the stage-recession analysis is performed.

Subsequently, each new incoming stage data define the following iterations of the real-time application. The following subsections will focus on the most crucial iterations.
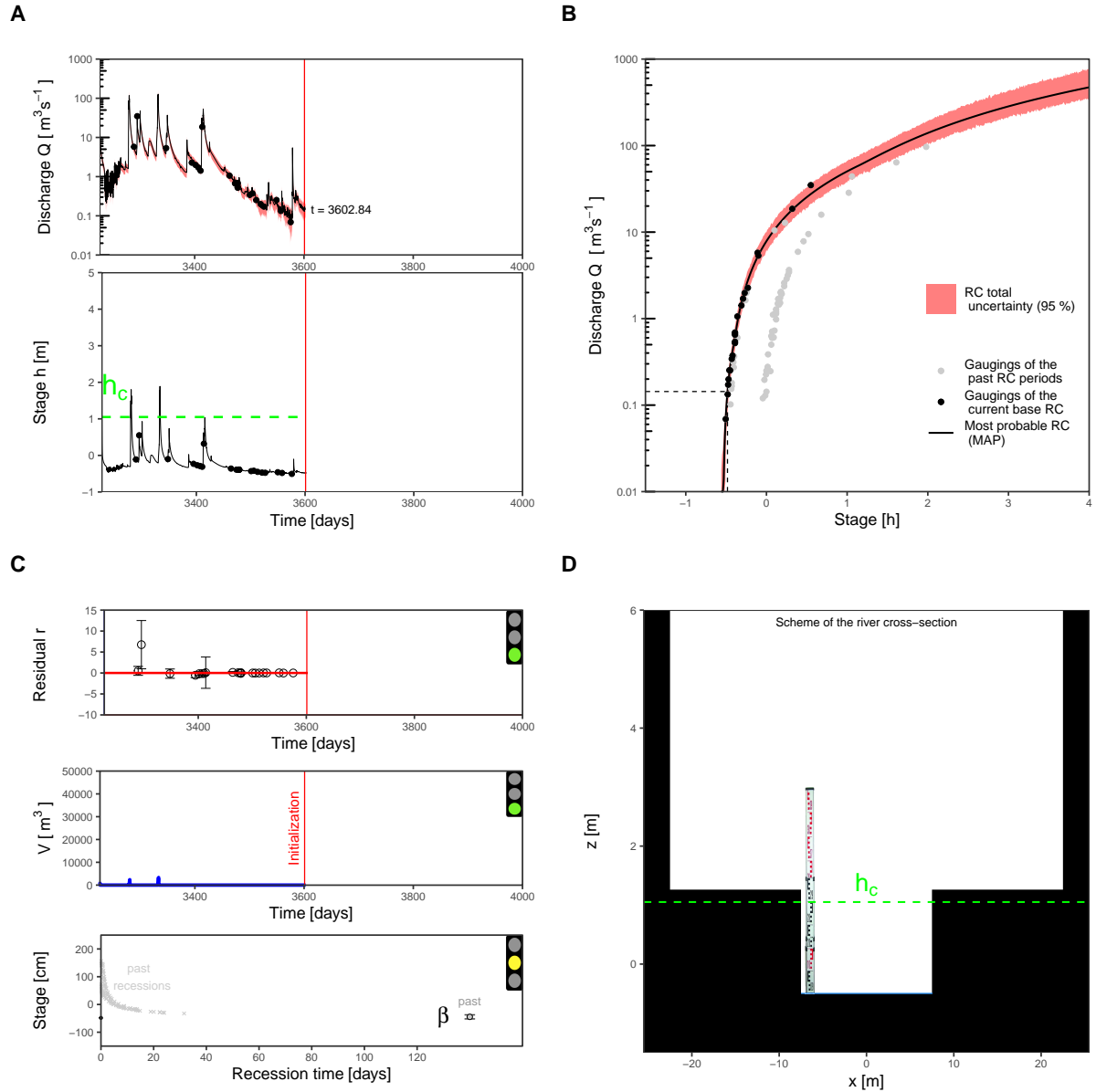
Figure 5.6: Results of the proposed real-time application to the Ardèche River at Meyras from the initialization time 3600. A) discharge and stage time series B) RC with uncertainty and gaugings, C) toolbox with three tools for rating shift detection, D) schematic representation of the river cross-section geometry. Iteration 0.

5.3.3 Iteration 15: recession analysis but no shift

Figure 5.7 illustrates the results for iteration 15. In the first period that follows the initial time t_0 the stage is located in a recession period and much below the triggering stage (hence there is no flood and the tool based on the sediment transport analysis is on stand-by). Moreover no new gaugings are performed, thus the tool based on the segmentation of gaugings is on standby.

Instead since the stage is decreasing the tool based on the stage-recession analyses is activated (light is turned on yellow) and since the recession is longer than 5 days the stage-recession estimation is performed. The uncertainty of the recession curve is represented in green. The asymptotic stage parameter of the current recession β is represented with a green dot with error bars. The segmentation of the time series of the current and past estimates of parameter β does not detect any shifts, mainly because of the large uncertainty of the recession estimation. Thus, the base RC is still valid.
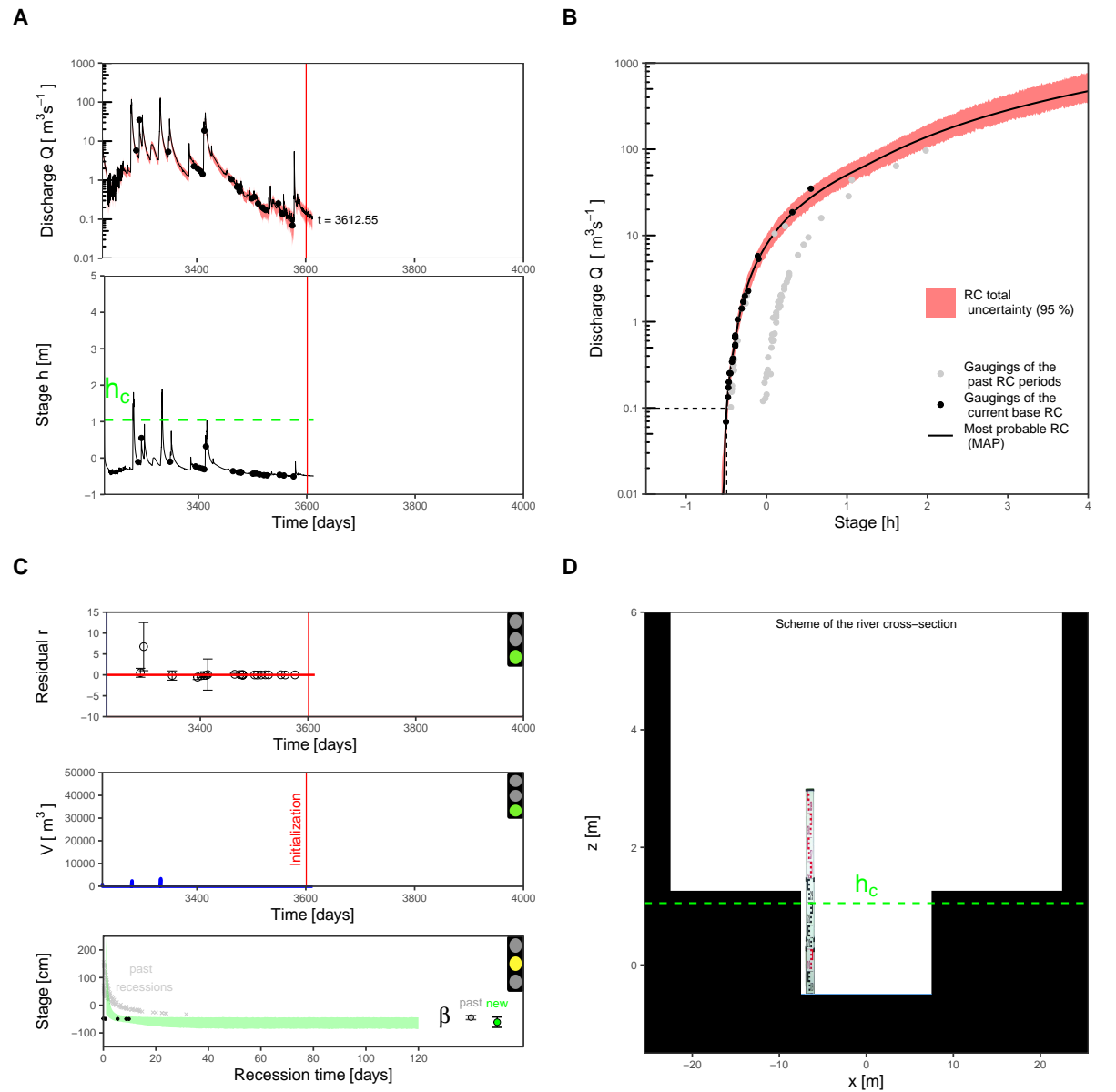
Figure 5.7: Same as Figure 5.6 for iteration 15.

5.3.4 Iteration 16: recession analysis and new gauging but no shift

Figure 5.8 illustrates the results for iteration 16. At this iteration the stage is still located in a recession period below the triggering stage, a new stage-recession regression is performed but still the segmentation of the time series of the estimates of β does not detect any shifts.

However between the previous and actual iteration a new gauging has been performed. It is added to the gaugings data set of the current stable period. The tool based on the segmentation of the residuals between the gaugings and the base RC is activated and the light turns on yellow. The tool does not detect any shifts. However the base RC is refined accounting for the new gauging.
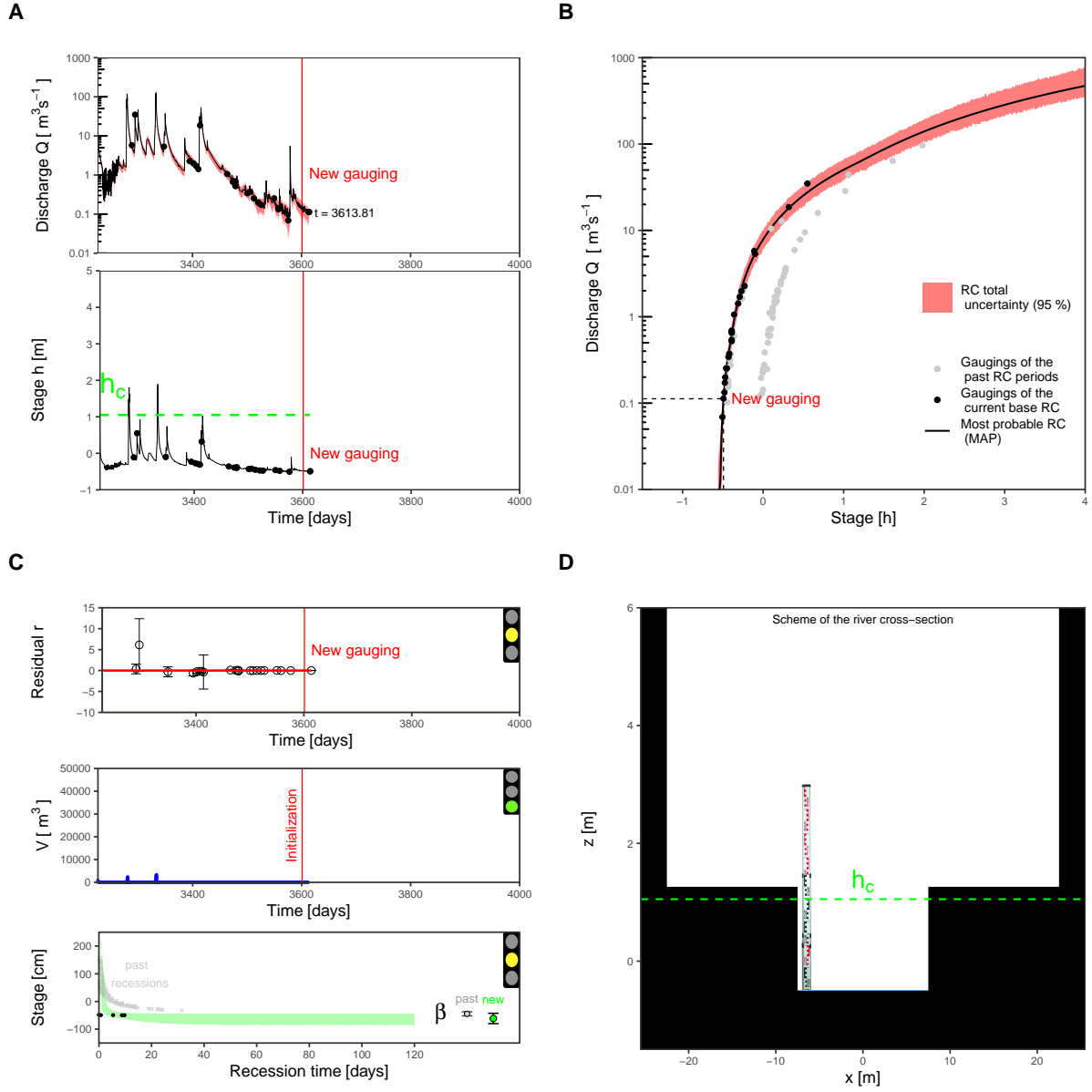
Figure 5.8: Same as Figure 5.6 for iteration 16.

5.3.5 Iteration 82: exceedance of the triggering stage and detection of a potential shift

Figure 5.9 illustrates the results for iteration 82. At this iteration the stage-recession analysis cannot be performed because the stage is increasing, thus the tool is kept on standby. Moreover, no new gaugings have been performed thus also the tool based on the segmentation of gaugings is kept on standby.

Instead, the stage $h(t)$ slightly exceeds the triggering stage $h_c(t)$ for sediment incipient motion. Hence, a potential flood-induced rating shift is detected and the tool based on the sediment transport analysis is activated (red light). This iteration defines the beginning of a morphogenic flood event. The volume of transported sediments cumulated from the beginning of the event $V(t)$ is computed through the proxy model described in Chapter 4. This tool provides also an estimate on the uncertainty of the rating shift through the relation $V - \Delta b_{ST}$ established in retrospective (Figure 5.5), so that for each value of V corresponds an estimate of the shift magnitude Δb and in particular of its uncertainty.

The priors of parameters $b_1(t)$ and $b_2(t)$ are thus updated accounting for the rating shift using Equation 5.3 with $\sigma_{\Delta b_1}(t)$ and $\sigma_{\Delta b_2}(t)$ around 0.0003 m and $V = 28$ m^3. At such an early stage of the flood, the potential shift cannot be too large. However, since the available gaugings are now potentially not valid anymore, the base RC is obsolete and the new provisional RC is now estimated through prior propagation only.
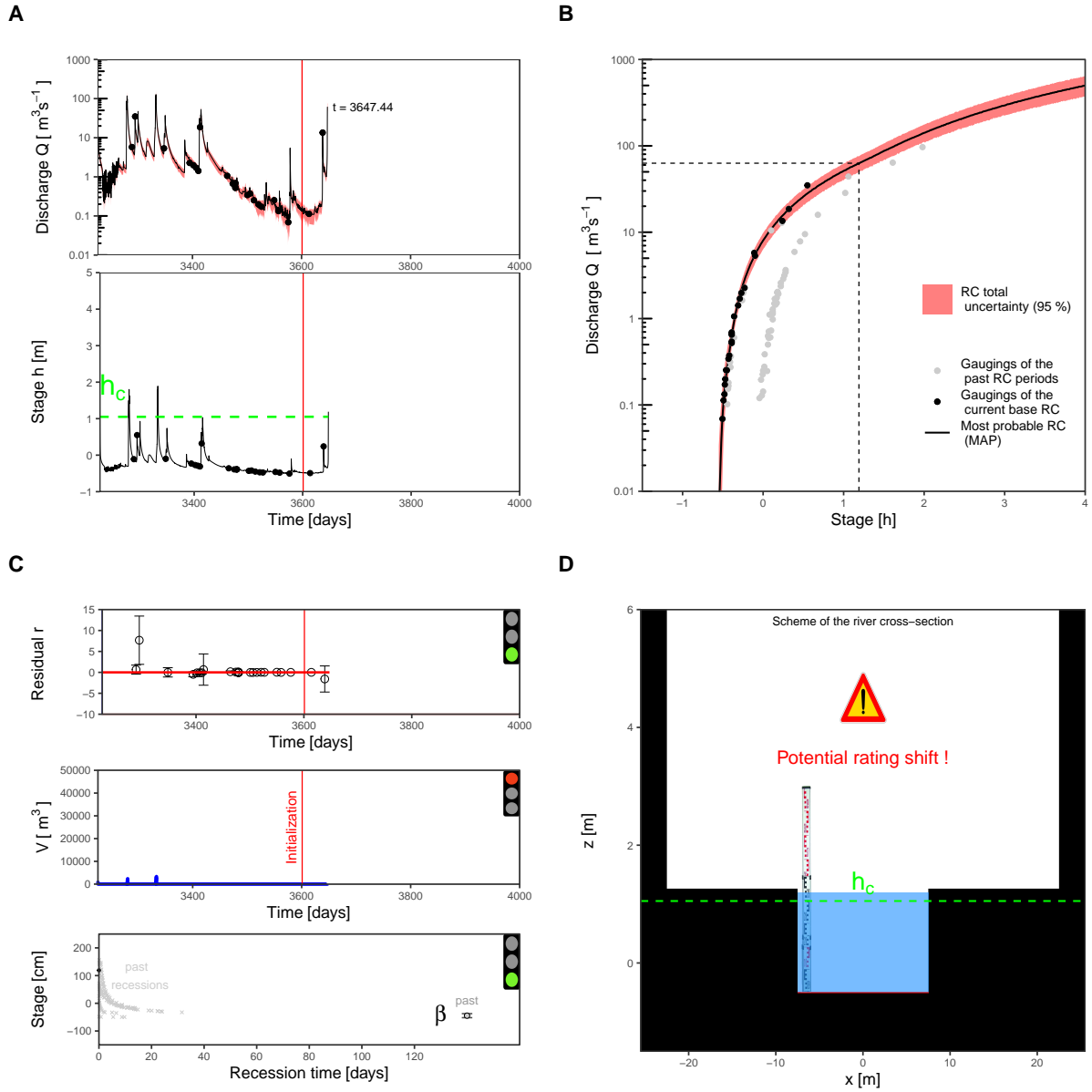
Figure 5.9: Same as Figure 5.6 for iteration 82.

5.3.6   Iteration 191: flood peak

Figure 5.10 illustrates the results of iteration 191. This iteration is similar to iteration 82. However the stage $h(t)$ is now well above the triggering stage $h_c(t)$ and the volume of transported sediments cumulated from the beginning of the event $V(t)$ is much larger than in iteration 82. The relation $V - \Delta b$ (Figure 5.5) is used to estimate the rating shift $\Delta b_{ST}(t)$ and in particular its uncertainty.

As for iteration 82 the RC is merely estimated through a prior estimation by updating the priors of parameters $b_1(t)$ and $b_2(t)$ of the base RC using Equation 5.3. However, at this iteration $\sigma_{\Delta b_1}(t)$ and $\sigma_{\Delta b_2}(t)$ assume values around 0.17 m and $V = 21520$ m^3, thus the uncertainty of the new provisional RC (and consequently of the discharge) is now very large. The uncertainty on prior b_2 is also illustrated with a red ribbon in Figure 5.10D.
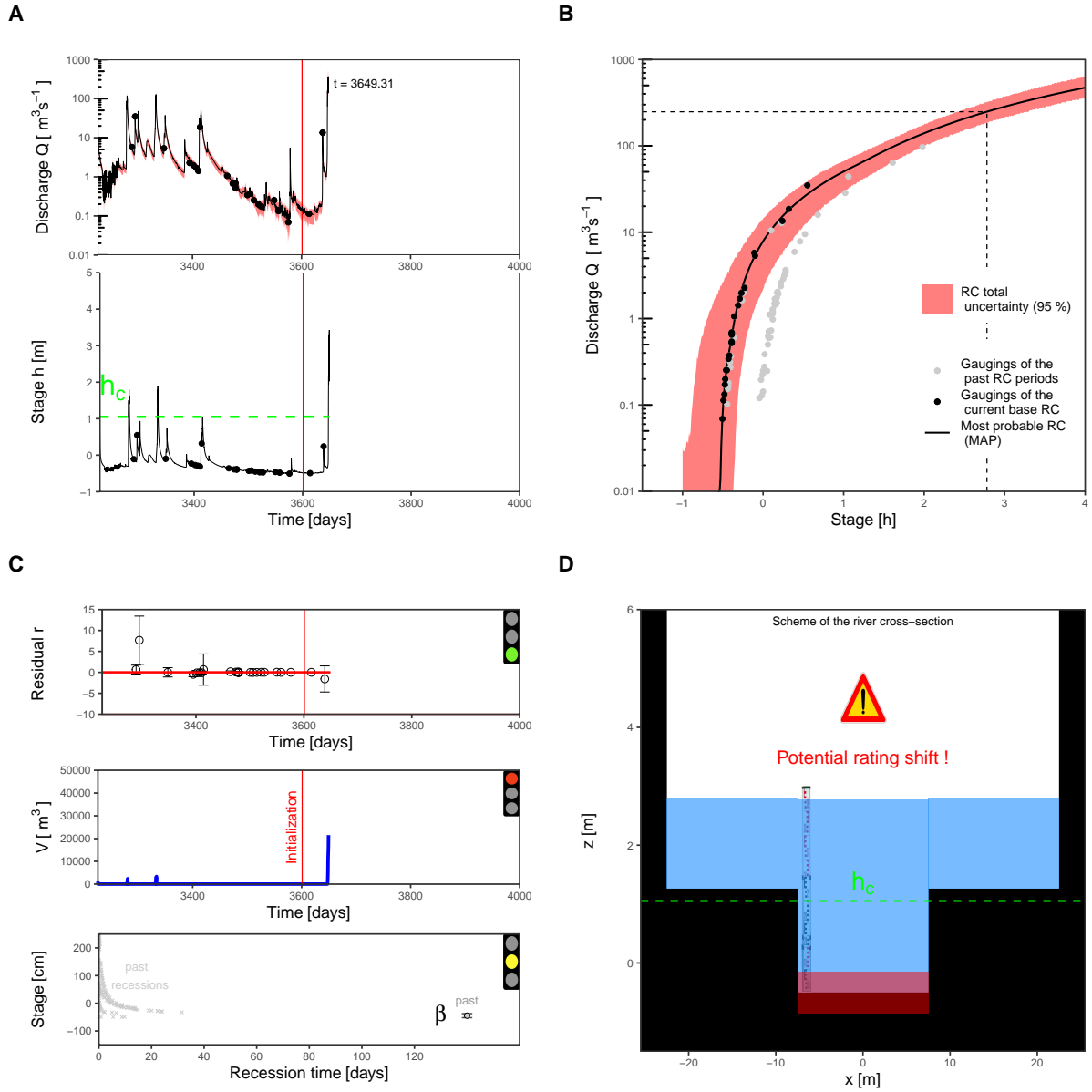
Figure 5.10: Same as Figure 5.6 for iteration 191.

5.3.7 Iteration 287: application of the stage-recession analysis after the flood

Figure 5.11 illustrates the results of iteration 287. At this iteration no new gaugings are performed thus the tool based on the segmentation of gaugings is kept on standby. Instead, the stage is located in a recession period after the flood peak, with a length larger than 5 days. Thus a stage-recession analysis can be performed. The estimated recession is illustrated in green.

Then, the segmentation of the estimated asymptotic level parameters β does not lead to the detection of any shift. Even though the recession analysis does not detect at this iteration a rating shift, it does provide a valuable uncertainty $\Delta b_{rec}(t)$ on it as defined by Equation 5.1. If this uncertainty is inferior to the one obtained through the sediment transport analysis $\Delta b_{ST}(t)$ it can be used to refine the prior on $b_1(t)$ and $b_2(t)$ as explained in Section 5.2.5. Thus also the new provisional RC shows a smaller uncertainty compared with the previous iterations.
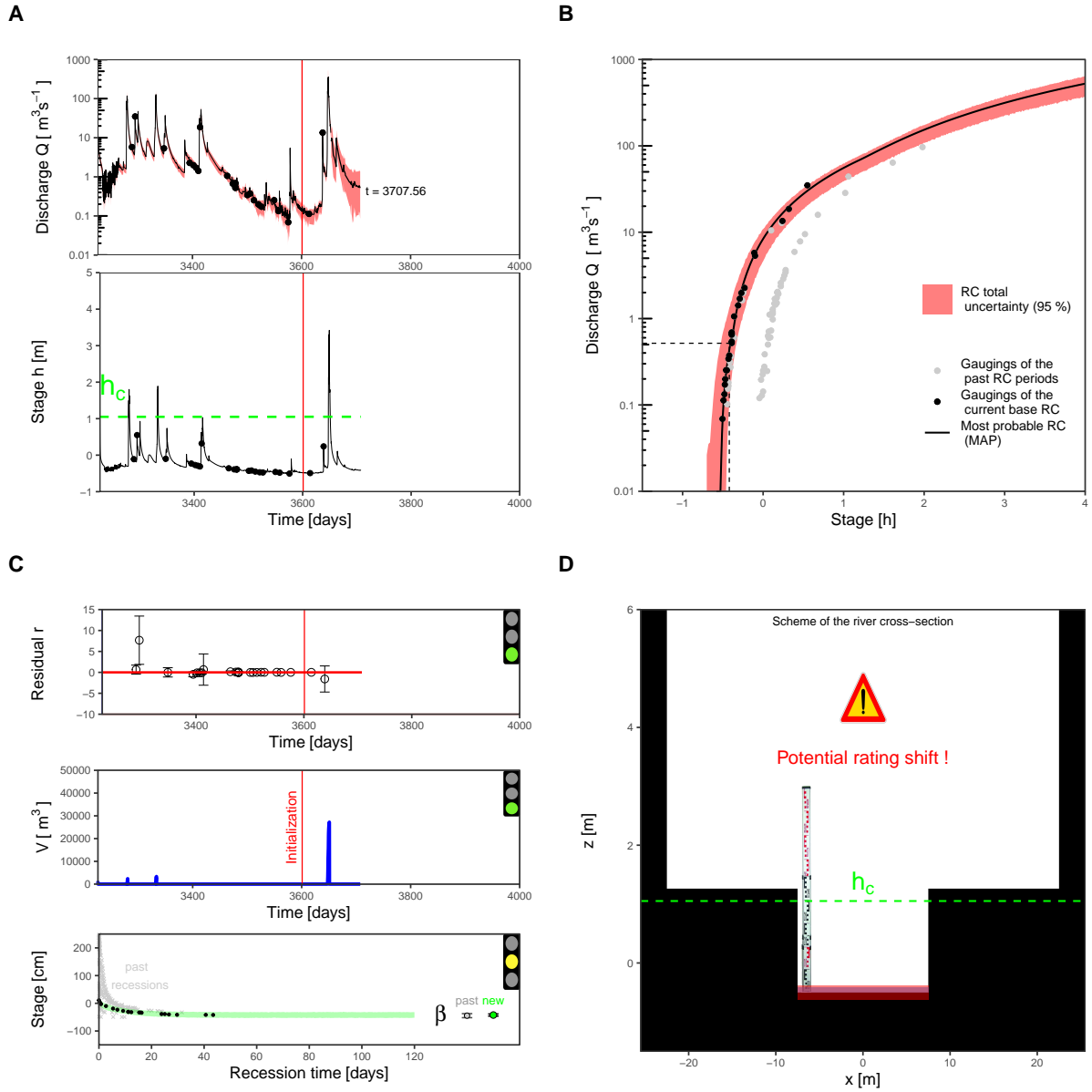
Figure 5.11: Same as Figure 5.6 for iteration 287.

5.3.8   Iteration 311: new gauging and rating shift confirmation

Figure 5.12 illustrates the results of iteration 311. At this time step a new gauging has been performed. Thus, the tool based on the segmentation of gaugings is activated. A shift is detected. Thus the ligth is turned on "red". This corresponds to an effective rating shift, which means that the provisional period is ended and that a new base RC can be estimated using the new gauging.

The stage is still located in a recession period, thus the estimation of the rating shift Δb_{rec} is used to update the prior before the RC estimation with the new gauging. The new gauging confirms the potential rating shift previously detected by the sediment transport analysis and refines the estimation of parameters b_1 and b_2. The estimated shifts Δb_1 and Δb_2 are quite small, around -0.066 m and -0.092 m, respectively. This possibly explains why the change wasn't detected by the stage-recession analysis.

This time step determines the beginning of a new stable period.

5.3.9   Summary of the application

In conclusion, during this application we have tested the tools for rating shift detection in real time during a morphogenic flood event known to have caused a minor shift of the RC. The tool based on the segmentation of gaugings does not detect any shifts when there are no shifts (before the flood) and instead detects the minor shift when the first gauging is performed after the flood. The sediment transport analysis properly detects a potential rating shift which is confirmed subsequently. Moreover the estimation of the shift uncertainty through the relation $V - \Delta b$ provides a useful information on the RC uncertainty during the flood. On the other hand the tool based on the stage-recession analysis shows some difficulties in detecting a minor shift. However, it provides a very useful information on the rating shift uncertainty which may reduce the one provided by the sediment transport analysis, leading to more reliable streamflow uncertainty.
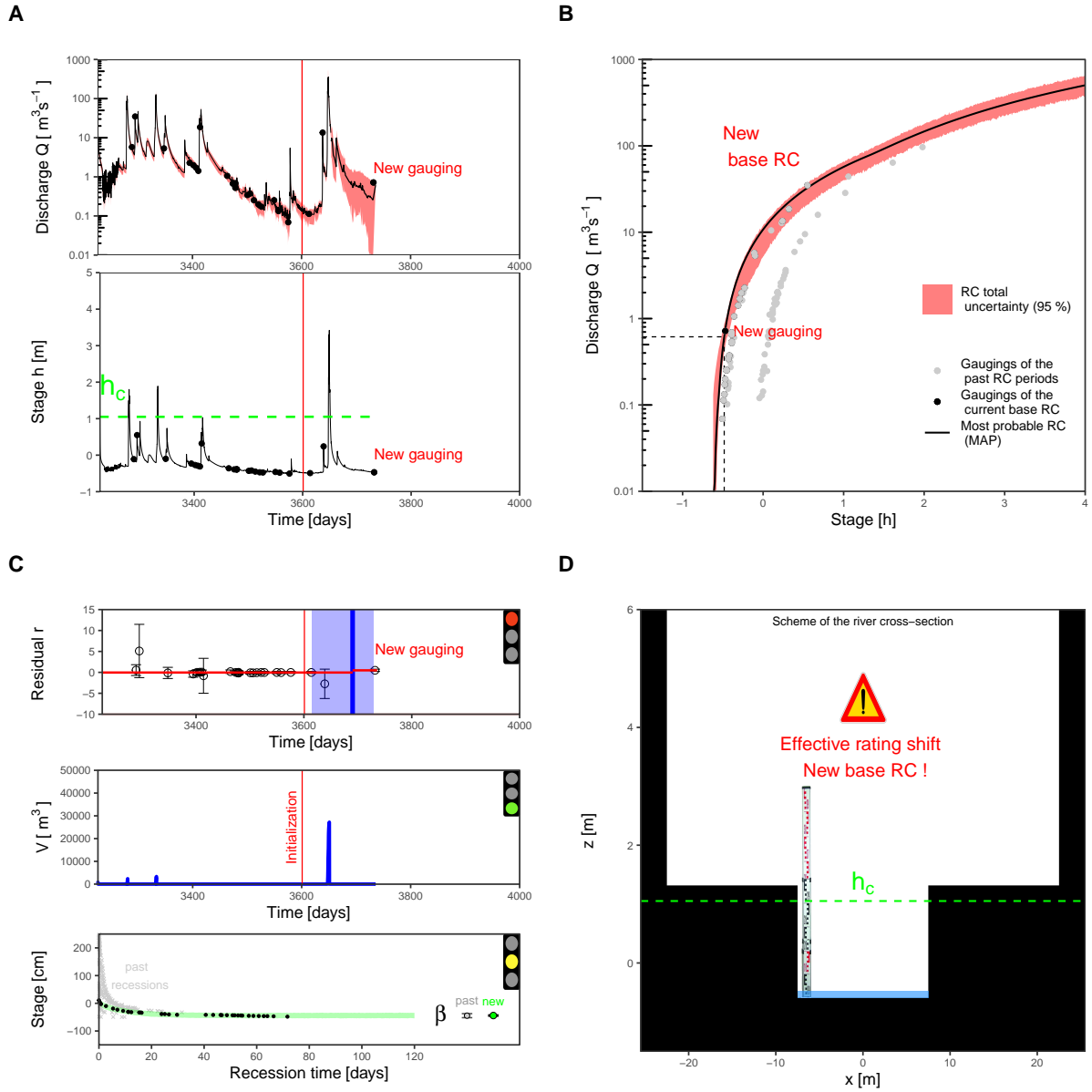
Figure 5.12: Same as Figure 5.6 for iteration 311.

5.4 Discussion

5.4.1 Main limitations

While the scheme of the proposed application for the real-time management of rating shifts is conceived to account for general real-time situations, it still have some limitations. Some of these limitations are related to the tools used for the shift detection and are already discussed in the previous chapters. More specifically related to the real-time framework itself, the structure of the proposed method is conceived for the management of rating shifts only. Instead, managing transient shifts, such as those induced by the growth/decline of aquatic vegetation, may require a dynamic RC modelling [Perret et al., 2021] which, in turn, may require a specific adaptation to the real-time context.

5.4.2 Stage pre-treatment

In this application the uncertainty in the stage input data is ignored. However, this uncertainty may sometimes be not negligible [Horner et al., 2018], especially in a real-time context. The stage observation may be affected by a general noise (due to instrument sensitivity or to the water surface oscillations induced by high flow conditions) that need to be filtered out, or by instrumental bugs (due to data logger issues or to icing conditions) that need to be corrected before the stage can be exploited (Figure 5.13).

Future perspectives of the proposed method include some pre-treatments of the raw stage measurements. Figure 5.13 schematizes three possible situations discussed in Puechberty et al. [2017]:

1. The instrument breaks down or is frozen, then the stage raw signal appears frozen too. As long as the instrument is out of order, no correction of the signal is possible. A solution needs to be found to provide streamflow estimate during this latent period.

2. Sudden instrumental bugs may also occur causing invalid aberrant stage values. These bugs can easily be corrected retrospectively by interpolation (on short periods at least), but this issue is more challenging in real time.
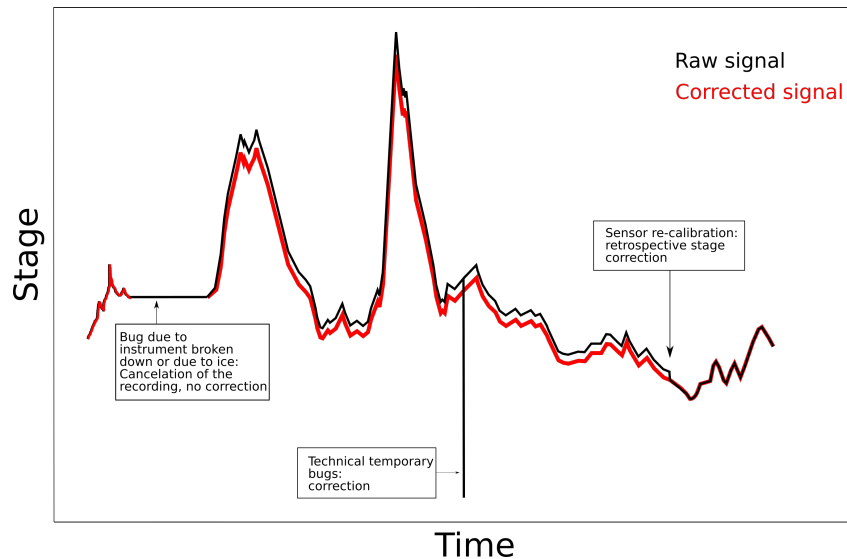
Figure 5.13: Stage errors examples. Adapted from Puechberty et al. [2017].

3. Moreover sensors may sometimes need to be re-calibrated and the stage data need to be retrospectively corrected.

5.4.3 Future perspectives

5.4.3.1 More thorough evaluation of the method

Several possible improvements and tests are planned for future work. Before its operational implementation the proposed real-time application certainly needs several validation tests in order to better understand its performance and its applicability conditions.

The proposed application needs to be tested on several other case studies preferably characterised by different hydraulic configurations (possibly more complex than the one of Meyras, such as twin-gauge stations), by different hydrological behavior (such as those with high-frequency floods) and by different sediment transport characteristics (different grain-size distribution).
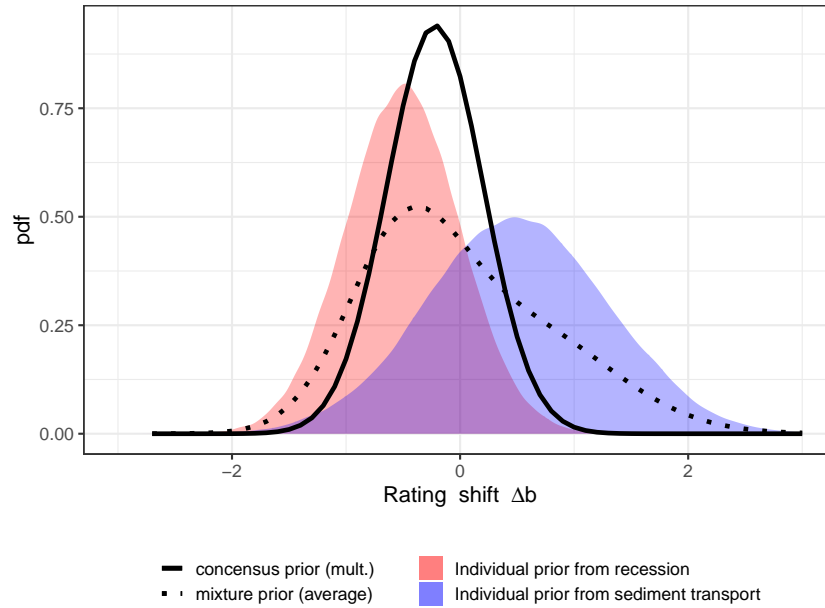
Figure 5.14: Example of two approaches for combining two distinct individual priors on the same rating shift Δb.

5.4.3.2 Combining the shift estimates from multiple sources

It may happen at some iterations that multiple sources of information are available about the rating shift. Therefore we may want to aggregate the different probability estimates. The issue of combining different "opinions" has been studied in the literature: e.g. by Genest and Zidek [1986] or more recently by Albert et al. [2012] and Dietrich and List [2014]. However no unique and general solutions have been provided yet.

Figure 5.14 proposes an example of two possible approaches for combining the prior on the rating shift obtained from the stage-recession analysis $\Delta b_{rec} \sim \mathcal{N}(\mu_{\Delta b_{rec}}, \sigma_{\Delta b_{rec}})$ with the one obtained by the sediment transport proxy analysis $\Delta b_{ST} \sim \mathcal{N}(\mu_{\Delta b_{ST}}, \sigma_{\Delta b_{ST}})$ into an unique prior by:

1. considering the product of the two pdfs (consensus prior) which in this case is also Gaussian.

2. averaging the two pdfs (mixture prior).

Further work is needed to apply the approaches proposed in the literature to the real-time operational management of RCs.

5.4.3.3 Adding other tools for detecting rating shifts

Other tools for rating shift detection and estimation are planned to be developed in future work and are further discussed in Chapter 6, such as:

- correlation analysis with the output of a rainfall-runoff hydrological model or with the discharge record of the hydropower plants [Puechberty et al., 2017];

- correlation analysis with the surface velocity measure by means of non-contact techniques (e.g. radar, Thollet et al. [2017]).

- on-site bathymetric surveys;

- other field observations (e.g. presence of dams built by beavers or swimmers; data logger bugs);

- information about mining operations in the river bed or civil works affecting the flow.

5.5   Conclusion

The proposed method for the real-time management of unstable rating curves is based on the application to the real-time context of the available tools for rating shift detection and estimation, and of the available tools for RC estimation with uncertainty.

Each iteration is based on the incoming new stage data, then it applies the aforementioned tools searching for a rating shift (potential or effective) and it eventually updates the RC with the estimation of a provisional RC, which in the Bayesian context is done by updating the prior specification. When an effective shift is estimated then a new base RC is defined and a new stable period begins.

The method has been applied to the case study of the Ardèche River at Meyras during one morphogenic flood event. The application yielded promising results with the detection of the potential shift by the sediment transport proxy model and the refining of the RC uncertainty by the stage-recession analysis and finally the confirmation of the shift by the first gauging. However, these results cannot be generalized yet. Further work is needed to test the performance of the method on several other case studies with different characteristics and define the applicability limitations.

CHAPTER 6

CONCLUSIONS AND PERSPECTIVES

6.1 Summary

In this dissertation the issue of unstable rating curves is investigated. In particular three original tools for the detection and estimation of rating shifts are proposed. They are a continuation of the PhD work of Valentin Mansanarez [Mansanarez, 2016] who developed the Stage-Period-Discharge method leading to the estimation of the multiple RCs at known times.

The first tool has been developed for the detection and estimation of effective rating shifts using the gaugings. It is based on an original recursive segmentation procedure applied to the time series of the residuals computed between the gaugings and a reference RC. In this segmentation method there are no assumptions on the number of homogeneous segments. Moreover its originality is to account for the uncertainty of the data (here, the gaugings residuals) which may have large and variable uncertainty. This avoids detecting false shifts, as demonstrated through the application to several synthetic data sets. Finally it also provides useful information about the uncertainty on the shift times, which allows searching for the causal event, e.g. the largest flood. Finally, the proposed segmentation procedure may be applied beyond the field of hydrometry to a wide range of problems. Some examples are reported in Section 6.2.1.1.

The second tool has been developed to detect and estimate effective shifts using a stage-recession analysis. Its originality is mainly to apply for the first time in hydrometry the recession analysis concepts, broadly studied in the literature, to the stage record instead of the streamflow record. The main assumption is that the stage-recession curve tends toward the elevation of the lowest control as streamflow tends toward zero and that a morphological change of the river bed induces a parallel change of this asymptotic stage. After having estimated all the available recession curves, the same segmentation procedure that was applied to the gaugings residuals is applied to the time series of asymptotic stage estimates. The method leads not only to the detection of a rating change but also to estimate its amplitude.

The first and second tools are limited for real-time applications since they need information (gauging, recession) that is only occasionally available in real time. For the same reason, these tools may miss rating shifts in the retrospective analysis. Thus a third tool has been proposed in this manuscript to detect potential rating shifts. While for effective shifts the magnitude can be estimated precisely enough, for potential shifts the primary objective is to estimate its uncertainty. This tool is based on a sediment transport proxy analysis using as input the stage record available in real time. The shift detection is issued when stage exceeds a triggering stage for incipient motion which is calibrated in retrospective by analysing all past rating shifts and the corresponding morphogenic floods. Then, a relation established between the cumulative volume of transported sediments (computed using classical models) and the past shift estimates can be used in real time to provide an uncertainty estimate on the detected potential shift. The advantages of using this approach are that it detects a potential shift while it is occurring, without delay, and that it requires only the stage record and some knowldege on the past rating shifts.

The three tools have been applied initially for the retrospective detection of rating shifts and identification of the stable periods. This may allow the managers of a station to review the historical series of hydrometic data and to reduce the number of stable periods when a conservative analysis led to over-segmentation of the periods (e.g. after each flood).

Finally the proposed methods are implemented together into an original framework for the

real-time management of shifts affecting the rating curves and the streamflow estimation. Such real-time scheme is an original outcome of this thesis work since it was never formally developed before in the hydrometry field. As a proof-of-concept, the method has been applied to the station of the Ardèche River at Meyras in France during a morphogenic flood. The combination of the three tools for shift detection and estimation yielded promising results and showed that they can be successfully used at least for gravel bed rivers affected by morphogenic floods. However further work is needed to validate the method and demonstrate its operational applicability, in particular by testing it on several other stations. The scheme of the proposed framework is also conceived to be general, thus other potential shift detection criteria can be included as detailed in the following perspectives sections.

Matteo Darienzo

6.2 Perspectives

The proposed tools for rating shift detection and estimation could be further improved in the future. Some ideas are discussed in the next subsections.

6.2.1 Improvement of the proposed tools for rating shift detection

6.2.1.1 Segmentation of gaugings

The tool based on the segmentation of the gaugings residuals could be improved by defining the most suitable criterion used for determining the optimal number of segments, among several proposed in the literature. The simulations using synthetic data in Chapter 2 have shown that the segmentation is sensitive to the chosen criterion. The criteria that yield the highest performance are the DIC and the BIC. A better understanding of the differences between BIC and DIC is needed in future work.

Finally, as a general perspective, the proposed segmentation procedure could probably be extended to other fields where the relation between two observed variables, estimated using uncertain calibration data, is subject to sudden changes. As an example, Figure 6.1 shows the results of the proposed segmentation method applied to the relation turbidity vs Total Suspended Sediment concentration. More generally, the proposed method could be used for segmenting uncertain time series. It can be applied to test the homogeneity of the series used for the analysis of the distributions of floods and droughts. It has been used in a recent report [Lang, 2020] to study the floods on the Rhine River and shows its utility in the case of data with uncertainty strongly varying in time (cf. historical floods, see Figure 6.2).

6.2.1.2 Stage-recession analysis

Chapters 3 and 5 have shown the value of the stage-recession analysis for detecting and estimating morphological changes. However while several recession models are proposed and applied for the retrospective analysis in Chapter 3, only one recession model has been applied in
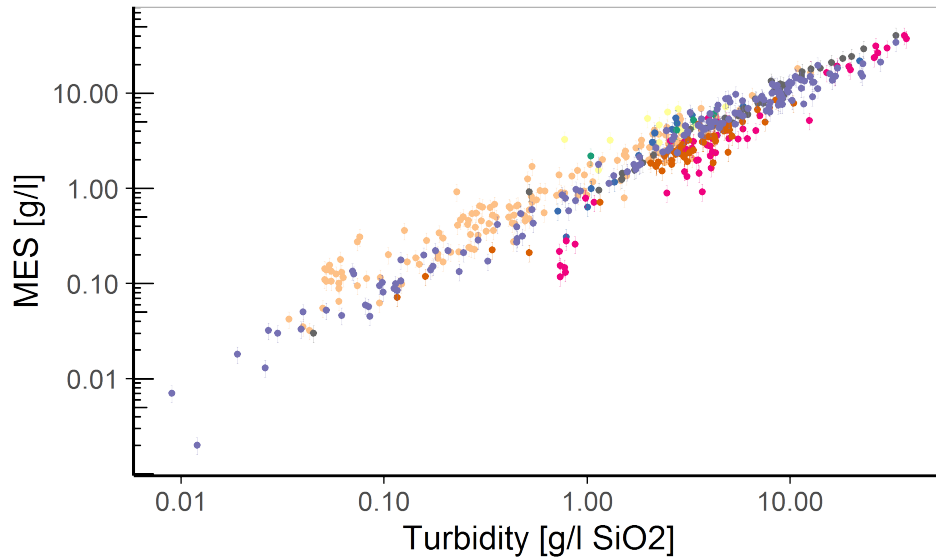
Figure 6.1: *Segmentation procedure proposed in Chapter 2 applied to the relation Turbidity vs Total Suspended Sediment concentration (MES in french) for the Arc River at Pontamafrey in France for the period 2011-2019.*
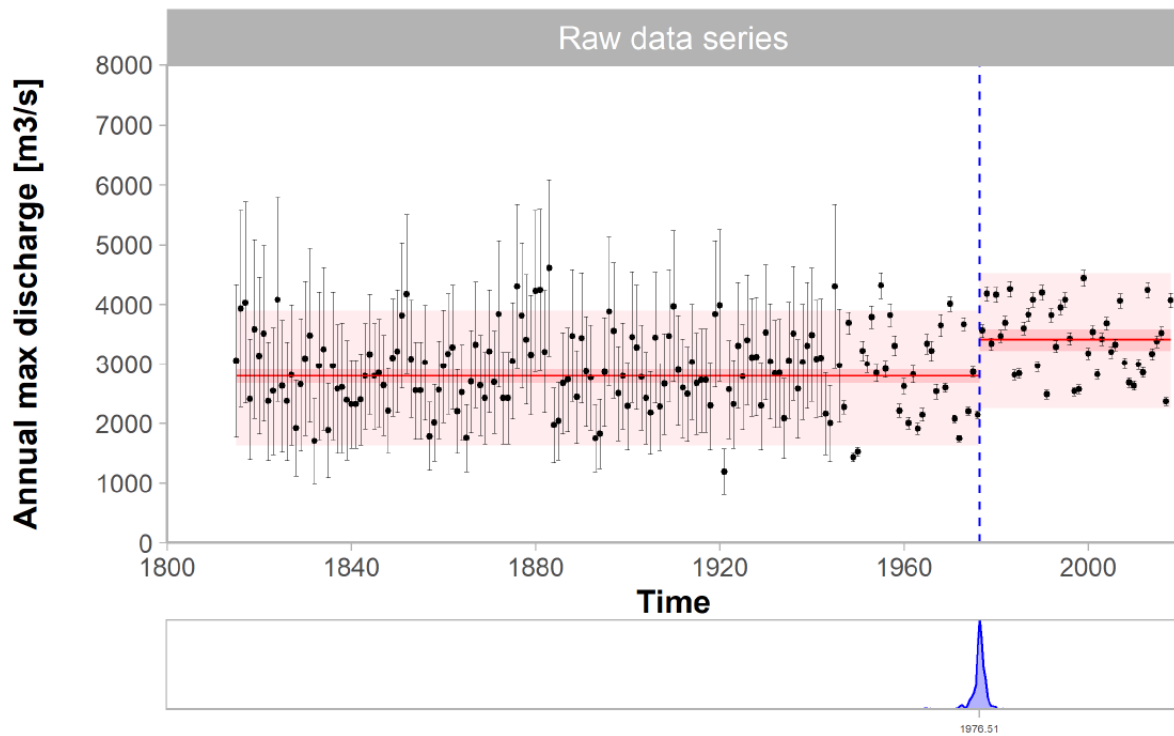
Figure 6.2: *The proposed segmentation procedure applied to the series of maximum annual discharge for the Rhine River at Maxau (Karlsruhe, Germany) during the period 1947-2017 [Lang, 2020]. Red and pink ribbons show the parametric and total uncertainty, respectively, of the segments mean. The shift time is represented by a dashed line and by its pdf in the graph below.*

the real-time application. The most suitable recession model might be different in retrospective and in real time. Further work is necessary in order to test other models in real time.

Other interesting perspectives include applying the stage-recession analysis to several case studies in order to provide some statistics on the stable parameters of the recession model (such as the recession rate λ), searching for hydrological signatures (as studied in the PhD thesis of Horner [2020]).

6.2.1.3 Sediment transport proxy analysis

According to the method proposed in Chapter 4, the criterion used for detecting potential shifts is based on the exceedance of the triggering stage h_c for incipient motion. This criterion leads to the detection of many events characterized by little sediment transport, thus by near-zero potential changes. This may certainly create practical problems for retrospective applications but also in real time when the manager of the station may not want to question the validity of the base RC too often to account for near-zero changes. An alternative to this may be to condition the detection of a rating shift to a minimum volume of transported sediments likely to cause a significant shift.

Finally another possible perspective, but not formalised yet, is the calibration of the triggering stage through a Bayesian framework. This may allow a more formal inclusion of the prior knowledge on the unknown parameters and considering some additional uncertainty that is otherwise ignored.

6.2.2 Performance evaluation using a wide range of hydrometric stations

Another important perspective of this work is the evaluation of the performance of the proposed methods on a range of different stations. While not described in this manuscript, we tested a few stations and the tests on a few others are planned in collaboration with several French and international services (e.g., CNR, EDF, DREAL, SCHAPI, NIWA, USGS, DEAL-Réunion). The stations to study are characterised by:

- Different river bed composition: gravel bed or sand beds. We focus in this manuscript on gravel bed rivers. We suppose that the application of the proposed methods to sand bed rivers (e.g. the Loire River at Montjean in France) may be more challenging due to the progressive river bed modification induced by continuous sediment transport and the great contribution of the suspended sediments to the erosion/deposition processes.

- Different frequency and intensity of shifts (e.g., the case of Séveraissette River at Vilar-Loubière, France which is highly unstable and the Illinois River at Tinley Creek, USA which has very small shifts) and input data (such as the available gaugings and recessions between the shift times). The ability of the segmentation of gaugings to detect rating shifts depends on the gaugings frequency with respect to the shift frequency, the gaugings uncertainty and their location along the RC. Two stations have been already processed: the results of the Wairau River at Barnetts Bank in New Zealand (Figure 6.3b) show that shifts occur very frequently with respect to the gaugings, thus many periods have few gaugings only. The results of the Mat River at Escalier, Reunion Island (Figure 6.3a) show that gaugings are mostly located at low flows leading to very uncertain base RCs and challenging segmentation. Moreover the stage-recession analysis depends on the number of long recessions that are available. Its application to stations with very frequent floods (e.g., the Wairau River at Barnetts Bank in New Zealand) may be very challenging and some improvements may be necessary.

- More complex controls and shifts which may affect other RC parameters (e.g., parameter a due to shifts of the channel width or the roughness coefficient or the longitudinal slope), such as braided or meandering rivers (e.g., the Drôme River at Loriol in France, the Rakaia River at Fighting Hill, in New zealand) or twin-gauge stations (e.g., the Isère River at Beaumont-Monteux).
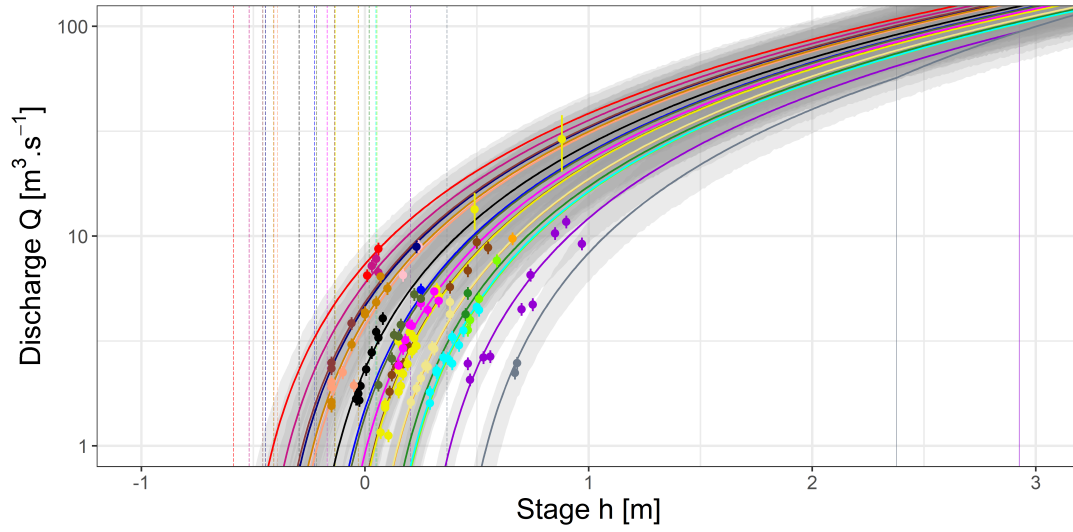
(a)
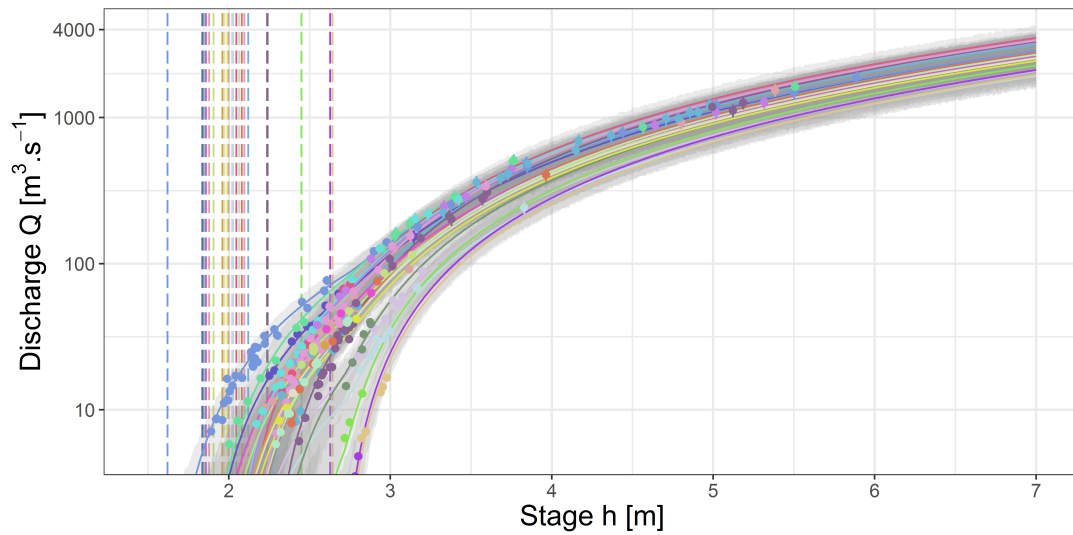
(b)

Figure 6.3: Proposed segmentation procedure applied to the gaugings of the Mat River at Escalier in Reunion Island (a) and the Wairau River at Barnetts Bank in New Zealand (b). Dashed vertical lines indicate the most probable values of the offset of the lowest control, b_1, for each stable period. Solid vertical lines in panel a) indicate the estimates of b_2. Ribbons around each rating curve represent the 95% uncertainty intervals obtained through the Bayesian approach of Mansanarez et al. [2019].

6.2.3 Development of other tools for potential rating shift detection

6.2.3.1 Correlation with the output of a rainfall-runoff model

The correlation analysis between the discharge time series produced at the station and the output of a hydrological rainfall-runoff model might be the most promising perspective. Many watersheds have models of this type. A rating shift may be detected by applying a segmentation procedure to the series of residuals derived from a linear regression between the two sets of discharge data. This approach is mentioned in the national (French) hydrometry quality plan [Puechberty et al., 2017]. Moreover, Lucas [2018] has tested this approach by using the hydrological model MORDOR [Garçon, 1996]).

Such residuals are characterized by large and strongly varying uncertainties, like the gaugings residuals (Chapter 2). Thus the segmentation procedure proposed in Chapter 2 would be well suited to them. However, a big difference with gaugings is that the number of data is much larger and their errors not independent (model bias). The risk may be a bias towards overconfidence in model outputs (cf. Sikorska and Renard [2017]). Moreover this tool depends on the availability of the input climatic data such as the precipitation and of the calibration streamflow data, and one problem to solve is how to quantify the model output uncertainty.

6.2.3.2 Correlation with neighboring stations

Also the spatial and temporal analysis of neighboring stations can be a powerful tool. It consists of comparing the discharge time series of the studied station with the discharge time series of another station with comparable hydrological behavior (e.g., located upstream or downstream along the same river, located in a tributary river, located in a neighboring catchment, etc.). Again, a segmentation procedure can be applied to the residuals. This approach is discussed in Puechberty et al. [2017] and the issue of characterizing the spatial correlation of daily streamflows has been studied by several authors, such as Betterle et al. [2017].

However, it is necessary to consider a sufficiently long time step (e.g., monthly) to ensure some reasonable degree of correlation between the two stations. Moreover this analysis cannot

be done without the existence of a hydrologically comparable and stable station, which is never granted.

This correlation approach could also be used for sites where independent discharge measurement from a structure (e.g. dam gates / turbines) is available. Usually it is much less precise than the RC but insensitive to bed evolution, hence "stable" (e.g. the Isère River at Beaumont-Monteux and the stations of the Vieux-Rhône by-passed channels, in France).

6.2.3.3 Analysis of residuals of the stage-surface velocity relation

Another tool possibly useful for detecting potential shifts in real time during floods is the analysis of the residuals between the stage and the surface velocity measured by non contact techniques such as radar or image velocimetry. This approach has been studied by Thollet et al. [2017] and Jacob [2014] with encouraging results: Figure 6.4 shows the stage - velocity relation at a station in France evidencing the existence of at least two distinct periods.

More and more hydrometric/hydrological services start to equip their stations with this type of instrumentation. Thus the analysis of the stage-surface velocity relation may become a valuable alternative to the sediment transport proxy analysis since it is based on measurements and available in real time during floods.
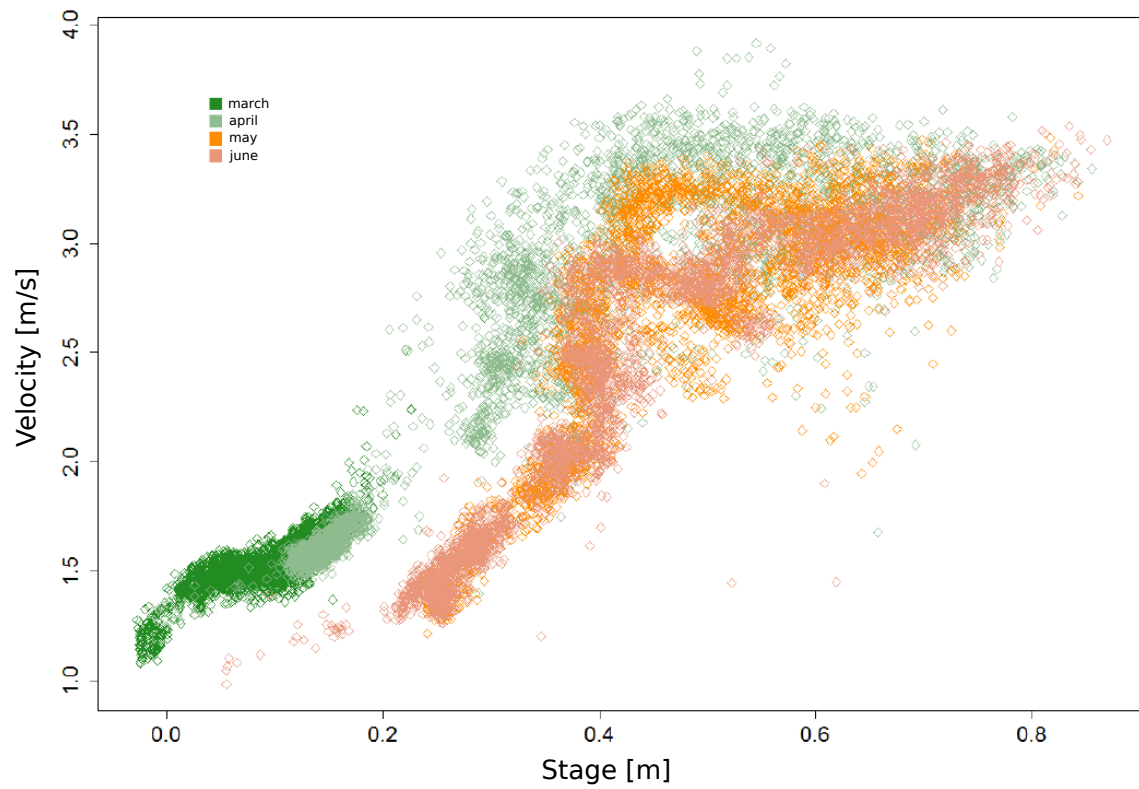
Figure 6.4: Stage-velocity radar-based measurements for the Arvan River at Saint-Jean de Maurienne in France, for the period March-June 2013 (modified from Jacob [2014]).

6.2.4 Choice of the tools for shift detection/estimation

The framework proposed in Chapter 5 for the real-time management of rating shifts is conceived to be complemented by any kind of information available in real time: e.g., the notice of dams built by beavers or swimmers; data logger bugs or instrumental failure reports, bathymetric surveys; information about sediment mining operations in the river bed or about works.

Before starting the real-time application shift detection tools must be selected. This choice may depend on the available data (e.g., gaugings, stage record, bathymetry) but also on the flow conditions (flood, drought), the tool-specific limitations and the shift causes. Table 6.1 summarises the conditions of application of the main shift detection tools from the literature and for those proposed in this manuscript.

The delay for precisely identifying and estimating a rating shift depends on the type of process causing the shifts: e.g., during floods the rating change induced by morphological change or due to hysteresis may occur in a period of a few hours or a few days; during a period of growth of aquatic vegetation the rating change may occur for several months in a progressive way.

Table 6.1: Summary of the principal shift detection tools from the literature and those proposed in this manuscript.

Shift detection method	Data required	Time step	Effective/ potential change	Cause of the detected change	Shifting RC parameters	Real-time applicability conditions
Tools proposed in this manuscript						
Segmentation of gaugings	Gaugings	Gauging frequency (e.g. month)	effective	all	all	Availability of gaugings
Analysis of stage-recessions	Stage record	Stage frequency (e.g. 15 min)	effective	Processes related to morphological changes	« b » of the lowest controls	During recession phase only and starting from few days after the flood peak
Sediment transport proxy analysis	Stage record	Stage frequency (e.g. 15 min)	potential	Morphogenic floods	« b » of the lowest controls	During floods only
Other tools proposed in the literature and not studied in this manuscript						
Comparison with neighboring stations [Puechberty et al., 2017]	Discharge time series of both stations	Week/month (to ensure independence of residuals)	potential	all	all	Availability of a « stable » and comparable neighboring station
Comparison with the ouput of a rainfall-runoff model [Puechberty et al., 2017]	Discharge time series + climatic data (e.g. precipitation)	Time step of the model (Day/week/month)	potential	all	all	availability of the inputs (catchment precipitation in particular)
Analysis of the surface velocity measurements [Thollet et al., 2017]	Surface velocity + stage record	Measurements time step	potential	all	all	Availability of surface velocity data
Analysis of the minimum stage values [Łapuszek, 2003]	Stage record	year	effective	Processes related to morphological changes	« b » of the lowest controls	Not suitable for real time purposes

6.3   Implementation into operational applications

The transfer of the methods proposed in this manuscript to their operational use may require additional improvements and adjustments. First of all a pre-treatment or visual checking of the input data is necessary in order to detect anomalies (e.g., errors due to wrong selection of rating shift date, sensor fault) and this must be done at different time scales (e.g., month, year) [Puechberty et al., 2017].

Regarding the computational costs, the tools proposed in this manuscript may take some time (from days to a week) when applied in retrospective to a long series and when several tests need to be carried out (e.g., to find the most adequate stage-recession model). Instead in real time the required computations for detecting a shift, updating the RC and providing the streamflow estimate are performed within 5 minutes for each time iteration, thus within the typical time step of the stage records (e.g., 15 minutes). This makes the method applicable operationally. The graphical interface can certainly be improved and adjusted according to the specific purposes of the services. Moreover, while the method is based on the automatic detection and estimation of the shifts, their validation and the beginning of a new stable period may remain partly manual and rely on the hydrologist expertise.

Another possible use of the proposed methods is their integration into existing operational real-time flood forecasting systems to provide streamflow data with more realistically quantified uncertainty to be assimilated in real time [Ocio et al., 2017; Barbetta et al., 2018]. The proposed methods may also help improving and optimising the future strategies for gauging campaigns.

Finally, future perspectives can clearly extend the objectives of this manuscript to study the processes inducing transient rating changes, such as: growth and decline of the aquatic vegetation, hysteresis, sea tidal effects, scour and fill of the river bed. Some of these processes are an ongoing study in the literature. A dynamic modelling may be more adequate than the shift-oriented approach taken in this manuscript, but this requires a better understanding of the physics behind the processes and of what precisely makes the RC changing over time.

Akaike, H. (1974). A new look at the statistical model identification. *IEEE Transactions on Automatic Control*, 19(6):716–723. doi:10.1109/TAC.1974.1100705.

Albert, I., Donnet, S., Guihenneuc-Jouyaux, C., Low-Choy, S., Mengersen, K., and Rousseau, J. (2012). Combining expert opinions in prior elicitation. *Bayesian Analysis*, 7(3):503–532. doi:10.1214/12-BA717.

Alexandersson, H. (1986). A homogeneity test applied to precipitation data. *Journal of Climatology*, 6(6):661–675. url: https://rmets.onlinelibrary.wiley.com/doi/10.1002/joc.3370060607.

Aminikhanghahi, S. and Cook, D. J. (2017). A survey of methods for time series change point detection. *Knowledge and Information Systems*, 51(2):339–367. doi:10.1007/s10115-016-0987-z.

Auger, I. E. and Lawrence, C. E. (1989). Algorithms for the optimal identification of segment neighborhoods. *Bulletin of Mathematical Biology*, 51(1):39–54. doi:10.1007/BF02458835.

Barbetta, S., Coccia, G., Moramarco, T., and Todini, E. (2018). Real-time flood forecasting downstream river confluences using a Bayesian approach. *Journal of Hydrology*, 565:516 – 523. doi:10.1016/j.jhydrol.2018.08.043.

Barnes, B. S. (1939). The structure of discharge-recession curves. *Eos, Transactions American Geophysical Union*, 20(4):721–725. doi:10.1029/TR020i004p00721.

Basseville, M. and Nikiforov, I. (1993). *Detection of Abrupt Change - Theory and Application*, volume 15. PTR Prentice-Hall.

Betterle, A., Schirmer, M., and Botter, G. (2017). Characterizing the spatial correlation of daily streamflows. *Water Resources Research*, 53(2):1646–1663. doi:10.1002/2016WR019195.

Booth, N. and Smith, A. (1982). A Bayesian approach to retrospective identification of change-points. *Journal of Econometrics*, 19(1):7 – 22. doi:10.1016/0304-4076(82)90048-3.

Brooks, S. and Gelman, A. (1998). General methods for monitoring convergence of iterative simulations. *Journal of Computational and Graphical Statistics*, 7(4):434–455. doi:10.1080/10618600.1998.10474787.

Brutsaert, W. and Nieber, J. L. (1977). Regionalized drought flow hydrographs from a mature glaciated plateau. *Water Resources Research*, 13(3):637–643. doi:10.1029/WR013i003p00637.

Buckland, S. T., Burnham, K. P., and Augustin, N. H. (1997). Model selection: An integral part of inference. *Biometrics*, 53:603–618. doi:10.2307/2533961.

Buffington, J. M. and Montgomery, D. R. (1997). A systematic analysis of eight decades of incipient motion studies, with special reference to gravel-bedded rivers. *Water Resources Research*, 33(8):1993–2029. doi:10.1029/96WR03190.

Burnham, K. P. and Anderson, D. R. (2004). Multimodel Inference: Understanding AIC and BIC in Model Selection. *Sociological Methods & Research*, 33:261 – 304. doi:10.1177/0049124104268644.

Camenen, B. and Larroudé, P. (2003). Comparison of sediment transport formulae for the coastal environment. *Coastal Engineering*, 48(2):111 – 132. doi:10.1016/S0378-3839(03)00002-4.

Camenen, C. (2007). Simple and general formula for the settling velocity of particles. *Journal of Hydraulic Engineering*, 133(2):229–233. doi:10.1061/(ASCE)0733-9429(2007)133:2(229).

Cappé, O., Moulines, E., and Ryden, T. (2005). *Inference in Hidden Markov Models (Springer Series in Statistics)*. Springer-Verlag. doi:10.1007/0-387-28982-8.

Chapman, T. (1999). A comparison of algorithms for stream flow recession and baseflow separation. *Hydrological Processes*, 13(5):701–714. doi:10.1002/(SICI)1099-1085(19990415)13:5<701::AID-HYP774>3.0.CO;2-2.

Chen, J. and Gupta, A. (2012). *Parametric statistical change point analysis: With applications to genetics, medicine, and finance.* Birkhäuser Boston. doi:10.1007/978-0-8176-4801-5.

Chen, J., Gupta, A., and Pan, J. (2006). Information criterion and change point problem for regular models. *Sankhyā: The Indian Journal of Statistics (2003-2007)*, 68(2):252–282. url: http://www.jstor.org/stable/25053496.

Chernoff, H. and Zacks, S. (1964). Estimating the current mean of a normal distribution which is subjected to changes in time. *The Annals of Mathematical Statistics*, 35(3):999–1018. url: https://www.jstor.org/stable/2238232.

Chib, S. (1998). Estimation and comparison of multiple change-point models. *Journal of Econometrics*, 86(2):221 – 241. doi:10.1016/S0304-4076(97)00115-2.

Coleman, S. E. and Smart, G. M. (2011). Fluvial sediment-transport processes and morphology. *Journal of Hydrology (New Zealand)*, 50(1):37–58. url: https://www.jstor.org/stable/43945013.

Coxon, G., Freer, J., Westerberg, I. K., Wagener, T., Woods, R., and Smith, P. J. (2015). A novel framework for discharge uncertainty quantification applied to 500 UK gauging stations. *Water Resources Research*, 51(7):5531–5546. doi:10.1002/2014WR016532.

Darienzo, M., Renard, B., Le Coz, J., and Lang, M. (2021). Detection of Stage-Discharge Rating Shifts Using Gaugings: A Recursive Segmentation Procedure Accounting for Observational and Model Uncertainties. *Water Resources Research*, 57,e2020WR028607. doi:10.1029/2020WR028607.

Davies, A., Ribberink, J., Temperville, A., and Zyserman, J. (1997). Comparisons between sediment transport models and observations made in wave and current flows above plane beds. *Coastal Engineering*, 31(1):163 – 198. doi:10.1016/S0378-3839(97)00005-7.

Davies, T. and Griffiths, G. (1996). Physical model study of stage-discharge relationships in a braided river gorge. *Journal of Hydrology (NZ)*, 35(2). url: https://www.jstor.org/stable/43944774.

Dewandel, B., Lachassagne, P., Bakalowicz, M., Weng, P., and Al-malki, A. (2003). Evaluation of aquifer thickness by analysing recession hydrographs. Application to the Oman ophiolite hard-rock aquifer. *Journal of Hydrology*, pages 248–269. doi:10.1016/S0022-1694(02)00418-3.

Dietrich, F. and List, C. (2014). Probabilistic opinion pooling. *Oxford Handbook of Probability and Philosophy*. url: http://philsci-archive.pitt.edu/11349/.

Drogue, C. (1972). Analyse statistique des hydrogrammes de decrues des sources karstiques. Statistical analysis of hydrographs of karstic springs. *Journal of Hydrology*, 15(1):49 – 68. doi:10.1016/0022-1694(72)90075-3.

Ducré-Robitaille, J.-F., Vincent, L. A., and Boulet, G. (2003). Comparison of techniques for detection of discontinuities in temperature series. *International Journal of Climatology*, 23(9):1087–1101. doi:10.1002/joc.924.

Engelund, F. and Hansen, E. (1967). A monograph on sediment transport in alluvial streams (3rd edition). *Hydraulic Engineering Reports, Technical University of Denmark Ostervoldgade 10, Copenhagen K*. url: http://resolver.tudelft.nl/uuid:81101b08-04b5-4082-9121-861949c336c9.

Garçon, R. (1996). Prévision opérationnelle des apports de la Durance à Serre-Ponçon à l'aide du modèle MORDOR. Bilan de l'année 1994-1995. *Houille Blanche-revue Internationale De L Eau*, 51:71–76. doi:10.1051/lhb/1996056.

Gelman, A., Carlin, J. B., Stern, H. S., and Rubin, D. B. (2004). *Bayesian Data Analysis*. Chapman and Hall/CRC.

Genest, C. and Zidek, J. V. (1986). Combining probability distributions: A critique and an annotated bibliography. *Statistical Science*, 1(1):114–135. doi:10.1214/ss/1177013825.

Green, P. (1995). Reversible jump Markov chain Monte Carlo computation and Bayesian model determination. *Biometrika*, 82(4):711–732. doi:10.1093/biomet/82.4.711.

Guerrero, J.-L., Westerberg, I. K., Halldin, S., Xu, C.-Y., and Lundin, L.-C. (2012). Temporal variability in stage–discharge relationships. *Journal of Hydrology*, 446-447:90 – 102. doi:10.1016/j.jhydrol.2012.04.031.

Hall, F. R. (1968). Base-flow recessions—a review. *Water Resources Research*, 4(5):973–983. doi:10.1029/WR004i005p00973.

Hannan, E. J. and Quinn, B. G. (1979). The determination of the order of an autoregression. *Journal of the Royal Statistical Society. Series B (Methodological)*, 41(2):190–195. url: http://www.jstor.org/stable/2985032.

Hawkins, D. M. (1977). Testing a sequence of observations for a shift in location. *Journal of the American Statistical Association*, 72(357):180–186. url: http://www.jstor.org/stable/2286934.

Herschy, R. W. (1998). *Streamflow measurement*, pages 635–637. Springer Netherlands, Dordrecht. doi:10.1007/1-4020-4497-6_214.

Hinkley, D. V. (1970). Inference about the change-point in a sequence of random variables. *Biometrika*, 57(1):1–17. doi:10.2307/2334932.

Horner, I. (2020). *Design and evaluation of hydrological signatures for the diagnostic and improvement of a process-based distributed hydrological model*. PhD thesis. Thèse de doctorat dirigée par Branger, Flora Océan, Atmosphère, Hydrologie Université Grenoble Alpes 2020, url: http://www.theses.fr/2020GRALU014/document.

Horner, I., Renard, B., Le Coz, J., Branger, F., McMillan, H. K., and Pierrefeu, G. (2018). Impact of stage measurement errors on streamflow uncertainty. *Water Resources Research*, 54(3):1952–1976. doi:10.1002/2017WR022039.

Horton, R. E. (1933). The rôle of infiltration in the hydrologic cycle. *Eos, Transactions American Geophysical Union*, 14(1):446–460. doi:10.1029/TR014i001p00446.

Hubert, P. and Carbonnel, J.-P. (1987). Approche statistique de l'aridification de l'Afrique de l'Ouest. *Journal of Hydrology*, 95(1):165 – 183. doi:10.1016/0022-1694(87)90123-5.

Hubert, P., Carbonnel, J.-P., and Chaouche, A. (1989). Segmentation des séries hydrométéorologiques. Application à des séries de précipitations et de débits de l'Afrique de l'Ouest. *Journal of Hydrology*, 110(3):349 – 367. doi:10.1016/0022-1694(89)90197-2.

Ibbitt, R. P. and Pearson, C. P. (1987). Gauging frequency and detection of rating changes. *Hydrological Sciences Journal*, 32(1):85–103. doi:10.1080/02626668709491164.

Jacob, E. (2014). Débits et incertitudes issus d'enregistrements de niveau et de vitesse par radar sur des cours d'eau de montagne à lit instable. *Rapport de stage encadré par Fabien Thollet, Jérôme Le Coz et Benoît Camenen, INRAE Lyon-Villeurbanne*, page 1–60.

Jalbert, J., Mathevet, T., and Favre, A.-C. (2011). Temporal uncertainty estimation of discharges from rating curves using a variographic analysis. *Journal of Hydrology*, 397(1):83 – 92. doi:10.1016/j.jhydrol.2010.11.031.

Matteo Darienzo

Jandhyala, V., Fotopoulos, S., MacNeill, I., and Liu, P. (2013). Inference for single and multiple change-points in time series. *Journal of Time Series Analysis*, 34(4):423–446. doi:10.1111/jtsa.12035.

Jia, L., Luo, Z., Yang, Q., Ou, S., and Lei, Y. (2007). Impacts of the large amount of sand mining on riverbed morphology and tidal dynamics in lower reaches and delta of the dongjiang river. *Journal of Geographical Sciences*, 17:197–211. doi:10.1007/s11442-007-0197-4.

Johnson, E. A. and Dils, R. E. (1956). Outline for Compiling Precipitation, Runoff, and Ground Water Data from Small Watersheds. *USDA Forest Service, Southeastern Forest Experiment Station, Old Station Paper*, (68). url: https://www.fs.usda.gov/treesearch/pubs/1790.

Keogh, E., Chu, S., Hart, D., and Pazzani, M. (2003). Segmenting time series: A survey and novel approach. *Data Mining in Time Series Databases*, 57. doi:10.1142/9789812565402_0001.

Kiang, J. E., Gazoorian, C., McMillan, H., Coxon, G., Le Coz, J., Westerberg, I. K., Belleville, A., Sevrez, D., Sikorska, A. E., Petersen-Øverleir, A., Reitan, T., Freer, J., Renard, B., Mansanarez, V., and Mason, R. (2018). A comparison of methods for streamflow uncertainty estimation. *Water Resources Research*, 54(10):7149–7176. doi:10.1029/2018WR022708.

Killick, R. and Eckley, I. (2014). Changepoint: An R Package for Changepoint Analysis. *Journal of statistical software*, 58. doi:10.18637/jss.v058.i03.

Killick, R., Fearnhead, P., and Eckley, I. A. (2012). Optimal detection of changepoints with a linear computational cost. *Journal of the American Statistical Association*, 107(500):1590–1598. doi:10.1080/01621459.2012.737745.

Kruskal, W. H. and Wallis, W. A. (1952). Use of ranks in one-criterion variance analysis. *Journal of the American Statistical Association*, 47(260):583–621. doi:10.2307/2280779.

Lang, C. and Gille, E. (2006). Une méthode d'analyse du tarissement des cours d'eau pour la prévision des débits d'étiage. *Norois*. doi:10.4000/norois.1743.

Lang, M. (2020). Expertise sur l'hydrologie du Rhin sur les biefs de Gambsheim et Iffezheim. *Rapport INRAE pour la DREAL Grand-Est*, page 98.

Langbein, W. B. (1938). Some channel-storage studies and their application to the

determination of infiltration. *Eos, Transactions American Geophysical Union*, 19(1):435–447. doi:10.1029/TR019i001p00435.

Łapuszek, M. (2003). The investigation of riverbed erosion in a mountainous river. *Archives of Hydro-Engineering and Environmental Mechanics*, 50:21–35.

Łapuszek, M. and Lenar-Matyas, A. (2015). Methods of analysis the riverbed evolution. A case study of two tributaries of the upper Vistula River. *Infrastructure and Ecology of Rural Areas, Nr IV/3/2015, Polska Akademia Nauk.* doi:10.14597/infraeco.2015.4.3.095.

Laronne, J., Outhet, D., Carling, P., and McCabe, T. (1994). Scour chain employment in gravel bed rivers. *CATENA*, 22(4):299 – 306. doi:10.1016/0341-8162(94)90040-X.

Larue, J.-P. and Giret, A. (2004). L'assèchement de cours d'eau dans le bassin de la Maine entre 1989 et 1992. *Norois.* doi:10.4000/norois.944.

Lavielle, M. and Lebarbier, E. (2001). An application of mcmc methods for the multiple change-points problem. *Signal Processing*, 81(1):39 – 53. Special section on Markov Chain Monte Carlo (MCMC) Methods for Signal Processing. doi:10.1016/S0165-1684(00)00189-4.

Le Coz, J., Mansanarez, V., Renard, B., Horner, I., and Lang, M. (2017). Towards the real-time management of unstable rating curves. *Congrès SHF: Hydrométrie 2017, Lyon 14-15 mars 2017*, page 1–12.

Le Coz, J., Renard, B., Bonnifait, L., Branger, F., and Le Boursicaud, R. (2014). Combining hydraulic knowledge and uncertain gaugings in the estimation of hydrometric rating curves: A Bayesian approach. *Journal of Hydrology*, 509:573 – 587. doi:10.1016/j.jhydrol.2013.11.016.

Le Coz, J., Smart, G., Hicks, M., Mansanarez, V., Renard, B., Camenen, B., and Lang, M. (2018). Estimating the long-term evolution of river bed levels using hydrometric data. *E3S Web Conf.*, 40:06003. doi:10.1051/e3sconf/20184006003.

Leduc, P., Ashmore, P., and Sjogren, D. (2018). Technical note: Stage and water width measurement of a mountain stream using a simple time-lapse camera. *Hydrology and Earth System Sciences*, 22(1):1–11. doi:10.5194/hess-22-1-2018.

Lee, A. F. S. and Heghinian, S. M. (1977). A shift of the mean level in a sequence of

independent normal random variables: A bayesian approach. *Technometrics*, 19(4):503–506. doi:10.2307/1267892.

Legleiter, C. J., Kinzel, P., and Overstreet, B. (2011). Evaluating the potential for remote bathymetric mapping of a turbid, sand-bed river: 2. application to hyperspectral image data from the platte river. *Water Resources Research*, 47. doi:10.1029/2011WR010592.

Legleiter, C. J. and Overstreet, B. T. (2012). Mapping gravel bed river bathymetry from space. *Journal of Geophysical Research: Earth Surface*, 117(F4). doi:10.1029/2012JF002539.

Lucas, M. (2018). Développement d'une méthode de détection en temps-réel des ruptures dans la relation hauteur/débit. *Rapport de stage de fin d'études, encadré par Pierre Brigode, Polytech Nice-Sophia, et Damien Sevrez, EDF-DTG*, page 1–59.

Luong, T., Perduca, V., and Nuel, G. (2012). Hidden markov model applications in change-point analysis. *arXiv*. url: https://arxiv.org/abs/1212.1778.

Mansanarez, V. (2016). *Non-unique stage-discharge relations: Bayesian analysis of complex rating curves and their uncertainties*. PhD thesis, Université Grenoble Alpes. url: https://tel.archives-ouvertes.fr/tel-01495985.

Mansanarez, V., Renard, B., Le Coz, J., and Lang, M. (2020). Stage-gradient-discharge models: Bayesian analysis of hysteresis due to unsteady flows. *Water Resources Research*. Manuscript submitted to Water Resources Research on 25/06/2020.

Mansanarez, V., Renard, B., Le Coz, J., Lang, M., and Darienzo, M. (2019). Shift Happens! Adjusting Stage-Discharge Rating Curves to Morphological Changes at Known Times. *Water Resources Research*, 55(4):2876–2899. doi:10.1029/2018WR023389.

McGilchrist, C. A. and Woodyer, K. D. (1975). Note on a distribution-free cusum technique. *Technometrics*, 17(3):321–325. doi:10.2307/1268068.

McMillan, H., Freer, J., Pappenberger, F., Krueger, T., and Clark, M. (2010). Impacts of uncertain river flow data on rainfall-runoff model calibration and discharge predictions. *Hydrological Processes*, 24(10):1270–1284. doi:10.1002/hyp.7587.

McMillan, H., Krueger, T., and Freer, J. (2012). Benchmarking observational uncertainties for

hydrology: rainfall, river discharge and water quality. *Hydrological Processes*, 26(26):4078–4111. doi:10.1002/hyp.9384.

McMillan, H., Seibert, J., Petersen-Øverleir, A., Lang, M., White, P., Snelder, T., Rutherford, K., Krueger, T., Mason, R., and Kiang, J. (2017). How uncertainty analysis of streamflow data can reduce costs and promote robust decisions in water management applications. *Water Resources Research*, 53(7):5220–5228. doi:10.1002/2016WR020328.

Meyer-Peter, E. and Müller, R. (1948). Formulas for bed load transport. *IAHSR 2nd meeting, Stockholm, appendix 2, Hydraulic Engineering Reports*.

Morlet, J., Arens, G., Fourgeau, E., and Glard, D. (1982). Wave propagation and sampling theory—part i: Complex signal and scattering in multilayered media. *Geophysics*, 47(2):203–221. doi:10.1190/1.1441328.

Morlot, T. (2014). *La gestion dynamique des relations hauteur-débit des stations d'hydrométrie et le calcul des incertitudes associées : un indicateur de gestion, de qualité et de suivi des points de mesure*. PhD thesis. Thèse de doctorat dirigée par Favre Pugin, Anne-Catherine et Perret, Christian Sciences de la terre et de l'univers, et de l'environnement Grenoble 2014 http://www.theses.fr/2014GRENU029.

Morlot, T., Perret, C., Favre, A.-C., and Jalbert, J. (2014). Dynamic rating curve assessment for hydrometric stations and computation of the associated uncertainties: Quality and station management indicators. *Journal of Hydrology*, 517:173–186. doi:10.1016/j.jhydrol.2014.05.007.

Nam, C. F. H., Aston, J. A. D., and Johansen, A. M. (2012). Quantifying the uncertainty in change points. *Journal of Time Series Analysis*, 33(5):807–823. doi:10.1111/j.1467-9892.2011.00777.x.

Nathan, R. J. and McMahon, T. A. (1990). Evaluation of automated techniques for base flow and recession analyses. *Water Resources Research*, 26(7):1465–1473. doi:10.1029/WR026i007p01465.

Ocio, D., Le Vine, N., Westerberg, I., Pappenberger, F., and Buytaert, W. (2017). The role of rating curve uncertainty in real-time flood forecasting. *Water Resources Research*, 53(5):4197–4213. doi:10.1002/2016WR020225.

Olshen, A. B., Venkatraman, E. S., Lucito, R., and Wigler, M. (2004). Circular binary segmentation for the analysis of array-based DNA copy number data. *Biostatistics*, 5(4):557–572. doi:10.1093/biostatistics/kxh008.

Osorio, A. L. N. A. and Reis, D. S. (2016). A Bayesian Approach for the Evaluation of Rating Curve Uncertainties in Flood Frequency Analyses. *World Environmental and Water Resources Congress*, pages 482–491. doi:10.1061/9780784479858.050.

Page, E. S. (1954). Continuous Inspection Schemes. *Biometrika*, 41(1/2):100–115. doi:10.2307/2333009.

Perreault, L., Bernier, J., Bobée, B., and Parent, E. (2000a). Bayesian change-point analysis in hydrometeorological time series. Part 1. The normal model revisited. *Journal of Hydrology*, 235(3):221 – 241. doi:10.1016/S0022-1694(00)00270-5.

Perreault, L., Bernier, J., Bobée, B., and Parent, E. (2000b). Bayesian change-point analysis in hydrometeorological time series. Part 2. Comparison of change-point models and forecasting. *Journal of Hydrology*, 235(3):242 – 263. doi:10.1016/S0022-1694(00)00271-7.

Perreault, L., Haché, M., Slivitzky, M., and Bobée, B. (1999). Detection of changes in precipitation and runoff over eastern canada and u.s. using a bayesian approach. *Stochastic Environmental Research and Risk Assessment*, 13(3):201–216. doi:10.1007/s004770050039.

Perret, E. (2017). *Transport of moderately sorted gravels at low bed shear stress : impact of bed arrangement and fine sediment infiltration*. PhD thesis. Thèse de doctorat dirigée par Benoît Camenen, Céline Berni et Kamal El Kadi Abderrezak, Mécanique des fluides Lyon 2017. url: https://tel.archives-ouvertes.fr/tel-01737702.

Perret, E., Renard, B., and Le Coz, J. (2021). A Rating Curve Model Accounting for Cyclic Stage-Discharge Shifts due to Seasonal Aquatic Vegetation. *Water Resources Research*, 57(3):e2020WR027745. doi:10.1029/2020WR027745.

Pettitt, A. N. (1979). A Non-Parametric Approach to the Change-Point Problem. *Journal of the Royal Statistical Society. Series C (Applied Statistics)*, 28(2):126–135. doi:10.2307/2346729.

Phillips, J. and Eaton, B. (2009). Detecting the Timing of Morphologic Change Using Stage-Discharge Regressions: A Case Study at Fishtrap Creek, British Columbia, Canada. *Canadian Water Resources Journal*, 34:285–300. doi:10.4296/cwrj3403285.

Pooley, C. M. and Marion, G. (2018). Bayesian model evidence as a practical alternative to deviance information criterion. *Royal Society Open Science*, 5(3):171519. doi:10.1098/rsos.171519.

Puechberty, R., Perret, C., Poligot-Pitsch, S., Battaglia, P., Belleville, A., Bompart, P., Chauvel, G., Cousseau, J., Dramais, G., Glaziou, G., Hauet, A., Hélouin, S., Lang, M., Larrarte, F., Le Coz, J., Marchand, P., Moquet, P., Payrastre, O., Pierrefeu, G., and Rauzy, G. (2017). Charte qualité de l'hydrométrie: Guide de bonnes pratiques. *Groupe Doppler Hydrométrie. Ministère de l'Environnement, de l'Energie et de la Mer, France*, page 83. url: https://side.developpement-durable.gouv.fr/Default/doc/SYRACUSE/355845/charte-qualite-de-l-hydrometrie-guide-de-bonnes-pratiques.

Rainville, F., Hutchinson, D., Stead, A., Moncur, D., and Elliott, D. (2016). Hydrometric manual: Data computations, stage-discharge model development and maintenance.

Rantz, S. E. (1982). *Measurement and computation of streamflow. Volume 2: Computation of discharge*. USGS, Geological Survey Water-Supply Paper.

Reitan, T. and Petersen-Øverleir, A. (2011). Dynamic rating curve assessment in unstable rivers using Ornstein-Uhlenbeck processes. *Water Resources Research*, 47(2). doi:10.1029/2010WR009504.

Renard, B., Garreta, V., and Lang, M. (2006). An application of Bayesian analysis and Markov chain Monte Carlo methods to the estimation of a regional trend in annual maxima. *Water Resources Research*, 42(12). doi:10.1029/2005WR004591.

Rodrigues, S., Mosselman, E., Claude, N., Wintenberger, C., and Juge, P. (2014). Alternate bars in a sandy gravel bed river: Generation, migration and interactions with superimposed dunes. *Earth Surface Processes and Landforms*, 40. doi:10.1002/esp.3657.

Schmidt, A. (2002). *Analysis of Stage-Discharge Relations for Open-Channel Flows and Their Associated Uncertainties*. PhD thesis, University of Illinois at Urbana-Champaign. http://hdl.handle.net/2142/83191.

Schwarz, G. (1978). Estimating the dimension of a model. *The Annals of Statistics*, 6(2):461–464. url: https://www.jstor.org/stable/2958889.

Scott, A. J. and Knott, M. (1974). A cluster analysis method for grouping means in the analysis of variance. *Biometrics*, 30(3):507–512. doi:10.2307/2529204.

Shields, A. (1936). Application of similarity principles and turbulence research to bed-load movement (translated version). *Mitteilungen der Preußischen Versuchsanstalt für Wasserbau. 26. Berlin: Preußische Versuchsanstalt für Wasserbau.*

Sikorska, A. E. and Renard, B. (2017). Calibrating a hydrological model in stage space to account for rating curve uncertainties: general framework and key challenges. *Advances in Water Resources*, 105:51–66. doi:10.1016/j.advwatres.2017.04.011.

Soulsby, R. L. (1997). Dynamics of marine sands: a manual for practical applications. *London, Thomas Telford Publications*, page 249 pp.

Spiegelhalter, D. J., Best, N., Carlin, B. P., and Linde, A. (2002). Bayesian measures of model complexity and fit (with discussion). *Journal of the Royal Statistical Society, Series B*, 64:1–34. doi:10.1111/1467-9868.00353.

Sujono, J., Shikasho, S., and Hiramatsu, K. (2001). Hydrograph recession analysis using wavelet transforms. *Journal of the Faculty of Agriculture, Kyushu University*, 45(2):557–564.

Sujono, J., Shikasho, S., and Hiramatsu, K. (2004). A comparison of techniques for hydrograph recession analysis. *Hydrological Processes*, 18(3):403–413. doi:10.1002/hyp.1247.

Tallaksen, L. (1995). A review of baseflow recession analysis. *Journal of Hydrology*, 165(1):349 – 370. url: http://www.sciencedirect.com/science/article/pii/002216949402540R.

Thollet, F., Le Coz, J., Dramais, G., Nord, G., Le Boursicaud, R., Jacob, E., and Buffet, A. (2017). Mesure de débit en rivière par station radar hauteur / vitesse selon la méthode de la vitesse témoin [Streamflow monitoring at stage / velocity radar stations using the index velocity method]. *La Houille Blanche*, (5):9–15. doi:10.1051/lhb/2017038.

Toebes, C. and Strang, D. D. (1964). On recession curves: 1 — Recession Equations. *Journal of Hydrology (New Zealand)*, 3(2):2–14. url: http://www.jstor.org/stable/43944075.

UNDRR (2020). *Human cost of disasters: An overview of the last 20 years 2000-2019.* United Nations Office for Disaster Risk Reduction (UNDRR), Centre for Research on the Epidemiology of Disasters (CRED), Institute of Health and Society (UCLouvain).

van Rijn, L. C. (1984). Sediment Transport, Part I: Bed Load Transport. *Journal of Hydraulic Engineering*, 110(10):1431–1456. doi:10.1061/(ASCE)0733-9429(1984)110:10(1431).

Vogel, R. M. and Kroll, C. N. (1996). Estimation of baseflow recession constants. *Water Resources Management*, 10:303–320. doi:10.1007/BF00508898.

Wang, B. and Xu, Y. J. (2016). Long-term geomorphic response to flow regulation in a 10-km reach downstream of the mississippi–atchafalaya river diversion. *Journal of Hydrology: Regional Studies*, 8:10 − 25. doi:10.1016/j.ejrh.2016.08.002.

Werner, P. and Sundquist, K. (1951). On the groundwater recession curve for large watersheds. *IAHS Publications*, 33:202–212.

Westerberg, I., Guerrero, J.-L., Seibert, J., Beven, K., and Halldin, S. (2011). Stage-discharge uncertainty derived with a non-stationary rating curve in the Choluteca River, Honduras. *Hydrological Processes*, 25:603 − 613. doi:10.1002/hyp.7848.

Wilcoxon, F. (1945). Individual comparisons by ranking methods. *Biometrics Bulletin*, 1(6):80–83. doi:10.2307/3001968.

Wittenberg, H. (1994). Nonlinear analysis of flow recession curves. *IAHS Publications*, 221.

WMO (2010). *Manual on Stream Gauging, Vol. II: Computation of discharge*. No. 1044 edition.

Zhao, J. and Zhang, H. (2008). Research on precise monitoring method of riverbed evolution. In Xu, P., Liu, J., and Dermanis, A., editors, *VI Hotine-Marussi Symposium on Theoretical and Computational Geodesy*, pages 303–307. Springer Berlin Heidelberg.

Détection et estimation de détarages dans les modèles hauteur-débit pour la quantification du débit des cours d'eau en rétrospectif et en temps réel

Les séries temporelles de débit des rivières sont établies à l'aide de "courbes de tarage", qui sont des modèles avec les hauteurs d'eau en entrée et les débits en sortie. Malheureusement, de nombreuses stations hydrométriques ont une relation hauteur-débit instable, notamment à cause de l'évolution du lit de la rivière lors des crues. Ces "détarages" posent problème à la fois pour l'établissement des séries hydrologiques de long-terme (analyse rétrospective) et pour la fourniture de données en temps réel, par exemple pour la prévision des inondations, avec des incertitudes quantifiées et fiables. Les méthodes existantes pour la mise à jour de la courbe de tarage sont basées sur une analyse statistique des données de calibration (jaugeages) passées ou sur des règles empiriques. Cette thèse a permis de développer des méthodes originales pour la détection automatique des détarages et l'estimation de leur amplitude en rétrospectif et en temps réel : une méthode de segmentation des résidus entre les jaugeages et une courbe de référence, une analyse des récessions du limnigramme et une détection de détarages potentiels à partir d'un indicateur disponible en temps réel (par exemple, transport sédimentaire cumulé). L'approche probabiliste permet d'une part de prendre en compte l'incertitude des informations sur les détarages et d'autre part de quantifier les incertitudes sur les débits calculés. La combinaison des trois méthodes a été appliquée à la station de l'Ardèche à Meyras, en France, qui présente des détarages nets après chaque crue importante. Une bonne détection et estimation des détarages a été observée en rétrospectif et en temps réel. La méthode est générique et, après davantage de validation, applicable en opérationnel à d'autres sites.

Mots clés : courbes de tarage, analyse Bayésienne, temps réel, détarages, jaugeages, analyse rétrospective

Detection and estimation of stage-discharge rating shifts for retrospective and real-time streamflow quantification

River discharge time series are established using "rating curves", which are models with stage as input and discharge as output. Unfortunately, many hydrometric stations have an unstable stage-discharge relation, particularly because of the change in the river bed during floods. These "rating shifts" pose a problem both for the establishment of long-term hydrological series (retrospective analysis) and for the delivery of real-time data, for example for flood forecasting, with quantified and reliable uncertainties. The existing methods for updating the rating curve are based on a statistical analysis of past calibration data (the gaugings) or on empirical rules. This thesis aims at developing some original methods for the automatic detection of rating shifts and the estimation of their magnitude in both retrospective and real time: a method of segmentation of the residuals between the gaugings and a base rating curve, an analysis of the stage recessions and a method for detecting potential shifts from an indicator available in real time (e.g. cumulative sediment transport). The probabilistic approach allows on the one hand to take into account the uncertainty of the information on the shift and on the other hand to quantify the uncertainties of the calculated streamflow. The combination of the three methods has been applied to the Ardèche at Meyras, France, which shows net shifts after each major flood. Good detection and estimation of the rating shift has been observed retrospectively and in real time. The method is generic and, after further validation, operationally applicable to other sites.

Key words: rating curves, Bayesian analysis, real time, rating shifts, gaugings, retrospective analysis